REPORT MDC E2009

INVESTIGATION OF THE FREE FLOW ELECTROPHORETIC PROCESS

FINAL REPORT

VOLUME II
TECHNICAL ANALYSIS

NASA/MSFC
DR R.S. SNYDER
HUNTSVILLE, AL.

MCDONNELL DOUGLAS ASTRONAUTICS COMPANY-ST. LOUIS DIVISION

MCDONNELL DOUGLAS CORPORATION

COPY NO. 5

INVESTIGATION OF THE FREE FLOW ELECTROPHORETIC PROCESS

FINAL REPORT

MAY 1979

REPORT MDC E2000

VOLUME II
TECHNICAL ANALYSIS

SUBMITTED TO: NATIONAL AERONAUTICS AND SPACE ADMINISTRATION
MARSHALL SPACE FLIGHT CENTER
HUNTSVILLE, ALABAMA

CONTRACT NO: NAS 8-32200

WRITTEN BY: R. A. WEISS
J. W. LANHAM
D. W. RICHMAN
C. D. WALKER

MCDONNELL DOUGLAS ASTRONAUTICS COMPANY-ST. LOUIS DIVISION
Box 516, Saint Louis, Missouri 63166 (314) 232-0232

MCDONNELL DOUGLAS CORPORATION

PREFACE

This MDC report entitled "Investigation of the Free Flow Electrophoretic Process" is submitted under NASA Contract Number NAS 8-32200. It consists of two volumes as specified below:

. Volume I - Executive Summary
Volume II - Technical Analysis

Prepared as the final report of a seven-month study, with the same title, performed by McDonnell Douglas Astronautics Company - St. Louis Division, this document summarizes the results of a study that focused on demonstrating the effects of gravity on the process and comparing the demonstrated effects with predictions made by mathematical models. This contract was administered by the NASA Marshall Space Flight Center, Huntsville, Alabama.

This report was written by:

Ronald A. Weiss, PhD
Principal Investigator

Charles D. Walker
Design Engineer

James W. Lanham, PhD
Technical Specialist-Microbiology

David W. Richman
Lead Engineer-Technology

Other contributors to the study effort included S. J. Blaisdell, C. E. Cleveland, C. E. Roth and A. L. Hitt. This report was reviewed by A. V. Montgomery, MD, PhD-Director of Life Sciences and J. T. Rose-Space Processing Program Manager.

Questions regarding this study should be directed to:

Ronald A. Weiss, PhD
McDonnell Douglas Astronautics
Company - St. Louis Division
P.O. Box 516
St. Louis, Missouri 63166
Telephone: (314) 232-2008

Robert S. Snyder, PhD
Code: ES73
NASA Marshall Space Flight Center
Huntsville, Alabama 35812
Telephone: (205) 453-3537

TABLE OF CONTENTS

TABLE OF CONTENTS

LIST OF FIGURES

LIST OF FIGURES

LIST OF FIGURES

LIST OF PAGES

1.0 SUMMARY

The microgravity environment of space may provide advantages to the production and purification of biological materials in terms of greater availability and higher purity of therapeutic, research, and diagnostic materials. Experiments conducted in space have already demonstrated the advantages of using static (1) and free-flow (2) electrophoresis to separate biological materials in a microgravity environment. Cells separated using static electrophoresis showed increased production of urokinase and erythropoietin when subsequently subcultured in earth based laboratories (3). The previously noted experiments demonstrated the positive results that the space environment has on materials processing, but they were not intended to focus on process parameters. A necessary step toward NASA's goal of space industrialization is an in-depth study of the effects of gravity on the process. Understanding these effects will facilitate quantification of the advantages of space processing, allowing ground-space economic trade-off analyses to be made. The purpose of this study is to demonstrate the effects of gravity on the free-flow electrophoretic process and to compare the demonstrated effects with predictions made by mathematical models.

The free flow electrophoresis chamber used to demonstrate the effects of gravity on the process is of a proprietary design developed by McDonnell Douglas Astronautics Company - St. Louis Division. This chamber is 120 cm long, 8.25 cm wide, and 0.3 cm thick. The chamber and its supporting hardware are shown in Figure 1-1, AN Electrophoresis Test Setup. Flow in this chamber is in the upward direction and exits through 105 outlets at the top of the chamber. During electrophoresis a stream of sample is injected into the flow near the bottom of the chamber and an electrical field is applied across the width of the chamber. The field causes a lateral force on particles in the sample proportional to the inherent charge of the particle and the electrical field strength. Particle lateral velocity is then dependent on the force due to viscous drag which is proportional to particle size. The characteristic that describes particle motion is electrophoretic mobility, which is the lateral velocity divided by electrical field strength.

The free flow electrophoretic process depends on maintenance of a steady laminar flow of the carrier fluid. Time variant velocity fluctuations will cause corresponding fluctuations in the particle paths spoiling the intended separation. On

AN ELECTROPHORESIS TEST SET-UP

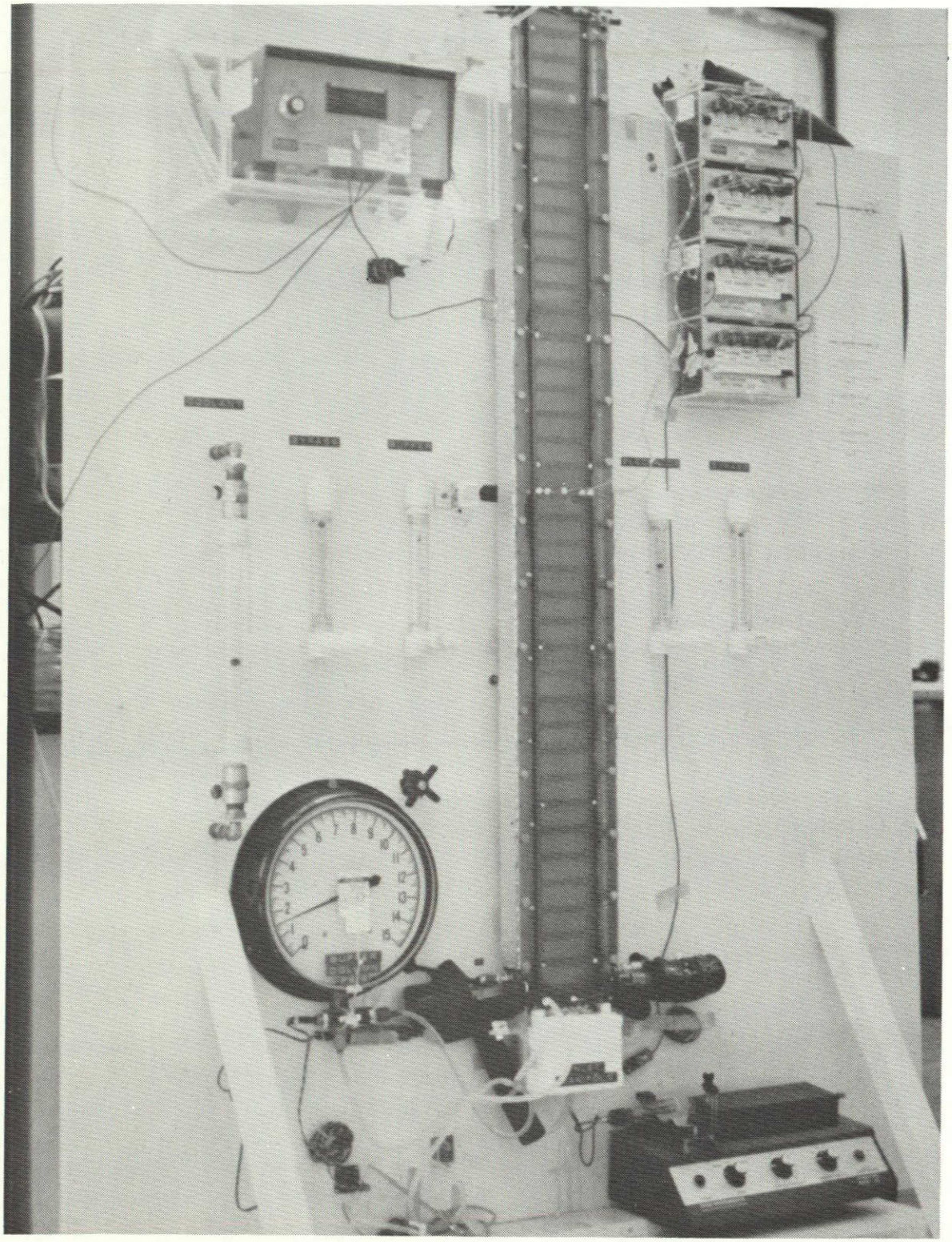

Figure 1–1

earth the primary source of velocity variations in the carrier fluid is convection currents. Free convection in turn is caused by density variations due to temperature differences in the fluid. These temperature differences are caused by Joule heating of the fluid by the electrical field. This problem is aggravated by the requirement that the carrier fluid must have sufficient ionic strength to insure stability of the biological materials being separated. This carrier fluid, or buffer, is therefore an electrically conductive medium.

1.1 EFFECTS OF GRAVITY ON CARRIER BUFFER

The purpose to Task 1.0 was to determine the effects of gravity induced thermal convection on the carrier buffer flow. Tests were performed to measure vertical centerline velocity as gauged by the motion of dye fronts in the carrier buffer flow. A dye front near the entrance of the chamber with no field applied is shown in Figure 1-2 and one at a field strength of 10 volts/cm near the outlet is shown in Figure 1-3. The results for the zero voltage case are what would be expected for flow between closely spaced parallel plates i.e. a nearly flat profile that falls off only near the sides of the chamber. With voltage however, peaks develop in the profile near the sides of the chamber. These peaks were found to be caused by heating of the fluid at the membranes, this conclusion was based on correlation with velocity predictions from a three dimensional mathematical model of the chamber flow velocities, pressures, and temperatures developed by McDonnell Douglas Astronautics Company - St. Louis Division.

Good correlation of test results with the mathematical model with no field applied may be demonstrated by comparing the observed data of Figure 1-4 with the model predictions of Figure 1-5. The mean of observed data (0.1890 cm/sec) is approximately one standard deviation (0.0135 cm/sec) less than the predicted mean velocity (0.2066 cm/sec).

When power was applied to the chamber the centerline velocities were significantly reduced by the return flow of the gravity induced convective cells evidenced by the velocity peaks seen in Figure 1-3. In this case the mathematical model centerline velocities were predicted to be significantly higher than the observed test data. This indicates that the mathematical model may have underestimated the return flow for the upward convection currents at the membranes. Therefore, the model predictions for sample residence times during test separations were less than the actual case.

VELOCITY PROFILE (0 VOLTS/CM)

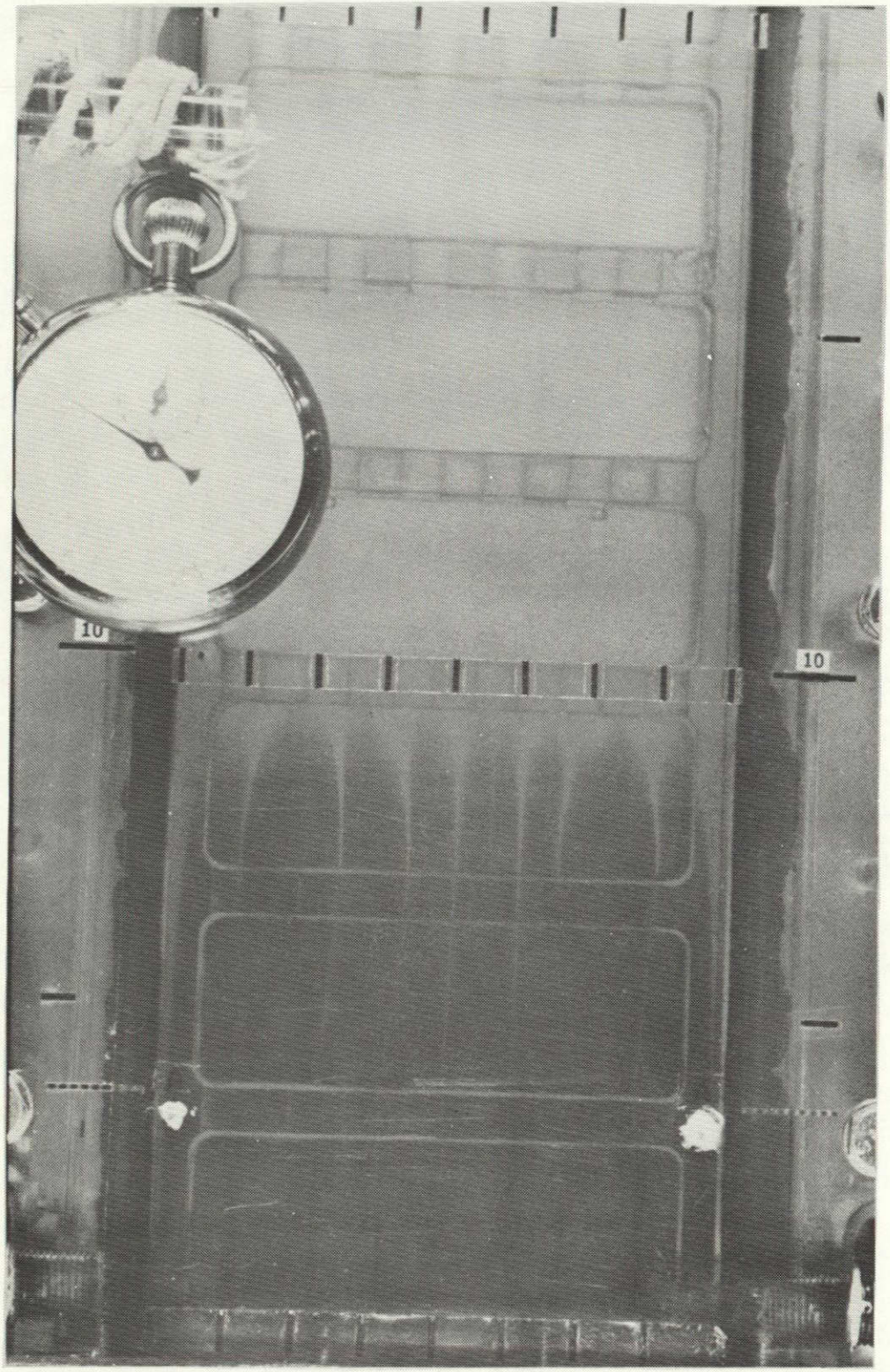

Figure 1–2

VELOCITY PROFILE (10 VOLTS/CM)

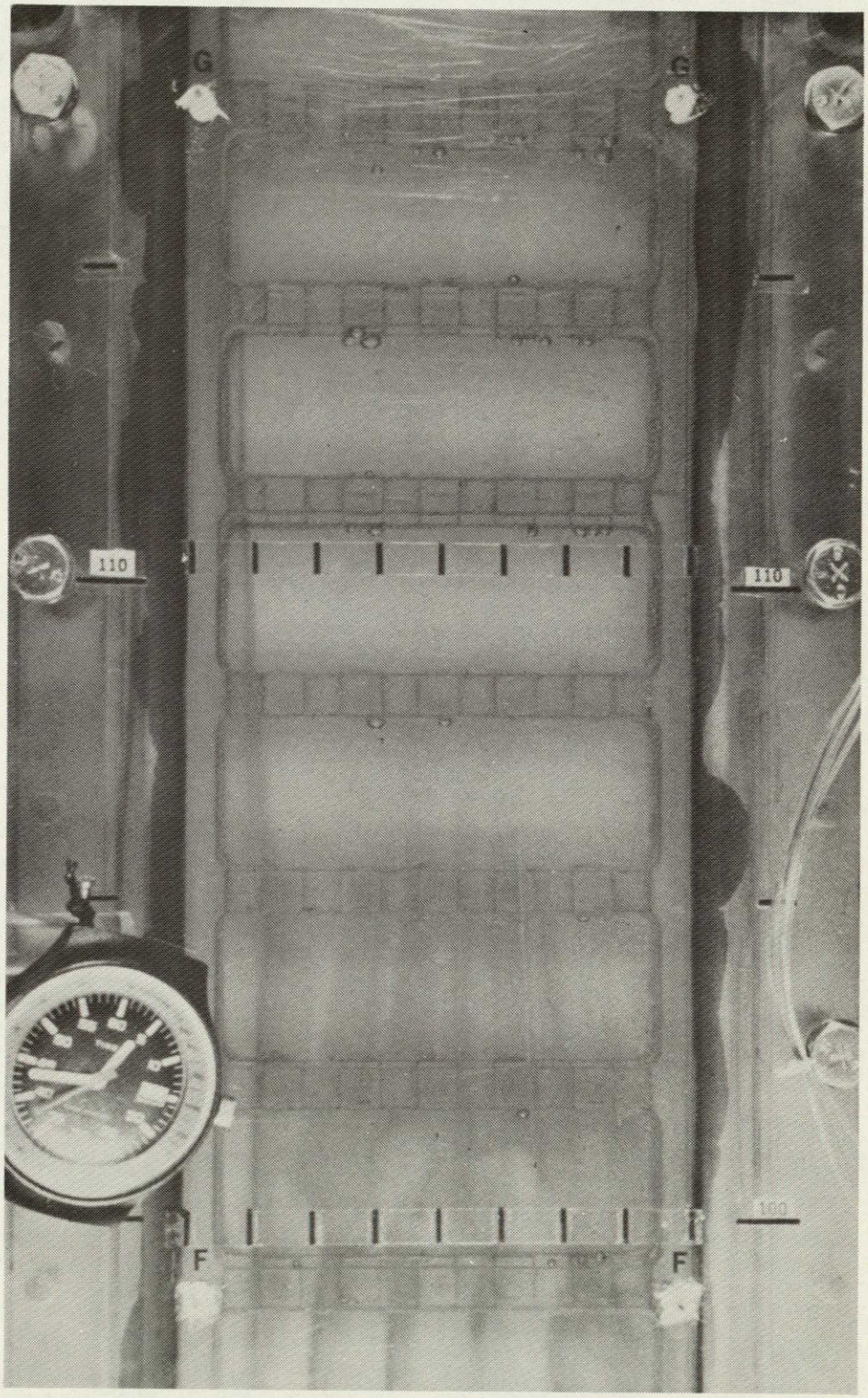

Figure 1–3

VERTICAL CENTERLINE VELOCITY DATA - CM/SEC

(0 VOLTS/ CM)

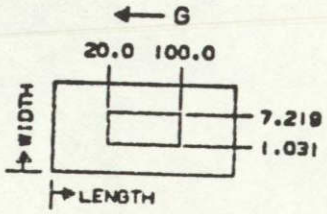

MDAC-STL ELECTROPHORESIS DATA REDUCTION
ORIGINATOR: D.W. RICHMAN 12/74

RUN NO. 1, TEST ENGINEER: C.D. WALKER
BUFFER FLOW 20.0 ML/MIN, INLET TEMP 6.9 C
FIELD STRENGTH 0.0 V/CM
BUFFER VERTICAL CENTERLINE VELOCITY
WIDTH

WIDTH										
8.250										
8.225										
8.200										
8.150										
8.050										
7.850										
7.219		.1805E+00	.2066E+00	.2084E+00	.2038E+00	.1851E+00				
6.188		.1792E+00	.1907E+00	.1937E+00	.1945E+00	.1795E+00				
5.156		.1802E+00	.1942E+00	.1925E+00	.1960E+00	.1820E+00				
4.125		.1809E+00	.1966E+00	.1931E+00	.1944E+00	.1916E+00				
3.094		.1815E+00	.1944E+00	.1923E+00	.1960E+00	.1974E+00				
2.063		.1768E+00	.1863E+00	.1846E+00	.1980E+00	.1989E+00				
1.031		.1748E+00	.1727E+00	.1516E+00	.1600E+00	.2249E+00				
.400										
.200										
.100										
.050										
.025										
0.000										
LENGTH	0.00	5.00	10.00	20.00	40.00	60.00	80.00	100.00	110.00	115.00	120.00

HEIGHTS > DATA = 0

Figure 1–4

PREDICTED VERTICAL CENTERLINE VELOCITY - CM/SEC

(0 VOLTS/CM)

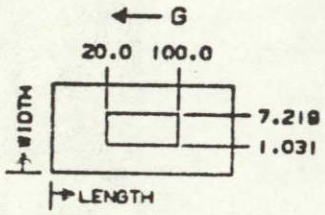

MDAC-STL ELECTROPHORESIS ANALYSIS PROGRAM
ORIGINATOR: D.W. RICHMAN 9/78

RUN NO. 1, TEST ENGINEER: C.D. WALKER
BUFFER FLOW 10.0 ML/MIN, INLET TEMP 6.9 C
FIELD STRENGTH 0.0 V/CM
BUFFER VERTICAL CENTERLINE VELOCITY
WIDTH

WIDTH											
8.250	.1347E+00	0.	0.	0.	0.	0.	0.	0.	0.	0.	0.
8.225	.1347E+00	.6981E-01	.6984E-01	.7006E-01	.7044E-01	.7081E-01	.7114E-01	.7155E-01	.7182E-01	.7211E-01	.1347E+00
8.200	.1347E+00	.1199E+00	.1198E+00	.1201E+00	.1206E+00	.1211E+00	.1216E+00	.1221E+00	.1225E+00	.1229E+00	.1347E+00
8.150	.1347E+00	.1770E+00	.1771E+00	.1773E+00	.1777E+00	.1781E+00	.1785E+00	.1789E+00	.1793E+00	.1796E+00	.1347E+00
8.050	.1347E+00	.2024E+00	.2033E+00	.2034E+00	.2036E+00	.2038E+00	.2040E+00	.2042E+00	.2045E+00	.2051E+00	.1347E+00
7.850	.1347E+00	.2052E+00	.2063E+00	.2065E+00	.2066E+00	.2068E+00	.2069E+00	.2072E+00	.2075E+00	.2081E+00	.1347E+00
7.219	.1347E+00	.2053E+00	.2044E+00	.2065E+00	.2067E+00	.2068E+00	.2070E+00	.2072E+00	.2075E+00	.2082E+00	.1347E+00
6.188	.1347E+00	.2052E+00	.2062E+00	.2063E+00	.2064E+00	.2065E+00	.2067E+00	.2069E+00	.2071E+00	.2077E+00	.1347E+00
5.156	.1347E+00	.2052E+00	.2062E+00	.2063E+00	.2064E+00	.2065E+00	.2067E+00	.2069E+00	.2071E+00	.2077E+00	.1347E+00
4.125	.1347E+00	.2052E+00	.2062E+00	.2063E+00	.2064E+00	.2065E+00	.2067E+00	.2069E+00	.2071E+00	.2077E+00	.1347E+00
3.094	.1347E+00	.2052E+00	.2062E+00	.2063E+00	.2064E+00	.2065E+00	.2067E+00	.2069E+00	.2071E+00	.2077E+00	.1347E+00
2.063	.1347E+00	.2052E+00	.2062E+00	.2063E+00	.2064E+00	.2065E+00	.2067E+00	.2069E+00	.2071E+00	.2077E+00	.1347E+00
1.031	.1347E+00	.2053E+00	.2063E+00	.2065E+00	.2067E+00	.2068E+00	.2070E+00	.2072E+00	.2075E+00	.2081E+00	.1347E+00
.400	.1347E+00	.2052E+00	.2062E+00	.2064E+00	.2066E+00	.2067E+00	.2069E+00	.2071E+00	.2074E+00	.2080E+00	.1347E+00
.200	.1347E+00	.2025E+00	.2033E+00	.2035E+00	.2037E+00	.2039E+00	.2041E+00	.2044E+00	.2047E+00	.2054E+00	.1347E+00
.100	.1347E+00	.1771E+00	.1774E+00	.1778E+00	.1784E+00	.1790E+00	.1795E+00	.1801E+00	.1807E+00	.1812E+00	.1347E+00
.050	.1347E+00	.1199E+00	.1202E+00	.1209E+00	.1217E+00	.1225E+00	.1232E+00	.1239E+00	.1245E+00	.1250E+00	.1347E+00
.025	.1347E+00	.6983E-01	.7014E-01	.7065E-01	.7133E-01	.7191E-01	.7242E-01	.7290E-01	.7328E-01	.7366E-01	.1347E+00
0.000	.1347E+00	0.	0.	0.	0.	0.	0.	0.	0.	0.	0.
LENGTH	0.00	5.00	10.00	20.00	40.00	60.00	80.00	100.00	110.00	115.00	120.00

Figure 1–5

Correlation of test results with the mathematical model requires reduction of the velocity profile data at the same locations within the chamber. This was accomplished by first measuring the profile coordinates for input to a data reduction program. These profile coordinates as a function of time were curve fitted and interpolated by computer at the analytical coordinate values. Velocities were interpolated at approximately one centimeter increments across the width of the chamber and 20 centimeter increments along the length of the chamber. The velocities are close to being constant, as would be expected from the flatness of the velocity profile. Analytical predictions were made for 1463 locations in a half thickness chamber model.

Tests were also conducted to determine horizontal centerline velocity. In these tests seven dye streams were injected into the carrier buffer flow at equal increments across the width of the chamber as shown in Figure 1-6. The tangent of the angle of the stream away from the vertical and the vertical velocity were used to calculate the horizontal velocity. It should be noted that in order to avoid the introduction of error due to the scatter in the vertical velocity test data, a constant analyzed vertical velocity was used for the calculation. Figure 1-6 shows that the dye streams are vertical with no applied electrical field indicating negligible horizontal velocity. The corresponding data reduction is shown in Figure 1-8. The horizontal velocities from the reduced test data are generally about 10^{-4} cm/sec in magnitude and either positive or negative in sign, indicating the limiting accuracy of the test method. The corresponding analytical predictions of velocity showed even lower values indicating residuals in the iterated solution. Figure 1-7 shows the dye streams near mid-chamber with an applied electrical field of 10 volts/cm. The corresponding data reduction is shown in Figure 1-9 where the test velocities approximate the predicted value of 0.002 cm/sec. Discrepancies are due to the values being almost of the same order of magnitude as the accuracy of the test method, as illustrated by the zero voltage case.

DYE STREAMS (0 VOLTS/CM)

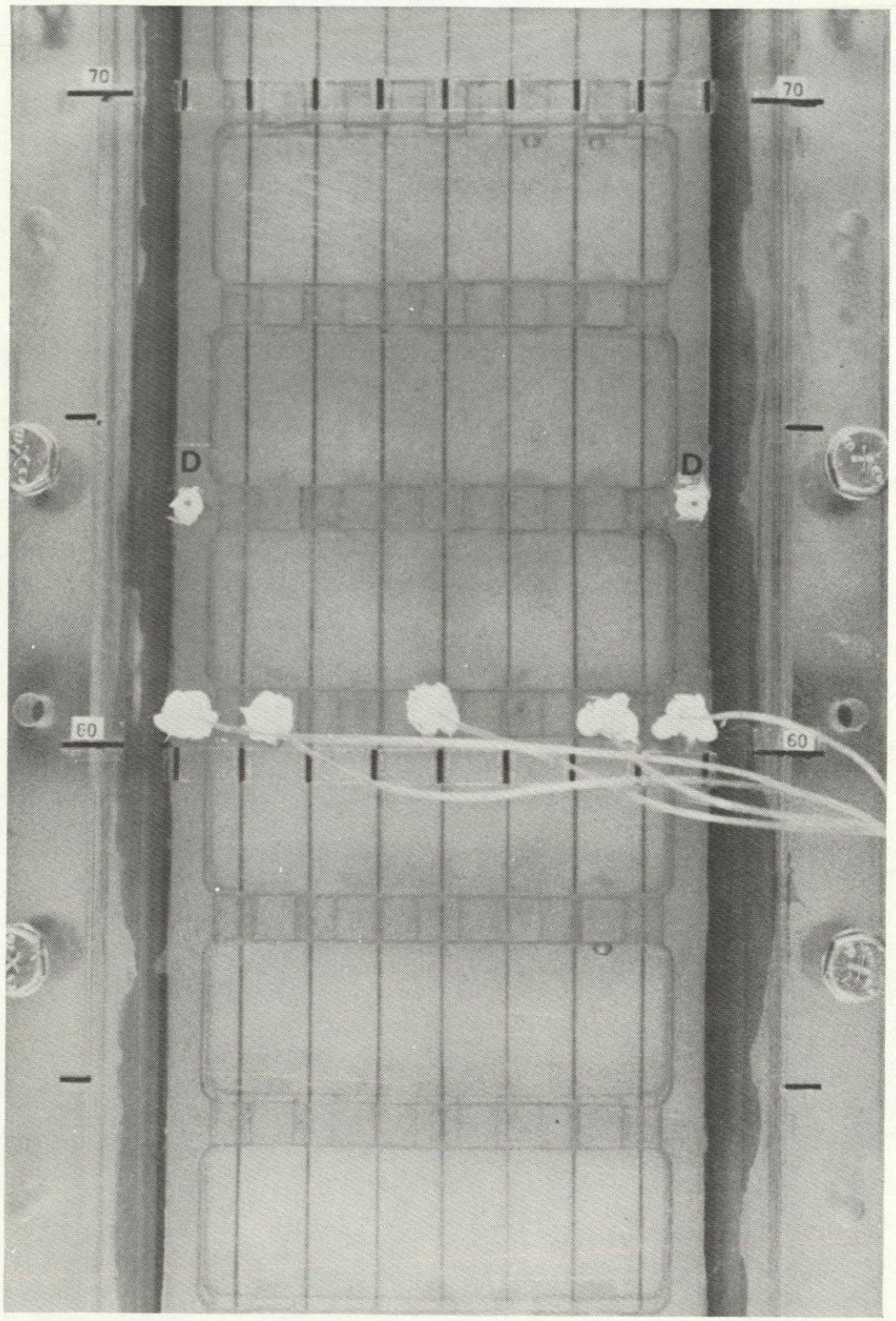

Figure 1–6

DYE STREAMS (10 VOLTS/CM)

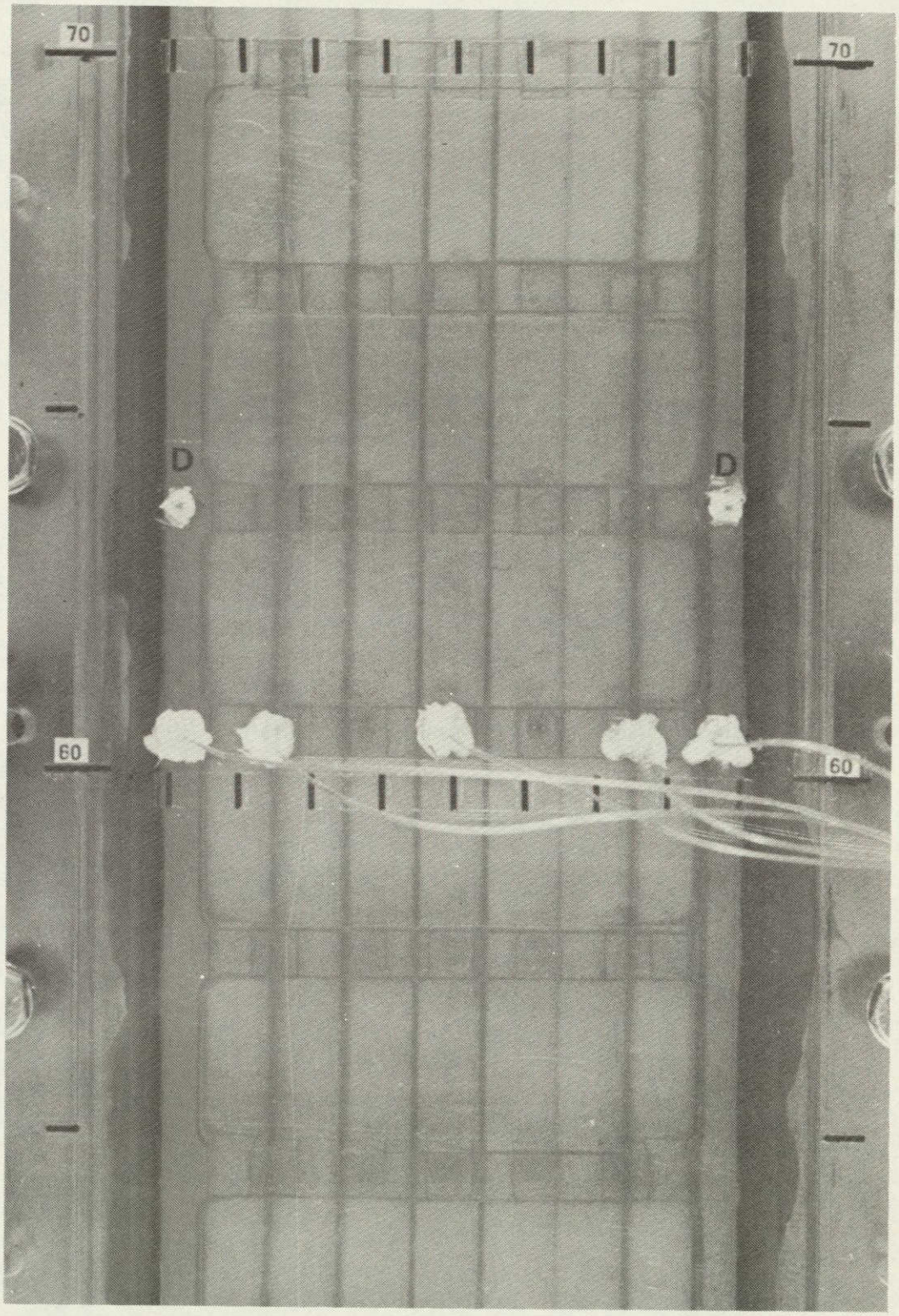

Figure 1–7

HORIZONTAL CENTERLINE VELOCITY DATA - CM/SEC

(0 VOLTS/CM)

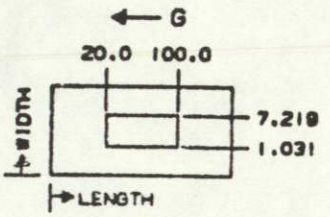

MDAC-STL ELECTROPHORESIS DATA REDUCTION
ORIGINATOR: D.W. RICHMAN 12/78

RUN NO. 16, TEST ENGINEER: C.D. WALKER
BUFFER FLOW 40.0 ML/MIN, INLET TEMP 7.4 C
FIELD STRENGTH 0.0 V/CM
BUFFER HORIZONTAL CENTERLINE VELOCITY

WIDTH						
8.250						
8.225						
8.200						
8.150						
8.050						
7.850						
7.219	0.	0.	.2929E-03	0.	0.	
6.188	.2155E-02	.1327E-02	-.2967E-03	-.1092E-02	-.3514E-03	
5.156	.2550E-02	.1112E-02	-.2021E-03	-.1197E-02	-.1896E-02	
4.125	.1848E-02	.1312E-02	-.3247E-03	-.1704E-02	-.1977E-02	
3.094	.4641E-02	.1365E-02	-.1047E-02	-.1904E-02	-.2124E-02	
2.063	.4447E-02	.7821E-03	-.8932E-03	-.1097E-02	-.1737E-02	
1.031	0.	0.	0.	0.	-.9203E-03	
.400						
.200						
.100						
.050						
.025						
0.000						

LENGTH	0.00	5.00	10.00	20.00	40.00	60.00	80.00	100.00	110.00	115.00	120.00

WIDTHS OUTSIDE DATA = 0

Figure 1—8

HORIZONTAL CENTERLINE VELOCITY DATA - CM/SEC

(10 VOLTS/CM)

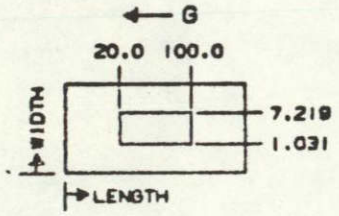

MDAC-STL ELECTROPHORESIS DATA REDUCTION
ORIGINATOR: D.W. RICHMAN 12/78

RUN NO. 17, TEST ENGINEER: C.D. WALKER
BUFFER FLOW 40.0 ML/MIN, INLET TEMP 6.9 C
FIELD STRENGTH 10.0 V/CM
BUFFER HORIZONTAL CENTERLINE VELOCITY

WIDTH						
8.250						
8.225						
8.200						
8.150						
8.050						
7.850						
7.219	0.	.3196E-02	.1977E-02	.2792E-03	.4134E-03	
6.188	.6804E-02	.3633E-02	.1473E-02	.1607E-02	.2268E-02	
5.156	.7117E-02	.2964E-02	.8563E-03	.1240E-02	.2141E-02	
4.125	.6525E-02	.2884E-02	.1083E-02	.9015E-03	.2345E-03	
3.094	.5587E-02	.2962E-02	.1351E-02	.9459E-03	.2644E-03	
2.063	.6066E-02	.3071E-02	.1654E-02	.1042E-02	.2764E-03	
1.031	0.	0.	0.	0.	0.	
.400						
.200						
.100						
.050						
.025						
0.000						

LENGTH	0.00	5.00	10.00	20.00	40.00	60.00	80.00	100.00	110.00	115.00	120.00

WIDTHS OUTSIDE DATA = 0

Figure 1—9

1.2 EFFECTS OF GRAVITY ON SAMPLE

The purpose of Task 2.0 was to determine the effects of gravity on the particle streams during electrophoresis. The limiting effects of gravity on sample streams in upward flow are illustrated by Figure 1-10. For a sample that is heavier than the carrier buffer, the sample falls back around the sample input tube. A sample stream that is lighter than the carrier buffer, however, is buoyed

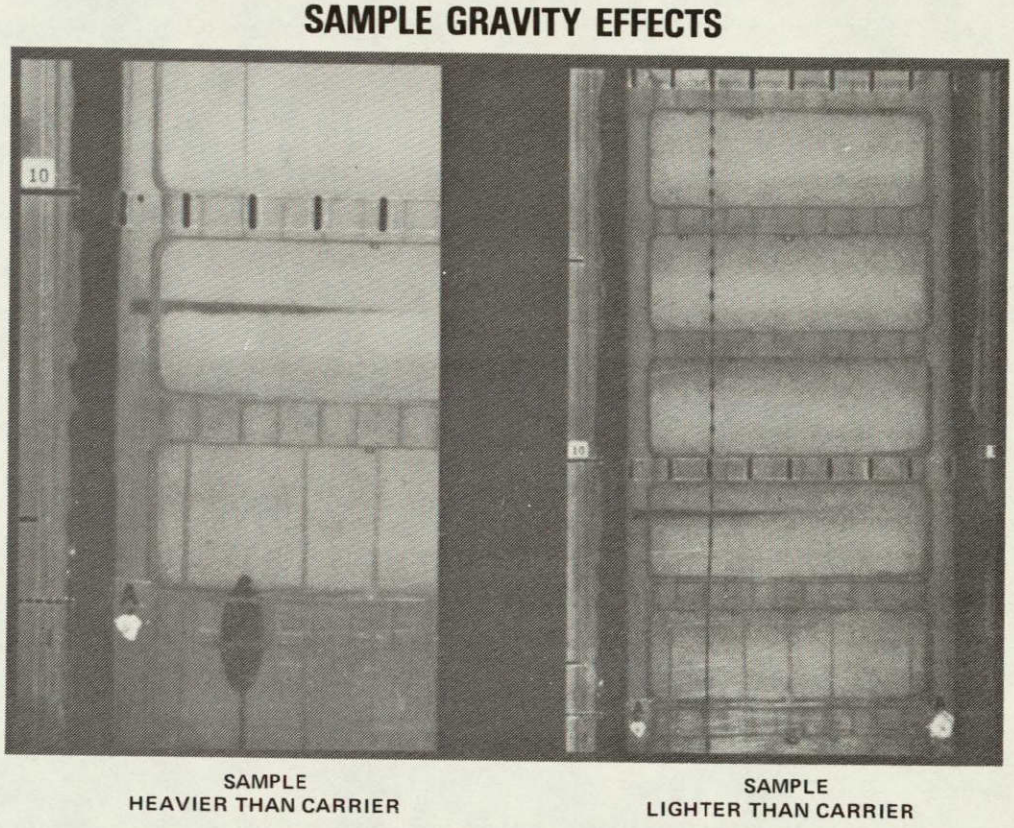

Figure 1–10

up in the flow and breaks up into beads. To assure realism and applicability of the results, biological materials, both proteins and cells, were used for these experiments. The selected materials had specific gravities greater than unity, as do most biological materials. This meant that fall back limited, for example, sample protein concentrations, to about 0.15% by weight per unit volume. To obtain good laminar sample streams, the protein samples were diluted to 0.12% maximum protein by weight.

The effects of gravity persist, however, even after the sample is diluted. The effect of gravity on sample streams that are heavier than the surrounding buffer in upward flow is to increase residence time and to widen the particle streams. Widening of the particle streams can cause overlapping so that the desired separation can not be obtained.

The mechanism involved in these gravity effects is that a negative buoyant force results on the particle when the buffer is displaced by a particle with a higher specific gravity. For equilibrium, this force must be balanced by the viscous shear due to a particle velocity that is less than that of the surrounding buffer. For particles the size of proteins and to some extent for cells, the velocity difference is negligible. However, for equilibrium of the particle stream with the surrounding buffer the force of viscous shear on the outside of the stream must be equal and opposite to the sum of the buoyant forces on the particles within the stream. For particle specific gravities higher than buffer specific gravity in upward flow, the particle stream velocity will be less than that of the surrounding buffer. Particle stream widening occurs under these conditions, because the particles with lower velocities will have longer residence times and greater lateral movement than particles with higher velocities near the edges of the particle stream. In upward flow therefore, the middle of the sample continuously overtakes the leading edge, while the trailing edge falls farther and farther behind in the lateral direction. The expected result is that the apparent mobility of the particle stream will increase with both increasing concentration and decreasing buffer flow rate.

Two proteins were separated at various concentrations and flow rates to demonstrate the gravity effects. The two proteins used were human albumin and human fibrinogen. In preparation for the separation of a mixture of fibrinogen and albumin, electrophoresis was performed on each of the proteins using a range of field strength and buffer flow rates. The test data was correlated with the mathematical model by using the apparent electrophoretic mobility at the maximum flow and minimum concentration as a constant input. The three dimensional mathematical model used for this correlation is similar to the buffer flow model except that it calculates conditions at 1001 points in the vicinity of the particle stream and it includes both particle diffusion and gravity effects. Test versus predicted outlet concentration distribution for human albumin and human fibrinogen are shown in Figure 1-11.

In general, the predicted spreading of the samples is less than for the test data, both with and without applied electrical field, indicating that this spreading is a characteristic of the MDAC-St. Louis chamber. In addition, the smaller predicted movement of the proteins with the field applied is caused by actual residence times being greater than predicted, as evidenced by the buffer gravity effects data correlation.

Predicted gravity effects on electrophoresis of mixed proteins are shown in Figure 1-12. The greater movement under electrophoresis in one-g is caused by the increased residence times due to the particle streams slipping with respect to the buffer. Widening of the particle streams is not evident, however, because each of the separating streams was only at a fraction of the limiting concentration.

The effects of gravity on cell samples at varying concentrations and flow rates were demonstrated using lymphocytes. Test versus predicted outlet concentration distributions for 33H human lymphocytes are shown in Figure 1-13. Again, the predicted spreading of the sample is less than the test data, both with and without electrical field, indicating that the spreading is characteristic of the chamber. And as in the case of proteins, the predicted movement is less than the measured movement due to the actual residence time being greater than predicted.

Predicted gravity effects on electrophoresis of cells are shown in Figure 1-14. The greater movement under electrophoresis in one-g is caused by the increased residence time due to the particle streams slipping with respect to the buffer. As in the case of proteins, widening of the particle streams would probably become evident at higher concentrations or at greater electrophoretic movement.

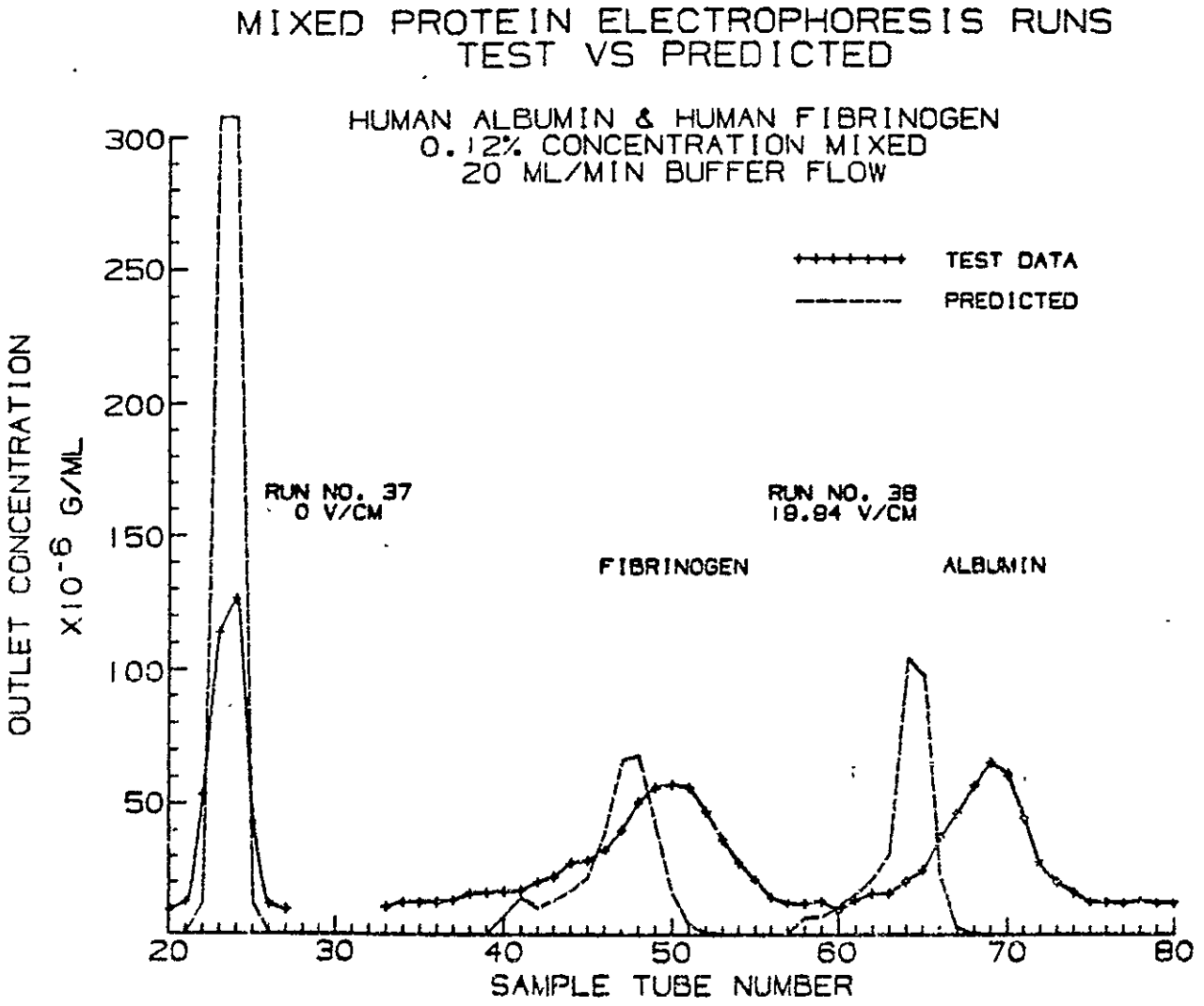
MIXED PROTEIN ELECTROPHORESIS RUNS
TEST VS PREDICTED
HUMAN ALBUMIN & HUMAN FIBRINOGEN
0.12% CONCENTRATION MIXED
20 ML/MIN BUFFER FLOW
TEST DATA
PREDICTED
RUN NO. 37
0 V/CM
RUN NO. 38
19.94 V/CM
FIBRINOGEN
ALBUMIN
OUTLET CONCENTRATION
X10-6 G/ML
300
250
200
150
100
50
20
30
40
50
60
70
80
SAMPLE TUBE NUMBER

FIGURE I-11

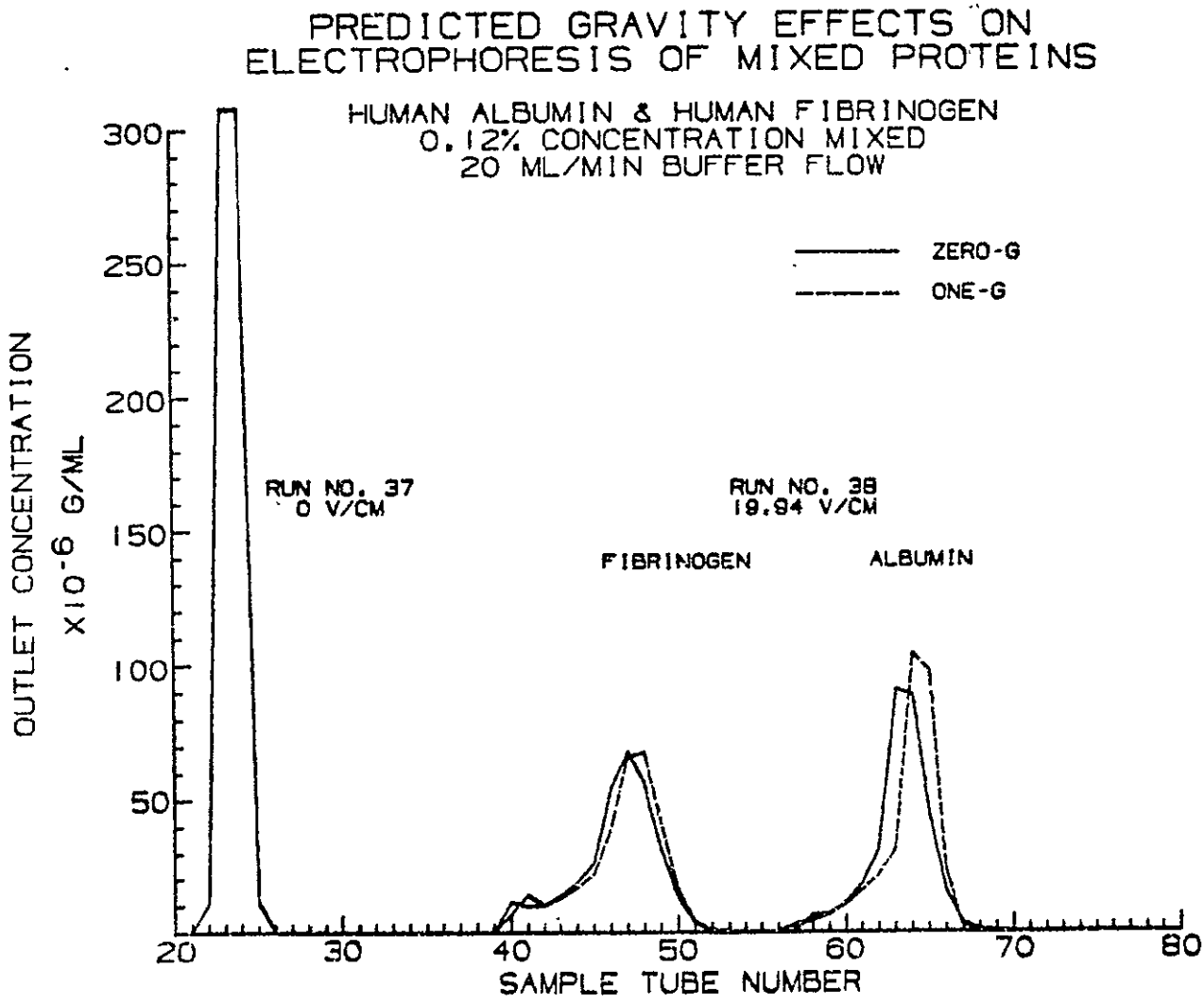
PREDICTED GRAVITY EFFECTS ON
ELECTROPHORESIS OF MIXED PROTEINS
HUMAN ALBUMIN & HUMAN FIBRINOGEN
0.12% CONCENTRATION MIXED
20 ML/MIN BUFFER FLOW
ZERO-G
ONE-G
RUN NO. 37
0 V/CM
RUN NO. 38
19.94 V/CM
FIBRINOGEN
ALBUMIN
OUTLET CONCENTRATION
X10-6 G/ML
300
250
200
150
100
50
20
30
40
50
60
70
80
SAMPLE TUBE NUMBER

FIGURE 1-12

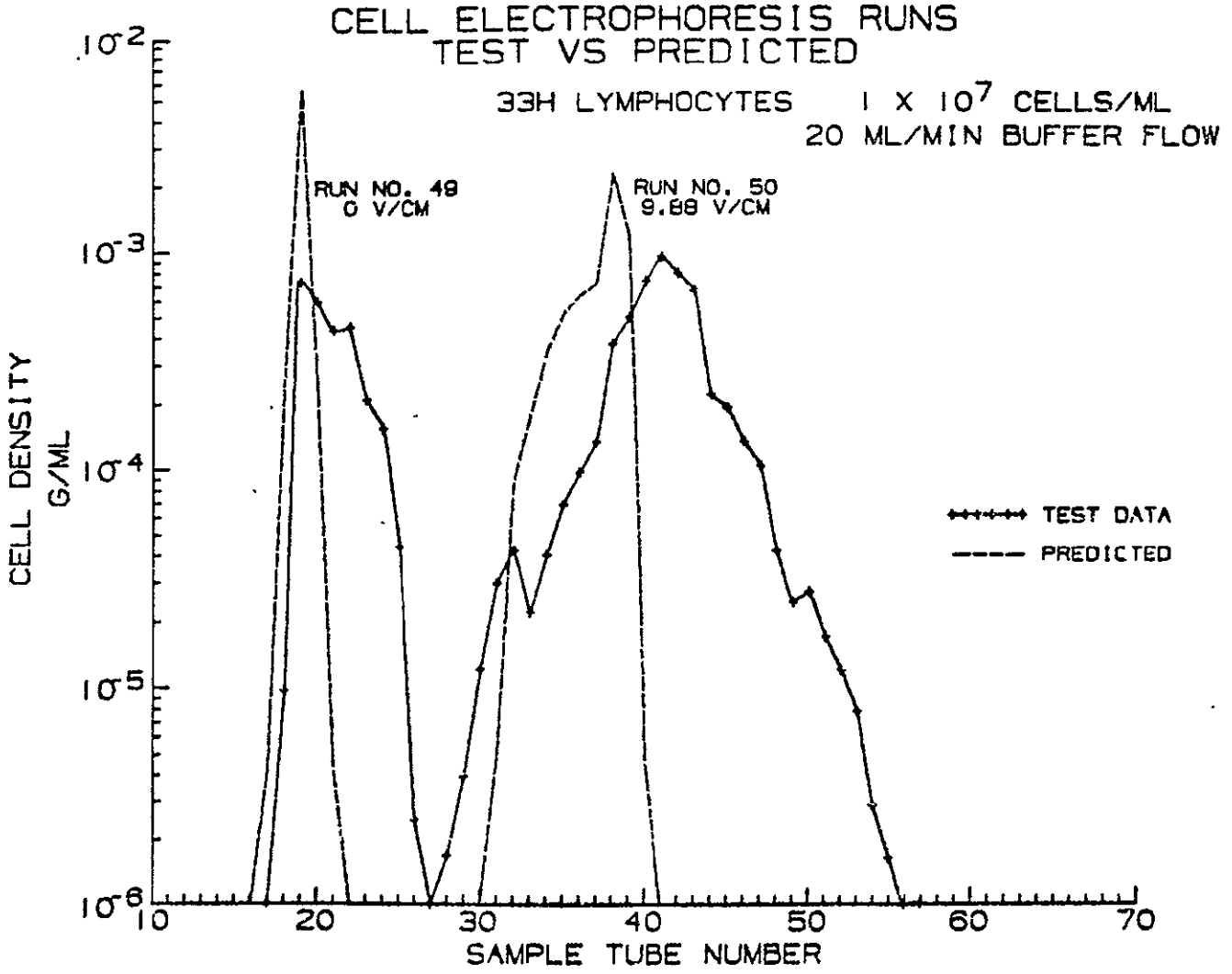
CELL ELECTROPHORESIS RUNS
TEST VS PREDICTED
33H LYMPHOCYTES 1 X 10^7 CELLS/ML
20 ML/MIN BUFFER FLOW
RUN NO. 49
0 V/CM
RUN NO. 50
9.88 V/CM
TEST DATA
PREDICTED
CELL DENSITY
G/ML
10^-2
10^-3
10^-4
10^-5
10^-6
10
20
30
40
50
60
70
SAMPLE TUBE NUMBER

FIGURE 1-13

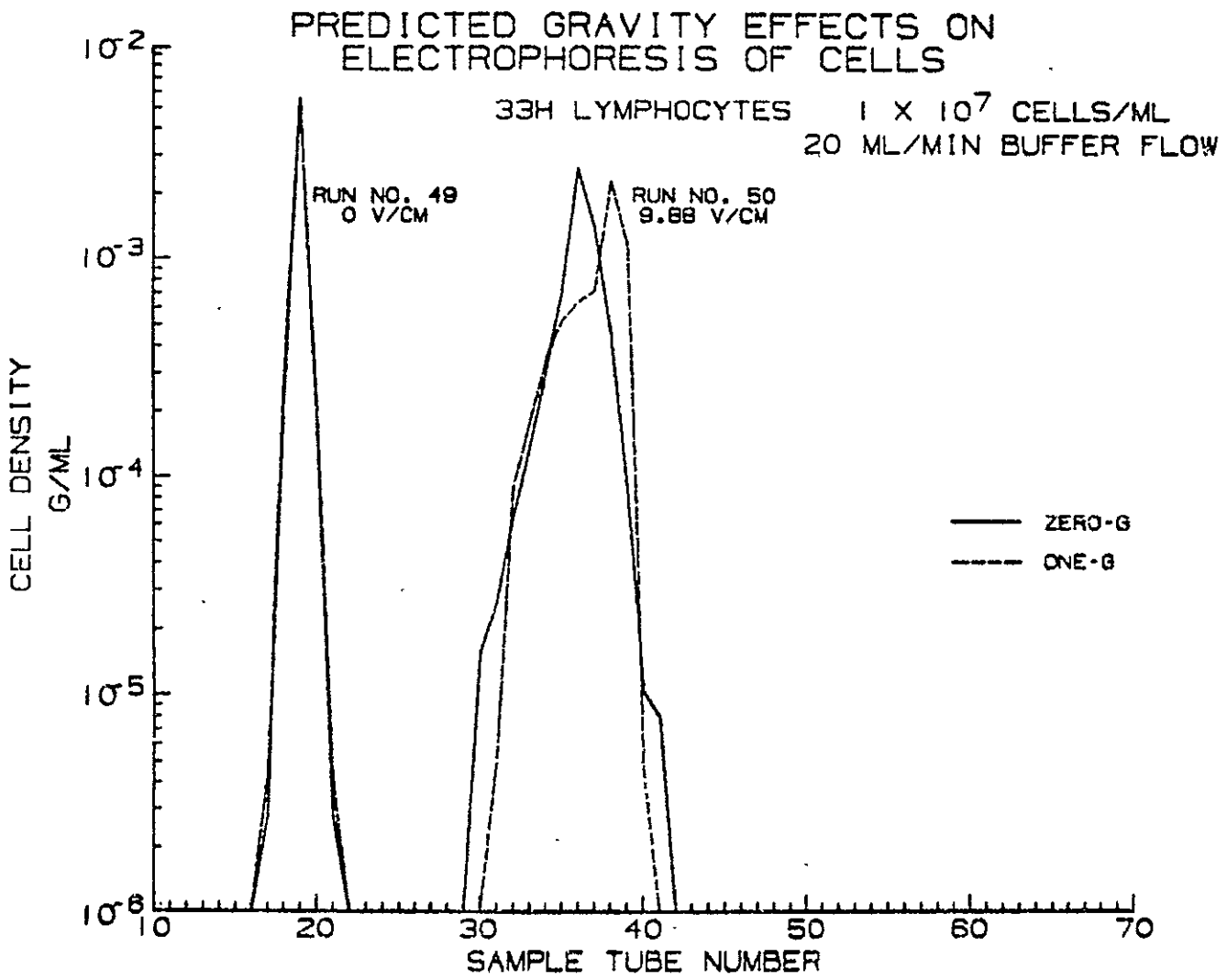
PREDICTED GRAVITY EFFECTS ON
ELECTROPHORESIS OF CELLS
33H LYMPHOCYTES 1 X 10^7 CELLS/ML
20 ML/MIN BUFFER FLOW
RUN NO. 49
0 V/CM
RUN NO. 50
9.88 V/CM
ZERO-G
ONE-G
CELL DENSITY
G/ML
10^-2
10^-3
10^-4
10^-5
10^-6
10
20
30
40
50
60
70
SAMPLE TUBE NUMBER

FIGURE 1-14

1.3 EFFECTS OF SAMPLE CONCENTRATION ON ELECTROPHORETIC MOBILITY

The purpose of Task 3.0 of this study was to determine if sample concentration has a significant effect on the electrophoretic mobility of the individual protein components of the sample. This is of interest because previous MDAC-St. Louis studies showed that only very dilute samples can be processed in a one-g environment by free flow electrophoresis, and that throughput in the microgravity environment could be increased substantially by processing more highly concentrated samples. Instead of diluting human plasma 70 times with water, for example, it may be possible to process concentrated plasma samples thus increasing the sample concentration from about 0.1% on Earth to 28% or even higher in the micro-gravity space environment.

Questions have arisen, however, concerning protein-protein interaction at concentrations above 0.1% which may change the electrophoretic mobility of individual proteins or in some other way interfere with their electrophoretic separation. If interfering interactions do occur, then the benefits of purity, attainable in space, would be offset by poor resolution as a result of these protein interactions.

In order to detect the possible effects of sample concentration on electrophoretic mobility three common ground based electrophoretic procedures were employed and the mobilities of various proteins in human plasma at several concentrations ranging from 0.109% to 28% total protein were studied.

Two of these methods, agar gel plate and polyacrylimide disc gel electrophoresis, gave consistent reliable test results and were used to evaluate mobilities of the various proteins. A third method, using cellulose acetate strip electrophoresis provided erratic data from day to day and was not used for evaluation.

Test results obtained using agar gel plate electrophoresis are summarized in Figure 1-15 and 1-16. No significant differences in protein mobilities were noted at any of the concentrations tested over a range of 0.875% to 28%.

MIGRATION OF PLASMA PROTEINS ON CORNING AGAR GEL PLATES
RUN 1

% PLASMA CONCENTRATION	PROTEIN MEASURED					
	ALBUMIN	α-1 GLOBULIN	α-2 GLOBULIN	β-1 GLOBULIN	FIBRINOGEN	γ GLOBULIN
	DISTANCE MOVED (cm) AT 85 VOLTS; FIELD STRENGTH 15 VOLTS/cm					
7.0	1.8	1.5	1.0	0.60	0.25	—0 25
3 5	1 8	1.5	1.0	0.60	0.25	—0.25
1.75	1.8	N.V.	1.0	0.60	0.25	N.V.
0.875	1 8	N.V.	N.V	0.55	0.25	N.V.

N.V. — BANDS WERE NOT VISIBLE DUE TO DILUTION

Figure 1—15

MIGRATION OF PLASMA PROTEINS ON CORNING AGAR GEL PLATES
RUN 2

% PLASMA CONCENTRATION	PROTEIN MEASURED					
	ALBUMIN	α-1 GLOBULIN	α-2 GLOBULIN	β-1 GLOBULIN	FIBRINOGEN	γ GLOBULIN
	DISTANCE MOVED (cm) AT 85 VOLTS; FIELD STRENGTH 15 VOLTS/cm					
7.0	1.9	1.55	1.0	0.65	0.25	—0.25
28.0	1 9	1.55	1.0	0.65	0.25	—0.25
7.0 (REDILUTED)	1.9	1.55	1.0	0.65	0.25	—0.25

Figure 1—16.

Results obtained using polyacrylamide gel electrophoresis are shown in Figure 1-17. In this procedure one anomaly occured. Albumin appeared to have increased mobility in the higher concentrated samples. However, this apparent increased mobility is probably the result of an overloading of the gel capacity and resultant exclusion of a portion of the albumin molecules from the molecular sieve action of the gel.

MIGRATION OF PLASMA PROTEINS IN POLYACRYLAMIDE DISC GEL ELECTROPHORESIS

% PLASMA CONCENTRATION	PROTEIN MEASURED					
	PRE-ALBUMIN	ALBUMIN	α-1 GLOBULIN	β-1 GLOBULINS (HEMOGLOBIN AND TRANSFERRIN)	α-2 GLOBULIN	γ GLOBULIN
	DISTANCE MOVED (cm) AT 150 VOLTS, FIELD STRENGTH, 12 VOLTS/cm					
7	5.8	4.4	3 3	2.1	1.4	0
3.5	5.8	4 4	3.3	2.2	1.4	0
1 75	N.V.	4 3	3.4	2.3	1.4	0
0.875	N.V.	4.2	3 3	2.3	1.4	0
0.437	N.V.	4.2	N.V.	2.2	N.V.	0
0.218	N.V.	4.2	N.V.	2.2	N.V.	0
0.109	N V.	4.1	N.V.	2.1	N.V.	0

N V — NOT VISIBLE DUE TO DILUTION

Figure 1—17

1.4 CONCLUSIONS AND RECOMMENDATIONS

Principal conclusions of this investigation are that the carrier buffer flow is affected by gravity induced thermal convection and that the movement of the separating particle streams is affected by gravity induced buoyant forces. Although much has been written about the fluid convection effects, the gravity effect on the particle streams is probably more important. It is this effect that limits the allowable density difference between the particle stream and the surrounding buffer to a fraction of a percent. And even within this allowable range of density difference, velocity variations within the stream cause widening of the particle streams during electrophoresis. Widening of the particle streams can cause the streams to overlap, limiting separation capability.

One finding of this investigation is that mathematical models, if they include the gravity induced buoyancy forces, should be able to effectively predict electrophoresis chamber separation performance. Additional work is recommended in the areas of correlation with the upward flow velocities with field applied and in testing to reliably determine wall electroosmotic flow velocities using microelectrophoresis for the tested combinations of wall material and buffers.

Another finding of this investigation is that sample concentration, using ground based electrophoresis procedures does not affect protein electrophoretic mobility over the range of 0.1% to 28%.

This investigation should provide a starting point for meaningful comparisons of free-flow electrophoresis chamber performance, i.e. output and separation capability, on the earth and under microgravity conditions and additional work in this area is planned.

2.0 CHARACTERIZATION METHOD

2.0 CHARACTERIZATION METHOD

Investigation of the free flow electrophoretic process required a method of demonstrating gravity effects on both the buffer and the sample and correlating the results with mathematical model predictions. The method selected for the buffer gravity effects demonstration was photographic recording of either horizontal dye front or vertical dye stream coordinates versus time and numerical differentiation to determine velocity distributions. The method selected for sample gravity effects demonstration was more straight forward, consisting of assaying the outlet tube concentration distributions for comparison with analytical predictions. In this section background information on the process is presented and details of the characterization method are discussed.

2.1 FREE FLOW ELECTROPHORETIC PROCESS

The free flow electrophretic process as shown in Figure 2-1 is a combination of several phenomena. In free flow electrophoresis the sample and a carrier buffer are continuously admitted to a chamber. An electric field is applied perpendicular to the direction of flow. The force of the field on charged particles of the

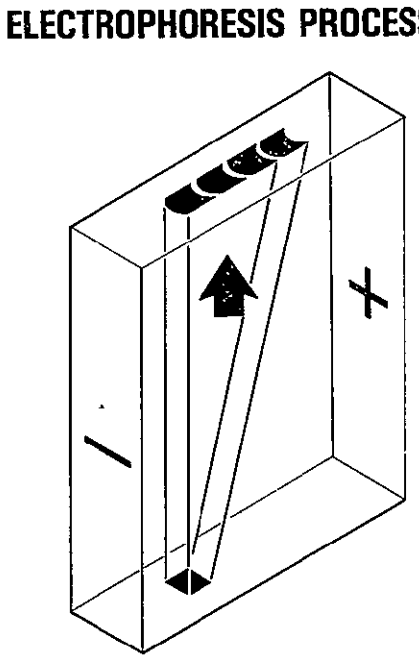

Figure 2–1

sample rapidly accelerates them to the terminal velocity for equilibrium with the viscous drag force. The distance particles travel in the direction of the electrical field is proportional to their residence time within the chamber. The increased residence time for particles near the wall due to fluid friction as illustrated in Figure 2-2 results in increased deflection near the wall. This distortion was described by Strickler and Sacks (4) as the crescent phenomenon.

ELECTROPHORESIS CRESCENT DISTORTION

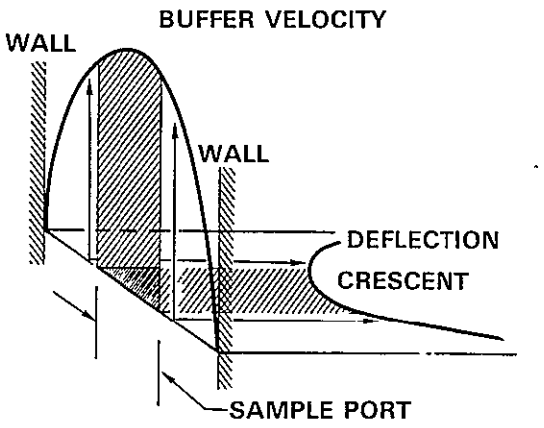

Figure 2–2

Electroosmosis is an effect of chamber wall material and can either reduce or exaggerate crescent phenomenon (distortion) as shown in Figure 2-3. Electroosmosis is dependent on the potential difference between the wall and the buffer. Since the wall is negatively charged, positive ions in the buffer are attracted by Coulomb forces. This causes the buffer very near the wall to have a positive charge differential relative to the bulk charge of the buffer and a force differential in favor of migration toward the negatively charged electrode. The force differential is proportional to the zeta potential (wall material characteristic) which is the potential difference between the surface of the double layer and the bulk of the buffer solution. The force is in equilibrium with the shear force due to the large velocity gradient at the wall. Because the chamber ends are closed, the buffer migrating toward the negatively charged electrode must circulate back along

the chamber centerline. The resulting velocity profile is parabolic, because the boundary conditions are the same as Poiseuille flow, i.e. constant wall velocity and constant pressure across the chamber. In this case, however, the velocity near the wall is not zero and the integral of velocity across the chamber is zero to satify conservation of mass. For these boundary conditions the chamber centerline electroosmotic velocity is the product of - 0.5 times the wall electroosmotic velocity, while the velocity is zero at a distance about 20% of chamber thickness from the walls.

ELECTROOSMOSIS CAN REDUCE CRESCENT DISTORTION

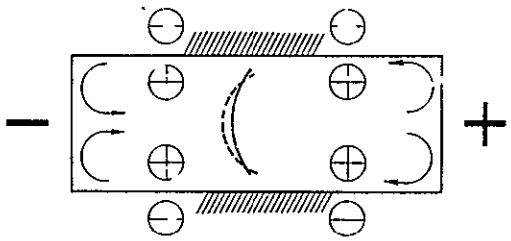

Figure 2–3

The other principal distortions are band - spreading effects. Recognized band - spreading effects are thermal diffusion, microheterogeneity, electrodiffusion, eddy migration and electrosorptive spreading (5). Of these, electrodiffusion is negligible for even moderate residence times and eddy migration does not occur because of lack of a supporting medium in free flow electrophoresis.

For operation on Earth, gravity affects the electrophoretic process as a result of buoyancy forces. These forces limit, (1) the allowable Joule heating in the buffer, because of convection currents, (2) the concentration of soluble species in samples because of large sample/buffer velocity differences, and (3) the movement of insoluble particles in samples because of sedimentation.

2.2 BUFFER GRAVITY EFFECTS

The method selected for the buffer gravity effects demonstration was photographic recording of either horizontal dye front or vertical dye stream coordinates versus

time and numerical differentiation to determine velocity differences. Advantages of this method include both the straight forward method of implementation and visibility of data in the raw integral form of position versus time. Such visible data was later to prove invaluable in providing evidence of velocity variations that were not evident in the reduced data. Another advantage of using horizontal dye fronts and vertical dye streams is that they facilitate obtaining the horizontal and vertical components of velocity. Obtaining the vertical component of velocity is important because the forces of gravity on the carrier buffer fluid, which are caused by temperature dependent density differences, manifest themselves as additive convective velocity increments. These vertical velocity increments in the three dimensional case also result in convection cells which have horizontal velocity components. Disadvantages of using dye fronts to visualize fluid motion include the fact that most dyes are not neutrally buoyant. This means that dyes that are heavier than the buffer, like the Coomassive Brilliant Blue R250 used in these tests, will increase the local density of the carrier fluid and induce downward slippage and attendant error in velocity determination. Another disadvantage is that most dyes including the dye used in these tests have significant electrophoretic mobility which must be accounted for in reducing the data.

Vertical velocity distribution was determined by photographically recording the coordinates of a horizontal dye front versus time. The front was created by tieing into the buffer inlet plane and injecting dye dissolved in buffer over an interval of a few seconds. This resulted in a well defined front as shown in Figure 1-2 for an applied field of zero volts. The results are what would be expected for Poiseuille flow, that is flow between parallel plates. To calculate vertical velocity in this case, the vertical position as a function of time is approximated by a second order polynomial fit. This polynomial is then numerically differentiated to find velocity. Data typical of the results are shown in Figure 1-4. Here velocities were calculated at about one centimeter increments across the chamber and at five increments along its length. When a field is applied to the chamber, the mobility of the dye requires that the calculation procedure be modified. Here the velocity profiles are not interpolated along a vertical line, but along a line inclined at an angle whose tangent is the electrophoretic velocity divided by the vertical velocity. This, of course,

results in an iterative procedure to calculate vertical velocity. Electrophoretic mobility of the R250 Brilliant Blue dye was determined from its movement in our chamber after the movement due to electroosmosis was subtracted. The reference data for determining electroosmotic movement was the work that Vanderhoff performed for NASA's Marshall Space Flight Center (MSFC) that gave an apparent electroosmotic mobility for a borate buffer/Lexan wall combination at the wall of -10.7×10^{-4} cm^2/volt-sec (6). In comparative testing the motion of R250 Coomassie Brilliant Blue dye was determined to be essentially the same in barbital and borate buffer. It was then assumed that both the electrophoretic movement and the electroosmotic movement for the R250 Coomassie Brilliant Blue were proportional to the total movement in each buffer and based on this, the electrophoretic mobility of R250 Coomassie Brilliant Blue dye and the wall electroosmotic mobility for the barbital buffer/Lexan wall combination were calculated to be 6.5×10^{-4} cm^2/volt-sec and -10.2×10^{-4} cm^2/volt-sec, respectively.

Horizontal velocity distribution, which is primarily due to osmotic flow, was determined by photographically recording the coordinates of vertical dye streams. These dye streams were injected into the buffer flow through seven capillary sample tubes near the bottom of the chamber and equally spaced across its width. A typical pattern with no field applied is as shown in Figure 1-6. The tangent of the stream angle away from the vertical to the right is equal to the horizontal velocity divided by the vertical velocity. It was at first anticipated that the vertical velocity used to calculate the horizontal velocity would be determined from the corresponding horizontal dye front test; however, noise in the data required that an assumed analytical value be substituted. With voltage, a typical pattern is as shown in Figure 1-8. To reduce this data it is necessary to subtract the effect of dye electrophoretic mobility, in this case the electrophoretic velocity must be subtracted from the apparent horizontal velocity.

The results of the horizontal and vertical velocity data reduction were compared with analytical results from an MDAC-STL developed three dimensional mathematical model of chamber flow. This model is based on finite difference approximations to the equations of motion and the continuity equation as presented in Figure 2-4. The equations of motion were solved subject to the simplifying assumptions given in Figure 2-5. The principal assumption is that density is assumed to be

EQUATION OF MOTION

$$\overline{F} = m\overline{a}$$

$$X - \frac{\partial p}{\partial x} - \left(\frac{\partial \tau_{xx}}{\partial x} + \frac{\partial \tau_{yx}}{\partial y} + \frac{\partial \tau_{zx}}{\partial z}\right) = \rho \frac{Du}{Dt}$$

X COMPONENT OF BODY FORCE PER UNIT VOLUME	X COMPONENT OF PRESSURE FORCE PER UNIT VOLUME	X COMPONENT OF VISCOUS FORCE PER UNIT VOLUME	MASS PER UNIT VOLUME TIMES X COMPONENT OF ACCELERATION

$$Y - \frac{\partial p}{\partial y} - \left(\frac{\partial \tau_{xy}}{\partial x} + \frac{\partial \tau_{yy}}{\partial y} + \frac{\partial \tau_{zy}}{\partial z}\right) = \rho \frac{Dv}{Dt}$$

$$Z - \frac{\partial p}{\partial z} - \left(\frac{\partial \tau_{xz}}{\partial x} + \frac{\partial \tau_{yz}}{\partial y} + \frac{\partial \tau_{zz}}{\partial z}\right) = \rho \frac{Dw}{Dt}$$

WHERE

$$\tau_{xx} = -2\mu \frac{\partial u}{\partial x} + \frac{2}{3}\mu \left(\overline{\nabla} \cdot \overline{V}\right)$$

$$\tau_{yy} = -2\mu \frac{\partial v}{\partial y} + \frac{2}{3}\mu \left(\overline{\nabla} \cdot \overline{V}\right)$$

$$\tau_{zz} = -2\mu \frac{\partial w}{\partial z} + \frac{2}{3}\mu \left(\overline{\nabla} \cdot \overline{V}\right)$$

$$\tau_{xy} = \tau_{yx} = -\mu \left(\frac{\partial u}{\partial y} + \frac{\partial v}{\partial x}\right)$$

$$\tau_{yz} = \tau_{zy} = -\mu \left(\frac{\partial v}{\partial z} + \frac{\partial w}{\partial y}\right)$$

$$\tau_{zx} = \tau_{xz} = -\mu \left(\frac{\partial w}{\partial x} + \frac{\partial u}{\partial z}\right)$$

FIGURE 2-4

EQUATION OF MOTION (CONT.)

$$X - \frac{\partial p}{\partial x} + \frac{\partial}{\partial x}\left[2\mu \frac{\partial u}{\partial x} - \frac{2}{3}\mu\,(\bar{\nabla} \cdot \bar{V})\right]$$

$$+ \frac{\partial}{\partial y}\left[\mu\left(\frac{\partial u}{\partial y} + \frac{\partial v}{\partial x}\right)\right] + \frac{\partial}{\partial z}\left[\mu\left(\frac{\partial w}{\partial x} + \frac{\partial u}{\partial z}\right)\right] = \rho \frac{Du}{Dt}$$

$$Y - \frac{\partial p}{\partial y} + \frac{\partial}{\partial x}\left[\mu\left(\frac{\partial v}{\partial x} + \frac{\partial u}{\partial y}\right)\right] + \frac{\partial}{\partial y}\left[2\mu \frac{\partial v}{\partial y} - \frac{2}{3}\mu\,(\bar{\nabla} \cdot \bar{V})\right] + \frac{\partial}{\partial z}\left[\mu\left(\frac{\partial w}{\partial y} + \frac{\partial v}{\partial z}\right)\right] = \rho \frac{Dv}{Dt}$$

$$Z - \frac{\partial p}{\partial z} + \frac{\partial}{\partial x}\left[\mu\left(\frac{\partial w}{\partial x} + \frac{\partial u}{\partial z}\right)\right] + \frac{\partial}{\partial y}\left[\mu\left(\frac{\partial w}{\partial y} + \frac{\partial v}{\partial z}\right)\right] + \frac{\partial}{\partial z}\left[2\mu \frac{\partial w}{\partial z} - \frac{2}{3}\mu\,(\bar{\nabla} \cdot \bar{V})\right] = \rho \frac{Dw}{Dt}$$

WHERE FOR A GRAVITY BODY FORCE

$X = \rho g_x$

$Y = \rho g_y$

$Z = \rho g_z$

FIGURE 2-4 CONT.

SIMPLIFYING ASSUMPTIONS

FOR LIQUIDS THE ONLY SIGNIFICANT EFFECT OF VARYING DENSITY IS BUOYANT FORCES &c WE ASSUME CONSTANT DENSITY FOR CONTINUITY, I.E.,

$$\nabla \cdot V = \frac{\partial u}{\partial x} + \frac{\partial v}{\partial y} + \frac{\partial w}{\partial z} = 0$$

$$X - \frac{\partial p}{\partial x} + 2\mu \frac{\partial^2 u}{\partial x^2} + \mu \left(\frac{\partial^2 u}{\partial y^2} + \frac{\partial^2 v}{\partial y \partial x}\right) + \left(\frac{\partial u}{\partial y} + \frac{\partial v}{\partial x}\right) \frac{\partial \mu}{\partial y} + \left(\frac{\partial^2 w}{\partial z \partial x} + \frac{\partial^2 u}{\partial z^2}\right) + \left(\frac{\partial w}{\partial x} + \frac{\partial u}{\partial z}\right) \frac{\partial \mu}{\partial z} = \rho \frac{Du}{Dt}$$

$$Y - \frac{\partial p}{\partial y} + \mu \left(\frac{\partial^2 v}{\partial x^2} + \frac{\partial^2 u}{\partial x \partial y}\right) + \left(\frac{\partial v}{\partial x} + \frac{\partial u}{\partial y}\right) \frac{\partial \mu}{\partial x} + 2\mu \frac{\partial^2 v}{\partial y^2} + \mu \left(\frac{\partial^2 w}{\partial z \partial y} + \frac{\partial^2 v}{\partial z^2}\right) + \left(\frac{\partial w}{\partial y} + \frac{\partial v}{\partial z}\right) \frac{\partial \mu}{\partial z} = \rho \frac{Dv}{Dt}$$

$$Z - \frac{\partial p}{\partial z} + \mu \left(\frac{\partial^2 w}{\partial x^2} + \frac{\partial^2 u}{\partial x \partial z}\right) + \left(\frac{\partial w}{\partial x} + \frac{\partial u}{\partial z}\right) \frac{\partial \mu}{\partial x} + \mu \left(\frac{\partial^2 w}{\partial y^2} + \frac{\partial^2 v}{\partial y \partial z}\right) + \left(\frac{\partial w}{\partial y} + \frac{\partial v}{\partial z}\right) \frac{\partial \mu}{\partial y} + 2\mu \frac{\partial^2 w}{\partial z^2} = \rho \frac{Dw}{Dt}$$

$$X - \frac{\partial p}{\partial x} + \mu \left(\frac{\partial^2 u}{\partial x^2} + \frac{\partial^2 u}{\partial y^2} + \frac{\partial^2 u}{\partial z^2}\right) + \left(\frac{\partial u}{\partial y} + \frac{\partial v}{\partial x}\right) \frac{\partial \mu}{\partial y} + \left(\frac{\partial w}{\partial x} + \frac{\partial u}{\partial z}\right) \frac{\partial \mu}{\partial z} = \rho \left(\frac{\partial u}{\partial t} + u \frac{\partial u}{\partial x} + v \frac{\partial u}{\partial y} + w \frac{\partial u}{\partial z}\right)$$

$$Y - \frac{\partial p}{\partial y} + \mu \left(\frac{\partial^2 v}{\partial x^2} + \frac{\partial^2 v}{\partial y^2} + \frac{\partial^2 v}{\partial z^2}\right) + \left(\frac{\partial v}{\partial x} + \frac{\partial u}{\partial y}\right) \frac{\partial \mu}{\partial x} + \left(\frac{\partial w}{\partial y} + \frac{\partial v}{\partial z}\right) \frac{\partial \mu}{\partial z} = \rho \left(\frac{\partial v}{\partial t} + u \frac{\partial v}{\partial x} + v \frac{\partial v}{\partial y} + w \frac{\partial v}{\partial z}\right)$$

$$Z - \frac{\partial p}{\partial z} + \mu \left(\frac{\partial^2 w}{\partial x^2} + \frac{\partial^2 w}{\partial y^2} + \frac{\partial^2 w}{\partial z^2}\right) + \left(\frac{\partial w}{\partial x} + \frac{\partial u}{\partial z}\right) \frac{\partial \mu}{\partial x} + \left(\frac{\partial w}{\partial y} + \frac{\partial v}{\partial z}\right) \frac{\partial \mu}{\partial y} = \rho \left(\frac{\partial w}{\partial t} + u \frac{\partial w}{\partial x} + v \frac{\partial w}{\partial y} + w \frac{\partial w}{\partial z}\right)$$

FIGURE 2-5

constant with respect to satisfying the continuity equation and is only assumed to be temperature dependent with respect to calculating the buoyant force terms in the equations of motion. As is apparent in the simplified equations the variation in viscosity with location has been retained, so that the effect of temperature on viscosity is included. This model was used to calculate the three components of velocity and the pressure at 1463 locations within the chamber including the locations at which the data was reduced. Additional points were required near the walls to effectively model the flow, so the calculation grid used is as shown in Figure 2-6.

Boundary conditions for the model were buffer flow into and out of the model at average vertical velocity and no flow through the membranes. A no slip, zero velocity condition was assumed at the chamber walls, except for the cases with an applied field where the wall electroosmotic velocity was assumed at the wall. The pressure boundary condition was zero pressure gage at the geometric center of the chamber. Temperature boundary conditions were calculated in the MDAC-STL mathematical model composed of 1583 nodes. This portion of the model solved finite difference approximations to the energy equation given in Figure 2-7. Boundary conditions for the solution of the energy equation were the input temperatures of fluid entering the chamber and the ambient environmental temperature.

2.3 SAMPLE GRAVITY EFFECTS

The method selected to demonstrate the effect of gravity on the separation of samples was to assay the outlet tube concentration distributions for comparison with analytical predictions. In these demonstrations the samples, including both proteins and cells, were heavier than the carrier buffers. The proteins used were human fibrinogen and human albumin, and the cells used were 33H human lymphocytes.

The predicted effect of gravity on sample streams heavier than the buffer is to widen the sample stream. This widening is a result of the sample column slipping relative to the surrounding buffer. The slip causes the force of viscous shear on the column to be equal and opposite to the net buoyant force, for equilibrium. This means that the vertical velocity decreases toward the middle of the

CALCULATION GRID

- WIDTH (19 NODAL POINTS)
  - EIGHT EQUAL INCREMENTS OF 1.03125 CM PLUS
  - ADDED NODES 0.25, 0.05, 0.1, 0.2, AND 0.4 CM FROM EACH END
- THICKNESS (7 NODAL POINTS)
  - SIX EQUAL INCREMENTS OF 0.025 CM
  - HALF THICKNESS WITH SYMMETRY
- HEIGHT (11 NODAL POINTS)
  - SIX EQUAL INCREMENTS OF 20.0 CM PLUS
  - ADDED NODES 5.0 AND 10.0 CM FROM EACH END
- 1463 NODAL POINTS
- 5972 DIFFERENTIAL EQUATIONS

FIGURE 2-6

ENERGY EQUATION

$$\frac{\partial}{\partial x}\left(k\frac{\partial T}{\partial x}\right) + \frac{\partial}{\partial y}\left(k\frac{\partial T}{\partial y}\right) + \frac{\partial}{\partial z}\left(k\frac{\partial T}{\partial z}\right) + Q = \rho C_p \frac{DT}{Dt}$$

NET X COMPONENT OF HEAT CONDUCTION RATE PER UNIT VOLUME	NET Y COMPONENT OF HEAT CONDUCTION RATE PER UNIT VOLUME	NET Z COMPONENT OF HEAT CONDUCTION RATE PER UNIT VOLUME	INTERNAL HEAT GENERATION RATE PER UNIT VOLUME	RATE OF CHANGE OF INTERNAL ENERGY PER UNIT VOLUME

$$k\left(\frac{\partial^2 T}{\partial x^2} + \frac{\partial^2 T}{\partial y^2} + \frac{\partial^2 T}{\partial z^2}\right) + \frac{\partial T}{\partial x}\frac{\partial k}{\partial x} + \frac{\partial T}{\partial y}\frac{\partial k}{\partial y} + \frac{\partial T}{\partial z}\frac{\partial k}{\partial z} + Q = \rho C_p \left(\frac{\partial T}{\partial t} + u\frac{\partial T}{\partial x} + v\frac{\partial T}{\partial y} + w\frac{\partial T}{\partial z}\right)$$

IN OUR SOLUTION WE ASSUME THAT Q CONSISTS OF JOULE HEATING ONLY, I.E.,

THAT GENERATED BY INTERNAL FRICTION IS NEGLIGIBLE

FIGURE 2-7

sample, increasing residence time and therefore lateral motion under electrophoresis. For a sample heavier than the carrier buffer in upward flow, this phenomena causes greater lateral motion of the middle of the sample, relative to the trailing edge, resulting in widening of the sample stream.

Of course, there are other factors that influence outlet concentration distribution. Included among these factors are crescent distortion, which causes widening of the distribution in the direction of the electrophoretic movements. Also included are electroosomotic flow which, depending on its magnitude and direction, can cause widening of the sample that can either increase, decrease, or compensate for the widening due to crescent distortion, as described by Strickler and Sacks (4). In addition to these effects, diffusion widens the streams by a continuous leveling of the concentration distribution. These effects are all well described in theory, but in addition there are the effects of the apparatus on the separation: that is, the stability and repeatability of electrophoresis chamber used.

Because of these variables the albumin and human fibrinogen samples were run separately before separation of mixtures was attempted. These tests were performed varying voltage and flowrate. Voltage was varied to identify any non-linearities in deflection with voltage. Flowrate was varied to identify the effects of gravity, which would be expected to increase with decreasing flowrate because the velocity variations due to slip in the column become more significant as velocity decreases.

After the single protein tests were completed mixtures of proteins were separated varying both concentration and flowrate. Here again, gravity effects, that is widening of the sample streams is expected to increase at decreasing flowrate. In addition, since the amount of slip in the sample column is proportional to concentration, gravity induced widening is expected to increase at increasing concentration.

Gravity effects were also demonstrated using a single cell type, 33H human lymphocytes. The resulting concentration distributions of cells and proteins were compared with analytical results from a three dimensional model of the flow and concentration in the vicinity of the sample. The area modeled was bounded by the front

wall and the chamber centerline and included enough of the flow on either side of the separating stream to minimize sample effects at the edges. Using this model the flow characteristics and sample concentration were calculated at 1001 locations within the chamber. Boundary conditions for this model were buffer flow into and out of all surfaces of the model and a known equilibrium pressure distribution at the inlet of the model where the sample was injected at carrier flow velocity. Temperature boundary conditions were calculated by an additional heat transfer model of 1274 nodes, which used input fluid temperatures and ambient temperature as boundary conditions.

In reduction of the protein separation outlet concentration data it appeared that the calculated wall electroosmotic mobility calculated for the buffer gravity effects tests as described in Section 2.2 was large enough that the mobility of human fibrinogen would be negative. This seemed unlikely, so tests were run to compare total movement of human albumin, the more mobile of the two proteins used, in both borate and barbital buffers. Again, it was assumed that both the electrophoretic movement and the electroosmotic movement for the human albumin were proportional to the total movement in each buffer, and based on this, the electroosmotic mobility for the barbital buffer/Lexan wall combination was calculated to be -7.9×10^{-4} cm^2/volt-sec and the analytical predictions of protein outlet concentration distributions were made using this value. It should be noted that the wall electroosmotic mobility calculated from the albumin data of -7.9×10^{-4} cm^2/volt-sec did not agree with one calculated from R250 Coomassie Brilliant Blue dye data of -10.2×10^{-4} cm^2/volt-sec. Because of the importance of the wall electroosmotic mobility, it is recommended that wall electroosmotic mobility measurements be made using a micro-electrophoresis device for the buffer/wall material combinations tested. Also because of the lack of agreement, further comparison tests were not attempted and the same wall electroosmotic mobility was used for the analytical prediction of cell outlet concentration distribution, although a different buffer had to be used to maintain cell viability.

For the protein and cell separations the mobilities used for the analytical predictions were the observed mobilities for those cases where gravity effects were at a minimum. The albumin mobility from Run 26 was 3.6×10^{-4} cm^2/volt-sec,

the fibrinogen mobility from Run 35 was 0.66 x 10^{-4} cm^2/volt-sec, and lymphocyte mobility from Run 59 was 6.6 x 10^{-4} cm^2/volt-sec.

3.0 TEST HARDWARE

3.0 TEST HARDWARE

A balanced investigation of the electrophoretic process requires that theoretical analysis be correlated with actual test data. The testing under this contract was intended to verify and quantify the influence of gravity-dependent factors upon the process. These factors include convection due to Joule heating of the buffer and the effects of sample stream buoyancy.

Tests necessary to demonstrate gravity effects in the free-flow electrophoretic process were performed with McDonnell Douglas Astronautics Company - St. Louis developed hardware. The test hardware was setup around a free flow electrophoresis chamber of 120 cm length as shown in Figure 1-1. Calibrated instrumentation was installed to measure internal temperatures, pressure, and electrical field strength. A detailed discussion of the hardware is provided in the following paragraphs.

3.1 FREE FLOW CHAMBER DESIGN

The basic functional characteristics of the McDonnell Douglas Astronautics Company - St. Louis chamber are as follows:

- o Upward carrier buffer flow
- o Parallel upward flow coolant jackets
- o Upward electrolyte buffer flow

Basic design features of the chamber are:

- o 120 cm flow length in electrical field
- o 0.3 cm separation chamber depth
- o 8.25 cm separation chamber width
- o Platinum electrodes
- o Reconstituted cellulose membrane material

Upward carrier buffer flow was chosen over downward flow because chamber buffer temperatures were above the temperature for maximum buffer density (4°C). Therefore, upward carrier buffer flow was compatible with the temperature gradient that was positive in the upward flow direction.

Parallel flow coolant jackets control the magnitude of this buffer temperature gradient. The coolant jackets' (one on each face of the chamber, front and back) flow covers the width and length (7.3 cm x 119.0 cm) of the carrier buffer chamber.

Separating each cooling jacket from the carrier buffer chamber is a wall of Lexan polycarbonate resin the primary structural material of the chamber.

Upward electrolyte buffer flow allowed the same upward increasing temperature gradient at the membranes separating the electrolyte flow from the carrier buffer flow. Upward flow also aided the buoyant forces on the bubbles (electrolysis products) in freeing them from the electrodes.

Chamber design was based upon several previous evolutionary models developed by McDonnell Douglas Astronautics Company - St. Louis. Incorporation of the practical lessons learned with previous units produced a chamber which can consistently provide sample residence times greater than ten minutes.

The 120 cm flow chamber length, a dimension considered most practical for Spacelab integration, allowed long sample residence times. The full 120 cm flow length was within the applied electric field. The field across the 8.25 cm wide 0.3 cm deep separation chamber was created between two platinum electrodes. Each electrode was surrounded by flowing electrolyte buffer. A membrane of reconstituted cellulose material segregated the carrier buffer flow from the electrolyte flow. The membrane porosity was picked to allow compounds of <14,000 molecular weight to move between flows.

3.2 ADDITIONAL CHAMBER FEATURES

Supplemental design features of the flow chamber were a manifolded carrier buffer inlet and a 105 tube outlet. The inlet provided uniform introduction of the carrier buffer across the separation chamber width through eight (8) channels. The manifold had provision for nearly homogeneous mixing of buffered dyes with the carrier buffer prior to introduction into the separation chamber. This feature was utilized in the first nine (9) Task 1 Buffer Gravity Effects test runs. The manifold also allowed sample introduction into the carrier buffer flow through any one or all of seven (7) glass capillary tubes (0.07 cm inside diameter) positioned vertically on the chamber centerline. Spacing between the sample inlet tubes was 1.06 cm. The tubes extended into the flow chamber 3.7 cm. This feature with all seven (7) tubes in place was utilized in the second set of nine (9) Task 1 test runs. All Task 2 test runs had the manifold configured with only one (1) inlet tube for sample. The single inlet tube was located 2.01 cm from the cathode side membrane.

At the separation chamber outlet, the flow exited through one-hundred five (105) capillary (0.066 cm nominal inside diameter) tubes across the separation chamber width.

3.3 INSTRUMENTATION

The flow chamber itself was instrumented for measurement of temperatures, pressures, and electrical field strength. Support equipment such as refrigerated reservoirs were also monitored for temperature.

Temperature instrumentation within the flow chamber consisted of seventeen (17) individual thermocouples located as shown in Figure 3-1. The thermocouples were Type T teflon sheathed copper-constantan. The nominal outside diameter of each sheath was 0.064 cm. At mid-chamber height (60 cm) and at the upper chamber (120 cm) two (2) thermocouples measured centerline carrier buffer temperatures. The remain-

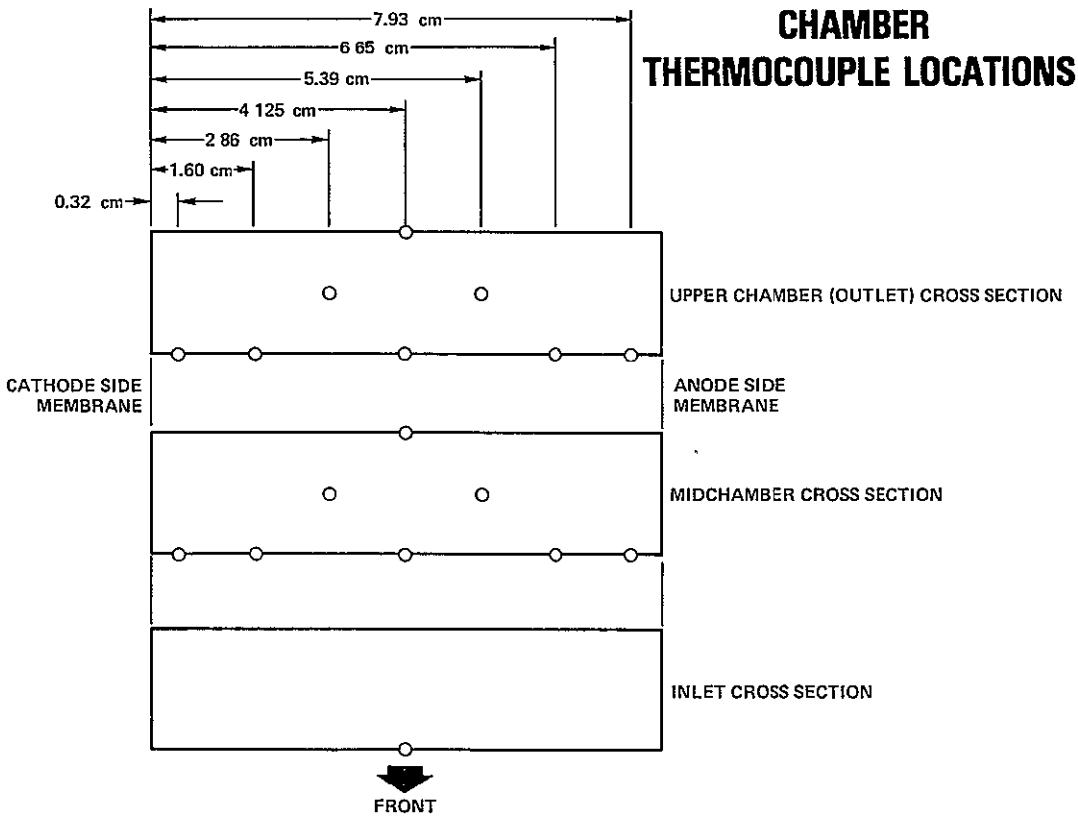

Figure 3–1

ing six (6) thermocouples at each location measured buffer flow chamber wall temperatures. Additional measurements of chamber inlet and outlet temperatures were gathered from thermocouples located at the coolant jacket inlet, electrode chamber inlet and both electrode chamber outlets. The thermocouples measured center stream temperatures, and were of the same teflon sheathed copper-constantan type as those installed within the chamber.

Pressure measurement was performed with one Bourdon direct pressure gage and two (2) differential pressure transducers. The direct pressure gage monitored the flow chamber static pressure at the inlet height. One each mechanical type differential transducer was utilized to measure the pressure drop across the cathode side membrane (i.e. between electrolyte and carrier buffer flow chambers) at the chamber inlet and 120 cm heights. Pressure measurement was not intended to provide data for correlation with analytically predicted chamber pressures but rather as an operational monitor against over-stressing the electrode membranes.

Electrical field strength instrumentation within the carrier buffer flow chamber consisted of seven (7) pairs of 0.1 cm diameter gold pins at chamber heights of 3.4 cm, 22.4 cm, 41.7 cm, 63.6 cm, 79.8 cm, 98.7 cm and 118.0 cm. Each pair of pins were 7.65 cm apart, with each pin approximately 0.3 cm from the adjacent membrane. Penetration of each pin into the buffer solution was approximately 0.1 cm. Flow chamber electrical field strength (volts) at each reference height was then measured between the two pins of each pair and reduced to volts per centimeter (v/cm).

3.4 CALIBRATION

All test hardware instrumentation was calibrated immediately preceeding the start of contract work. All twenty-two (22) thermocouples, cables and the digital readout were calibrated as a system. Thermocouple error was $\pm$0.55 C and gage pressure accuracies were $\pm$0.15 psi. Pressure transducers were calibrated to an accuracy of $\pm$0.075 psi. Chart record pressure readings were evaluated with accuracies of $\pm$0.25 psi. The digital voltmeter readout of electrical field strength values was calibrated to an accuracy of $\pm$1.02 volt over the range of chamber potentials measured.

In addition to test instrumentation installed on the flow chamber, fluid flow metering devices in the support setup were calibrated. Each fluid flowing through the chamber and cooling jackets, i.e. carrier buffer, electrolyte buffer, and jacket coolant, was metered prior to introduction at the chamber. The flowmeters were the spherical float type. Calibration curves were generated for each flowmeter at the conditions of flow while installed in the test setup. Carrier buffer flow measurement accuracy was the most critical from the standpoint of test-to-test flow rate control. The resulting instrument accuracy was $\pm$4.0% under steady flow conditions, over the range of test operation (20 - 40 milliliters/minute (ml/min)). With regard to potential sources of error in the test run data the fluid flow rates, most importantly carrier buffer, were the greatest hardware related errors.

Support equipment included two (2) sample syringe pumps that were calibrated at the discreet sample flow rate settings utilized during all runs. The pumps were individually calibrated for the particular syringe size used with each run. Calibrated sample flow rates were accurate to $\pm$5.0%.

4.0 BUFFER GRAVITY EFFECTS

4.0 BUFFER GRAVITY EFFECTS

Assessment of sample gravity effects in free-flow electrophoresis first requires definition of the carrier buffer gravity effects. Buffer gravity effects result from buoyancy forces due to temperature differences in the buffer through Joule heating. Joule heating of the buffer causes distortions of the parabolic velocity profile described for Poiseuille flow. This section presents test methodology, test results and correlation with the analytical predictions.

4.1 TEST DATA COLLECTION

Measurement of dye stream patterns was used to quantify the buffer flow profile. These measurements plus flow chamber temperatures and flow rates comprised the useful test data.

Preliminary to data gathering, test procedures and criteria were established. Carrier buffer flow rates of 20, 30 and 40 milliliters per minute (ml/min) provided a useful range of flow rates with the 120 cm length flow chamber utilized. A range of electrical field strengths across the chamber (0, 10 and 20 volts D.C. per centimeters (V/cm)) was chosen rather than applied voltage. This choice was made prior to the initiation of testing and was deemed necessary in order to simplify data gathering and presentation during the sample protein and cell studies. Sample movement can be considered a constant function of electrical field strength, but a variable function of applied voltage, because of flow chamber membrane day-to-day electrical resistance changes. For experimental control, electrical field strength was more appropriate and so used throughout the data collection.

Uniform coolant, electrolyte buffer and carrier buffer temperatures at the chamber inlets are desirable initial conditions for an optimum thermal balance when establishing laminar buffer flow. Therefore, as part of the test protocol, uniform temperature conditions were established at the mid-chamber and upper-chamber (Figure 4-1).

Fluid pressure differentials across one membrane were monitored during chamber operation. This was done in order to prevent over-pressures from occurring during filling of the electrode and buffer chambers which would damage the membrane material or

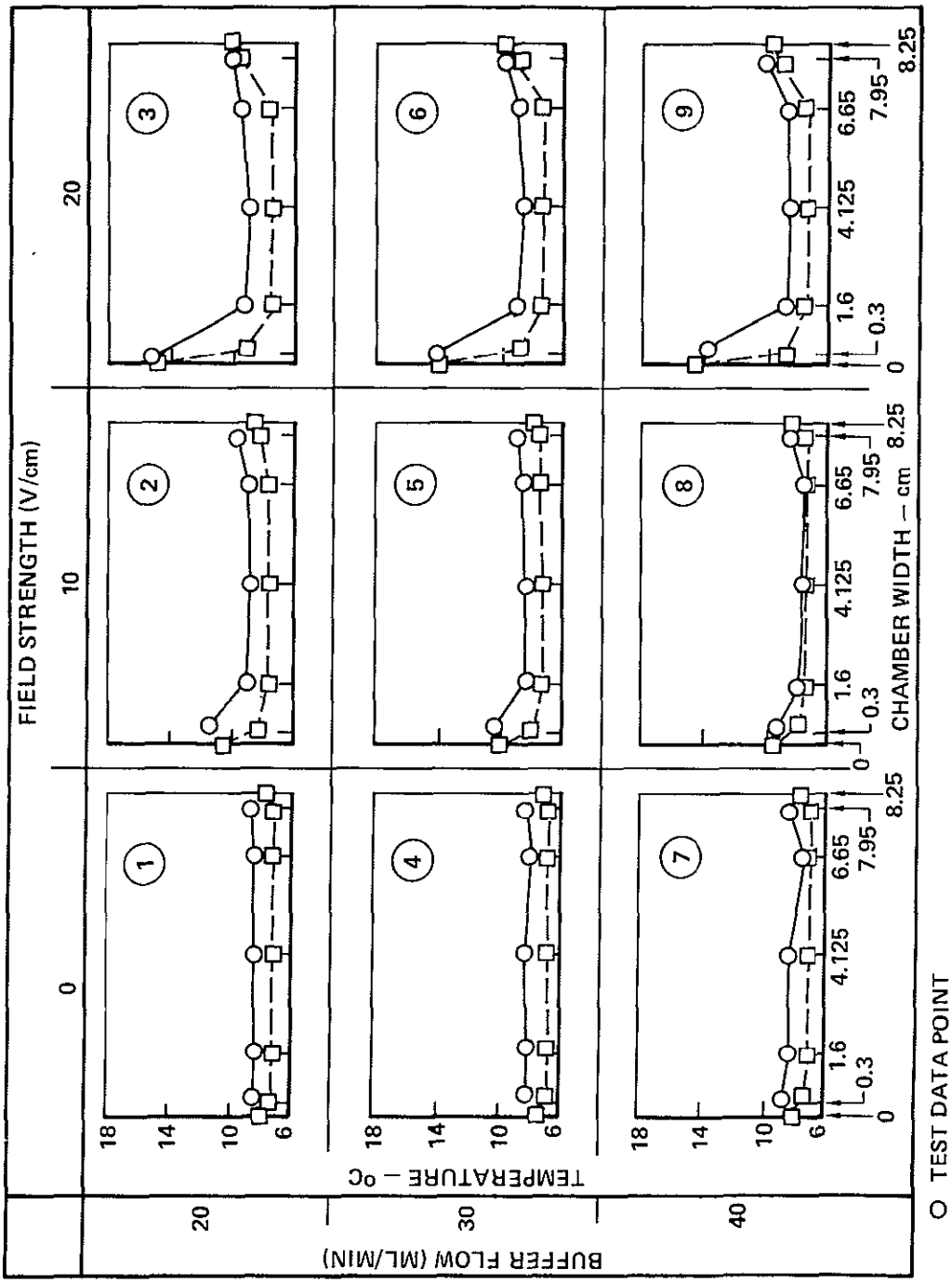
MID-CHAMBER BUFFER TEMPERATURES AT WALL
FIELD STRENGTH (V/cm)
0
10
20
BUFFER FLOW (ML/MIN)
20
30
40
TEMPERATURE – °C
18
14
10
6
CHAMBER WIDTH – cm
0
0.3
1.6
4.125
6.65
7.95
8.25
TEST DATA POINT
PREDICTED DATA POINT
RUN NUMBER

Figure 4-1(A)

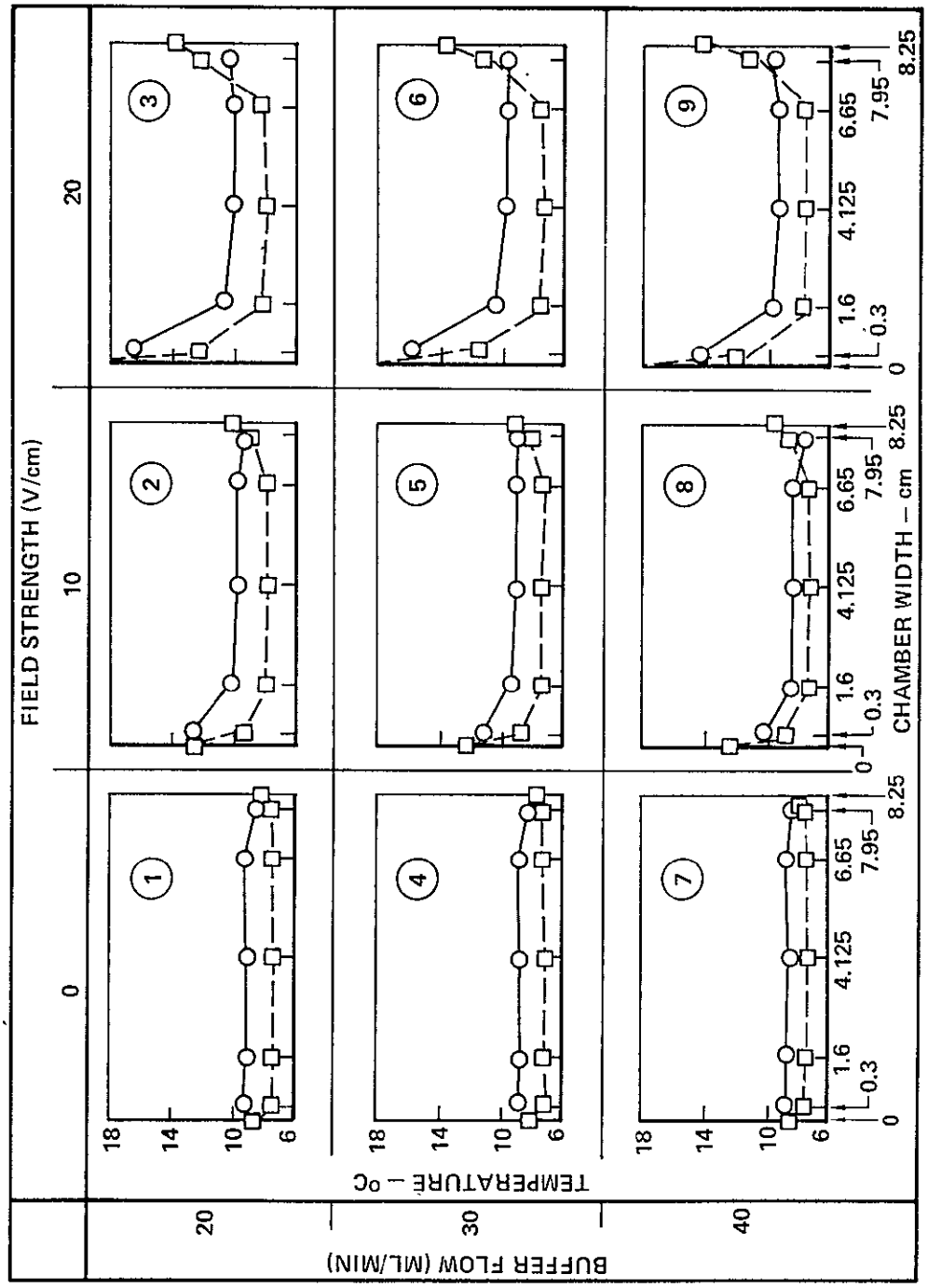
UPPER-CHAMBER BUFFER TEMPERATURES AT WALL
FIELD STRENGTH (V/cm)
0
10
20
BUFFER FLOW (ML/MIN)
20
30
40
TEMPERATURE – °C
18
14
10
6
CHAMBER WIDTH – cm
0
0.3
1.6
4.125
6.65
7.95
8.25
TEST DATA POINT
PREDICTED DATA POINT
RUN NUMBER

Figure 4-1(B)

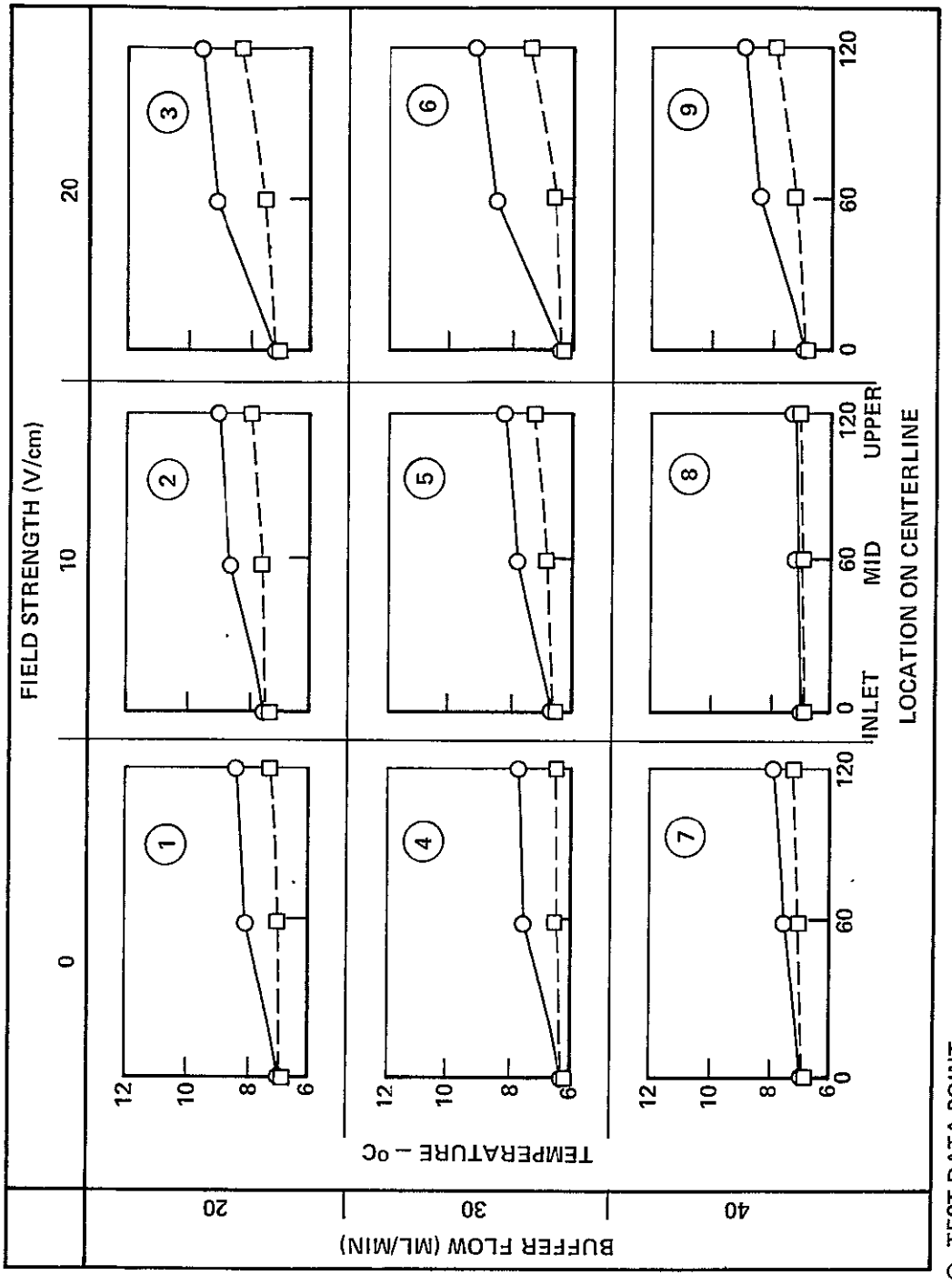
CENTERLINE BUFFER CHAMBER TEMPERATURES
FIELD STRENGTH (V/cm)
0
10
20
BUFFER FLOW (ML/MIN)
20
30
40
TEMPERATURE – °C
12
10
8
6
0
60
120
INLET
MID
UPPER
LOCATION ON CENTERLINE
1
2
3
4
5
6
7
8
9
TEST DATA POINT
PREDICTED DATA POINT
RUN NUMBER

Figure 4-1(C)

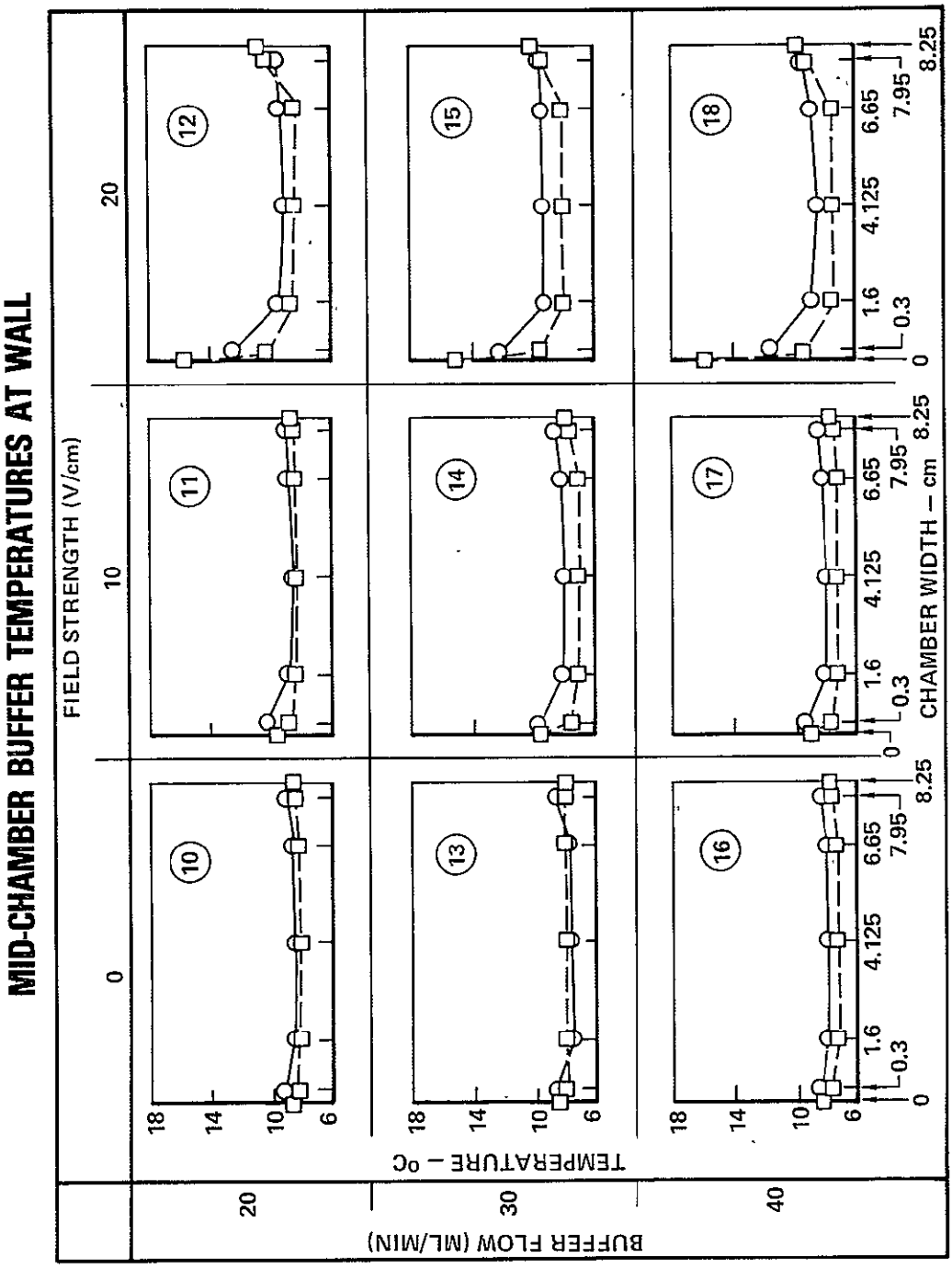
MID-CHAMBER BUFFER TEMPERATURES AT WALL
FIELD STRENGTH (V/cm)
0
10
20
BUFFER FLOW (ML/MIN)
20
30
40
TEMPERATURE – °C
18
14
10
6
CHAMBER WIDTH – cm
0
0.3
1.6
4.125
6.65
7.95
8.25
TEST DATA POINT
PREDICTED DATA POINT
RUN NUMBER

Figure 4-1(D)

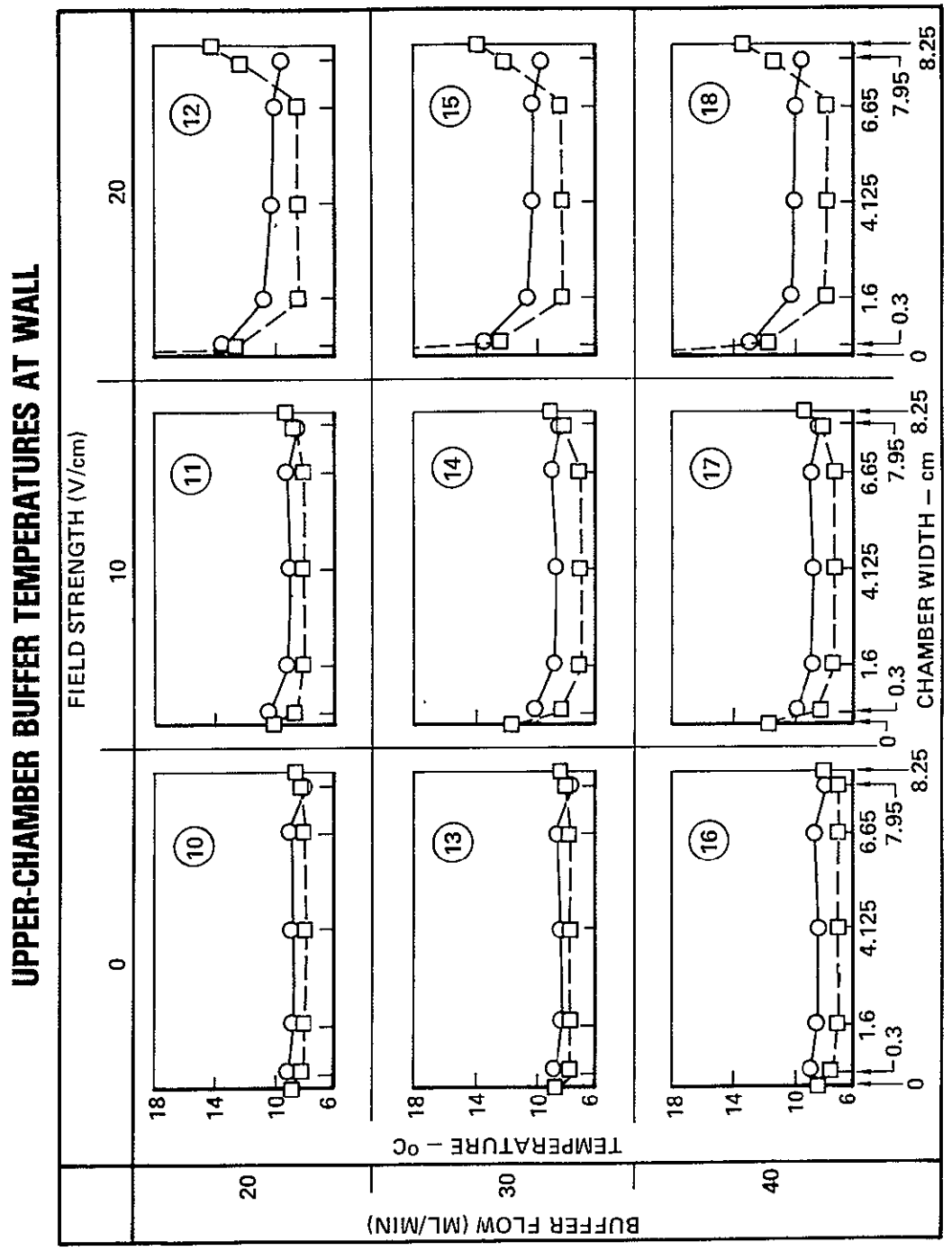
UPPER-CHAMBER BUFFER TEMPERATURES AT WALL
FIELD STRENGTH (V/cm)
0
10
20
BUFFER FLOW (ML/MIN)
20
30
40
TEMPERATURE – °C
18
14
10
6
CHAMBER WIDTH – cm
0
0.3
1.6
4.125
6.65
7.95
8.25
10
11
12
13
14
15
16
17
18
TEST DATA POINT
PREDICTED DATA POINT
RUN NUMBER

Figure 4-1(E)

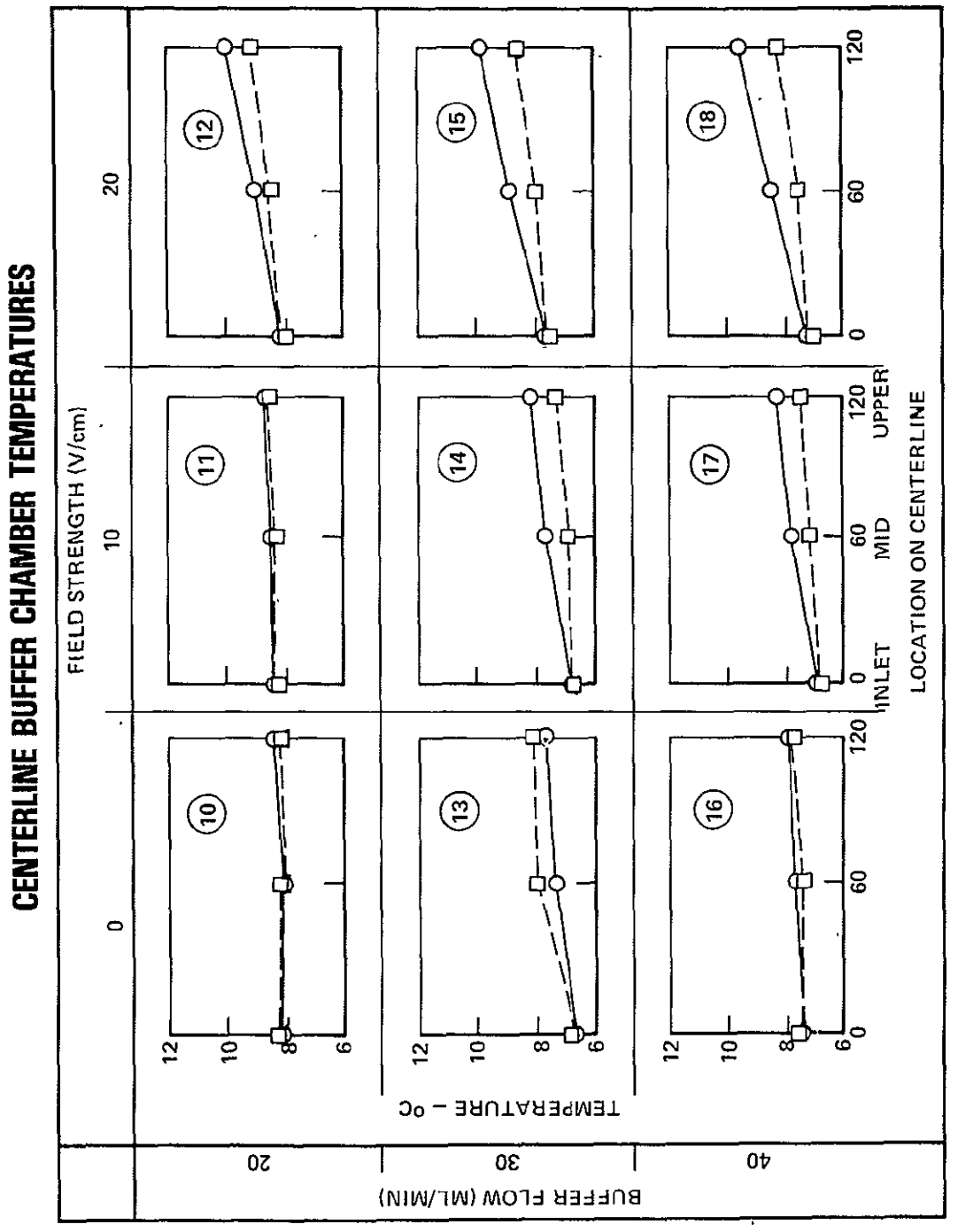
CENTERLINE BUFFER CHAMBER TEMPERATURES
FIELD STRENGTH (V/cm)
0
10
20
BUFFER FLOW (ML/MIN)
20
30
40
TEMPERATURE – °C
12
10
8
6
LOCATION ON CENTERLINE
INLET
MID
UPPER
0
60
120
TEST DATA POINT
PREDICTED DATA POINT
RUN NUMBER
10
11
12
13
14
15
16
17
18

Figure 4-1(F)

seals. Differential pressures of up to 1.0 psid are normal and do not substantially reduce the functional life of the membrane material..

Carrier buffer flow stability criteria were established to define laminar flow. Steady state laminar flow was defined as a lack of time variant visible fluctuations of continuous dye stream (or streams) over a five-minute period. Conversely, laminar flow disturbance was defined as visible fluctuations or discontinuities of a dye stream (or streams).

Flow profile visualization was necessary to allow measurement of the buffer velocity, specifically the centerline velocity. Measurement of velocities without physically disturbing the flow itself was achieved by making it visible with Coomassie Brilliant Blue R250 dye. An instantaneous record of the velocity profile was then possible by photographing the visible flow pattern. Neutrally buoyant particles of size, consistency and coloration necessary for photographic recording flow profiles were not readily available. Laser velocimetry was available, but programmatic conflicts, cost and questions of the laser's interference with flow chamber structure decided against this approach. Standard electrophoretic dyes were the simplest means. Coomassie Brilliant Blue R250 was chosen because of its visibility, mobility, and availability. Flow trials were performed to determine a minimum concentration of dye dissolved in buffer, which would flow well over the test range of buffer flow rates while remaining visible the length of the chamber. A concentration range of 1-2 milligram dye per milliliter buffer (1-2 mg/ml) was chosen. At test temperatures (approximately $8^{o}C$) the dye stream specific gravity was 0.0006-0.0008 greater than the surrounding buffer.

Buffer centerline velocity had to be measured in two parts, the vertical component and the horizontal component, which conformed with the analytical output. Two different dye flow patterns were necessary to visualize buffer movement due to each of these two velocity components. The vertical component had to be visualized at any instant across the entire width of the flow chamber. This meant a relatively uniform front of dye the width of the chamber moving with the flow. To do this dye was intermittently injected into the carrier buffer previous to the flow chamber inlet manifold. This allowed a homogeneous mix of dye and buffer to enter the chamber. The leading edge of the visible dye front would flow with the highest

velocity buffer, i.e. the centerline flow. Photographically recording the advance of the front at intervals allowed positional definition of any point on the front. Position or location information was referenced from metric unit scale markings on the flow chamber face. The horizontal velocity component was best visualized using streams of dye. Seven discrete vertical dye streams were formed simultaneously by dye injection into the buffer flow chamber through sample ports with equal spacings of 1.06 cm. In established laminar flow any differential horizontal movement of the continuous dye streams was photographically recorded in reference to the scaled chamber face. The crescent distortion phenomena would tend to spread each stream. Therefore centerline buffer movement was correlated with movement of the densest (darkest) visible portion of each dye stream.

Tests were performed in accordance with the two matrices of Figures 4-2 and 4-3. (The tests were not necessarily performed in order numerically, however). The first tests were the nine (9) vertical velocity component runs (Figure 4-2). Chamber inlet configuration for these tests provided the uniform mix of dye and carrier buffer across the separation chamber width as described in Section 3.2. Carrier and electrolyte buffer solutions sufficient for up to eight (8) hours of operation were prepared daily as described in Section 5.1. An electrolyte buffer solution concentration (and ionic strength) five (5) times that of the carrier buffer was used in order to reduce electrical resistance across the membrane.

Preliminary runs with photography evaluation of dye front visibility resulted in selection of a 1.5 mg dye per ml carrier buffer solution to mark the flow stream. A stock of this dye solution was stored at 4°C and kept for five (5) days before being discarded and new stock prepared. For each run the dye solution was injected at room temperature from a syringe into the carrier buffer.

The first run conducted each day was a zero-voltage case. This allowed confirmation that a steady state laminar flow condition was present in the separation chamber. Flow stability was determined by two means. First, a consistent stream pattern as visualized by short period (5 second) dye solution injection, at 5 minute intervals. Second, by even separation chamber wall temperatures at mid-chamber height and upper chamber. Here even was defined as temperatures falling within $\pm$0.4°C of the average at each chamber height.(Figures 4-1(A) and 4-1(B)).

TASK 1.0

TEST MATRIX, RUNS 1-9

BUFFER FLOW ML/MIN \ FIELD VOLTS/CM	0	10	20
20	1	2	3
30	4	5	6
40	7	8	9

- UNIFORM FRONT DYE INJECTION THROUGH BUFFER INLET
- NUMERICAL DIFFERENTIATION APPROXIMATES VERTICAL COMPONENT OF CENTERLINE VELOCITY

Figure 4–2

TASK 1.0

TEST MATRIX, RUNS 10-18

FIELD VOLTS/CM / BUFFER FLOW ML/MIN	0	10	20
20	10	11	12
30	13	14	15
40	16	17	18

- MULTI-STREAM DYE INJECTION THROUGH SAMPLE PORTS
- LOCAL VERTICAL COMPONENT OF CENTERLINE VELOCITY X TANGENT OF STREAM DEFLECTION ANGLE EQUALS HORIZONTAL COMPONENT OF VELOCITY PLUS ELECTROPHORETIC VELOCITY

Figure 4–3

The first daily run was commenced after steady laminar flow was established. Dye was injected into the carrier buffer flow for mixing immediately preceeding the inlet manifold. Dye injection for the 20 ml/min buffer flow cases was 8 ml/min over a 15 second period. For the 30 ml/min and 40 ml/min buffer flow cases it was 12 ml/min over 12 seconds and 15 ml/min over 12 seconds, respectively.

Timing of the run started at the first visible incursion of dye into the separation chamber at 0 cm chamber level. This inlet plane was viewed directly perpendicular to the flow. Timing was initiated manually. The advance of the dye front up the 120 cm chamber length was photographically recorded at regular intervals with the elapsed time of each photograph noted. Figure 1-2 shows a typical photograph. The number of photographs per run taken during the 20 ml/min buffer flow cases and used for data reduction averaged thirteen (13). The 30 ml/min and 40 ml/min buffer flow cases averaged ten (10) photographs each run for both cases.

Following the zero-voltage run voltage was applied to the electrophoresis chamber for the 10 volt/cm field strength case, then the 20 volt/cm case at the control buffer flow rate. Carrier buffer and coolant flow rates remained the same as for the zero-voltage case. The electrolyte buffer flow rates remained essentially the same with only minor ($\leq$15%) electrolyte buffer flow rate increases in order to maintain electrode chamber inlet temperatures at the same value set in the zero-voltage cases. Electrical field strength at pairs of pins on either side of the field was monitored regularly. Readings from seven pairs of pins along the vertical were averaged. For the applied voltage runs, flow stability was determined by first, a consistent stream pattern visualized as during zero-voltage cases, second, steady flow chamber temperatures, and third, an average chamber field strength varying not more than 0.35 v/cm over a 5 minute period. Typically, temperatures and field strengths were recorded immediately preceeding dye front introduction for photography.

The second set of tests were the nine (9) horizontal velocity component runs (Figure 4-3). For these tests the chamber inlet configuration was changed to inject seven (7) continuous and parallel dye streams into the carrier buffer flow. The inlet for this set of runs is described in Section 3.2. Buffer and sample dye preparations were as described for the vertical velocity component runs.

Preliminary run evaluations selected a dye solution of 1.0 mg/ml. Total dye sample injection rate was set at 0.15 ml/min, 0.20 ml/min and 0.30 ml/min for the 20 ml/min, 30 ml/min and 40 ml/min carrier buffer flow cases, respectively.

Zero-voltage run flow stability was confirmed by two means. First, steady dye streams as defined by lack of lateral movement or waivering over a 5-minute period and, second by the same even separation chamber wall temperature as defined for the vertical component runs. Carrier buffer, electrolyte buffer and coolant flow rates were the same as set for the zero-voltage vertical velocity component runs.

Timing during stream photography was not necessary with the continuous dye streams. Photographs of the flow chamber were taken at 20 cm intervals from 20 cm to 100 cm in height. Data reduction was later done by finding the lateral coordinate of each dye stream as it crossed the 20, 40, 60, 80 and 100 cm vertical level.

Conditions for the horizontal component runs with voltage applied, were established essentially as they were for the vertical component runs. Temperatures and field strengths were monitored and recorded in the same manner as discussed previously.

4.2 DATA REDUCTION AND CORRELATION

Effects of gravity on the buffer flow were evaluated by the tests given in the matrices of Figures 4-2 and 4-3. The first nine tests used horizontal dye fronts to determine vertical centerline velocity. The results of the test data reductions and the corresponding analytical predictions are presented in Figures 4-4 through 4-21. The reduced data for vertical centerline velocity at 0 volts/cm and 20 ml/min buffer flow is presented in Figure 4-4. Here the velocity varies little from side to side, as would be expected, particularly near the inlet. The expected profile is illustrated by the analytical predictions shown in Figure 4-5; that is, a constant velocity except in the vicinity of the membranes. It should be noted that the reduced test data, as well as the photographic data, show some rounding of the velocity profile with length in the chamber as shown in Figure 1-2 for a flow rate of 40 ml/min. This is probably the result of non-uniform heating of the buffer and coolant by conduction through the faces of the unit. These effects do not show up in the predictions, because a constant ambient temperature was used as a boundary condition. Similar results are shown in the 0 volt/cm data presented

in Figures 4-10 and 4-11 for a buffer flow rate of 30 ml/min and in Figures 4-16 and 4-17 for a buffer flow rate of 40 ml/min.

The reduced data for vertical centerline velocity at 10 volts/cm and 20 ml/min buffer flowrate is presented in Figure 4-6. Here the vertical centerline velocities appear to be constant across the chamber at the one centimeter increments where the data was reduced. The original photographs show additional peaks in the velocity profile near the membranes not evidenced by the reduced data. These peaks are illustrated by Figure 1-3 at a flowrate of 40 ml/min. The data reduction does not indicate the presence of these peaks, because it proved impossible to reliably measure the vertical height coordinates of the profiles in the area near the membranes, where the slope of the profiles was almost vertical. In addition to this, the electrophoretic mobility of the dye shifted the dye fronts away from the cathode in the direction of increasing width in the chamber. This caused all the points at 1.031 cm width to be beyond the velocity profiles as indicated by the "R's" in the reduced data. Calculation at these points would have required extrapolation instead of interpolation of the data; a risky procedure at best. The corresponding analytical predictions, as presented in Figure 4-7, do indicate the presence of velocity peaks within about 0.2 cm of both membranes. The velocity peaks near the outlet are about 5% greater than the velocity at mid chamber. Similar comparisons are indicated by Figures 4-12 and 4-13 for a buffer flow rate of 30 ml/min and by Figures 4-18 and 4-19 for a buffer flow rate of 40 ml/min.

The reduced data for vertical centerline velocity at 20 volts/cm and 20 ml/min buffer flow rate is presented in Figure 4-8 and the corresponding analytical prediction in Figure 4-9. Here the analytical predictions show even higher velocity peaks near the membranes, as would be expected at the higher voltage level. Similar results are indicated by Figures 4-14 and 4-15 for a buffer flow rate of 30 ml/min and by Figures 4-20 and 4-21 for a buffer flow rate of 40 ml/min.

MDAC-SEL ELECTROPHORESIS DATA PRODUCTION
ORIGINATOR: D.W. RICHMAN 12/78

RUN NO. 1, TEST ENGINEER: C.F. WALKER
BUFFER FLOW 20.0 ML/MIN, INLET TEMP 6.9 C
FIELD STRENGTH 0.0 V/CM
BUFFER VERTICAL CENTERLINE VELOCITY

WIDTH											
8.250											
8.225											
8.200											
8.150											
8.050											
7.850											
7.219			.1805E+00	.2066E+00	.2084E+00	.2038E+00	.1851E+00				
6.188			.1792E+00	.1907E+00	.1937E+00	.1945E+00	.1795E+00				
5.156			.1802E+00	.1942E+00	.1925E+00	.1960E+00	.1870E+00				
4.125			.1809E+00	.1966E+00	.1931E+00	.1964E+00	.1916E+00				
3.094			.1815E+00	.1944E+00	.1923E+00	.1960E+00	.1974E+00				
2.063			.1768E+00	.1663E+00	.1846E+00	.1980E+00	.1989E+00				
1.031			.1748E+00	.1727E+00	.1516E+00	.1600E+00	.2249E+00				
.400											
.200											
.100											
.050											
.025											
0.000											
LENGTH	0.00	5.00	10.00	20.00	40.00	60.00	80.00	100.00	110.00	115.00	120.00

HEIGHTS > DATA = P

FIGURE 4-4

MDAC-STL ELECTROPHORESIS ANALYSIS PROGRAM
ORIGINATOR: D.W. RICHMAN 9/78

RUN NO. 1, TEST ENGINEER: C.D. WALKER
BUFFER FLOW 10.0 ML/MIN, INLET TEMP 6.9 C
FIELD STRENGTH 0.0 V/CM
BUFFER VERTICAL CENTERLINE VELOCITY
WIDTH

8.250	.1347E+00	0.	0.	0.	0.	0.	0.	0.	0.	0.	0.
8.225	.1347E+00	.6981E-01	.6984E-01	.7006E-01	.7044E-01	.7081E-01	.7118E-01	.7155E-01	.7182E-01	.7211E-01	.1347E+00
8.200	.1347E+00	.1198E+00	.1198E+00	.1201E+00	.1206E+00	.1211E+00	.1216E+00	.1221E+00	.1225E+00	.1229E+00	.1347E+00
8.150	.1347E+00	.1773E+00	.1771E+00	.1773E+00	.1777E+00	.1781E+00	.1785E+00	.1789E+00	.1793E+00	.1796E+00	.1347E+00
8.050	.1347E+00	.2024E+00	.2033E+00	.2034E+00	.2036E+00	.2038E+00	.2040E+00	.2042E+00	.2045E+00	.2051E+00	.1347E+00
7.850	.1347E+00	.2052E+00	.2063E+00	.2065E+00	.2066E+00	.2068E+00	.2069E+00	.2072E+00	.2075E+00	.2081E+00	.1347E+00
7.219	.1347E+00	.2053E+00	.2064E+00	.2065E+00	.2067E+00	.2068E+00	.2070E+00	.2072E+00	.2075E+00	.2082E+00	.1347E+00
6.188	.1347E+00	.2052E+00	.2062E+00	.2063E+00	.2064E+00	.2065E+00	.2067E+00	.2069E+00	.2071E+00	.2077E+00	.1347E+00
5.156	.1347E+00	.2052E+00	.2062E+00	.2063E+00	.2064E+00	.2065E+00	.2067E+00	.2069E+00	.2071E+00	.2077E+00	.1347E+00
4.125	.1347E+00	.2052E+00	.2062E+00	.2063E+00	.2064E+00	.2065E+00	.2067E+00	.2069E+00	.2071E+00	.2077E+00	.1347E+00
3.094	.1347E+00	.2052E+00	.2062E+00	.2063E+00	.2064E+00	.2065E+00	.2067E+00	.2069E+00	.2071E+00	.2077E+00	.1347E+00
2.063	.1347E+00	.2052E+00	.2062E+00	.2063E+00	.2064E+00	.2065E+00	.2067E+00	.2069E+00	.2071E+00	.2077E+00	.1347E+00
1.031	.1347E+00	.2053E+00	.2063E+00	.2065E+00	.2067E+00	.2068E+00	.2070E+00	.2072E+00	.2075E+00	.2081E+00	.1347E+00
.400	.1347E+00	.2052E+00	.2062E+00	.2064E+00	.2066E+00	.2067E+00	.2069E+00	.2071E+00	.2074E+00	.2080E+00	.1347E+00
.200	.1347E+00	.2025E+00	.2033E+00	.2035E+00	.2037E+00	.2039E+00	.2041E+00	.2044E+00	.2047E+00	.2054E+00	.1347E+00
.100	.1347E+00	.1771E+00	.1774E+00	.1778E+00	.1784E+00	.1790E+00	.1795E+00	.1801E+00	.1807E+00	.1812E+00	.1347E+00
.050	.1347E+00	.1199E+00	.1202E+00	.1209E+00	.1217E+00	.1225E+00	.1232E+00	.1239E+00	.1245E+00	.1250E+00	.1347E+00
.025	.1347E+00	.6988E-01	.7014E-01	.7065E-01	.7133E-01	.7191E-01	.7242E-01	.7290E-01	.7328E-01	.7366E-01	.1347E+00
0.000	.1347E+00	0.	0.	0.	0.	0.	0.	0.	0.	0.	0.
LENGTH		0.00	5.00	10.00	20.00	40.00	60.00	80.00	100.00	110.00	115.00	120.00

FIGURE 4-5

MDAC-STL ELECTROPHORESIS DATA REDUCTION
ORIGINATOR: D.W. RICHMAN 12/78

RUN NO. 2, TEST ENGINEER: C.F. WALKER
BUFFER FLOW 20.0 ML/MIN, INLET TEMP 7.5 C
FIELD STRENGTH 9.8 V/CM
BUFFER VERTICAL CENTERLINE VELOCITY

WIDTH										
8.250										
8.225										
8.200										
8.150										
8.050										
7.850										
7.219			.1556E+00	.1556E+00	.1659E+00	.1910E+00	.1506E+00			
6.188			.1695E+00	.1768E+00	.1702E+00	.1735E+00	.1489E+00			
5.156			.1727E+00	.1765E+00	.1697E+00	.1737E+00	.1438E+00			
4.125			.1721E+00	.1765E+00	.1697E+00	.1744E+00	.1544E+00			
3.094			.1730E+00	.1720E+00	.1688E+00	.1679E+00	.1530E+00			
2.063			.1699E+00	.1715E+00	.1848E+00	.1921E+00	.1809E+00			
1.031			R	R	R	R	R			
.400										
.200										
.100										
.050										
.025										
0.000										
LENGTH	0.00	5.00	10.00	20.00	40.00	60.00	80.00	100.00	110.00	115.00	120.00

HEIGHTS > DATA < P

FIGURE 4-6

MDAC-STL ELECTROPHORESIS ANALYSIS PROGRAM
ORIGINATOR: D.W. RICHMAN 9/78

RUN NO. 2, TEST ENGINEER: C.D. WALKER
BUFFER FLOW 10.0 ML/MIN, INLET TEMP 7.5 C
FIELD STRENGTH 9.8 V/CM
BUFFER VERTICAL CENTERLINE VELOCITY

WIDTH											
8.250	.1347E+00	0.	0.	0.	0.	0.	0.	0.	0.	0.	0.
8.225	.1347E+00	.7295E-01	.7390E-01	.7341E-01	.7356E-01	.7421E-01	.7506E-01	.7580E-01	.7740E-01	.8043E-01	.1347E+00
8.200	.1347E+00	.1258E+00	.1274E+00	.1261E+00	.1260E+00	.1268E+00	.1282E+00	.1292E+00	.1321E+00	.1374E+00	.1347E+00
8.150	.1347E+00	.1851E+00	.1875E+00	.1855E+00	.1847E+00	.1855E+00	.1869E+00	.1880E+00	.1916E+00	.1985E+00	.1347E+00
8.050	.1347E+00	.2066E+00	.2094E+00	.2084E+00	.2080E+00	.2085E+00	.2094E+00	.2102E+00	.2126E+00	.2176E+00	.1347E+00
7.850	.1347E+00	.2056E+00	.2075E+00	.2073E+00	.2073E+00	.2076E+00	.2083E+00	.2085E+00	.2095E+00	.2117E+00	.1347E+00
7.219	.1347E+00	.2047E+00	.2042E+00	.2063E+00	.2063E+00	.2066E+00	.2069E+00	.2072E+00	.2079E+00	.2093E+00	.1347E+00
6.188	.1347E+00	.2043E+00	.2057E+00	.2057E+00	.2058E+00	.2060E+00	.2062E+00	.2065E+00	.2071E+00	.2082E+00	.1347E+00
5.156	.1347E+00	.2043E+00	.2057E+00	.2057E+00	.2058E+00	.2060E+00	.2062E+00	.2065E+00	.2071E+00	.2082E+00	.1347E+00
4.125	.1347E+00	.2043E+00	.2057E+00	.2057E+00	.2058E+00	.2060E+00	.2062E+00	.2065E+00	.2071E+00	.2082E+00	.1347E+00
3.094	.1347E+00	.2043E+00	.2057E+00	.2057E+00	.2058E+00	.2060E+00	.2062E+00	.2065E+00	.2071E+00	.2082E+00	.1347E+00
2.063	.1347E+00	.2043E+00	.2057E+00	.2057E+00	.2058E+00	.2060E+00	.2062E+00	.2065E+00	.2071E+00	.2082E+00	.1347E+00
1.031	.1347E+00	.2047E+00	.2042E+00	.2062E+00	.2063E+00	.2065E+00	.2068E+00	.2072E+00	.2078E+00	.2091E+00	.1347E+00
.400	.1347E+00	.2055E+00	.2074E+00	.2072E+00	.2072E+00	.2075E+00	.2079E+00	.2084E+00	.2094E+00	.2115E+00	.1347E+00
.200	.1347E+00	.2061E+00	.2092E+00	.2083E+00	.2080E+00	.2087E+00	.2099E+00	.2108E+00	.2135E+00	.2189E+00	.1347E+00
.100	.1347E+00	.1858E+00	.1890E+00	.1873E+00	.1870E+00	.1884E+00	.1906E+00	.1924E+00	.1973E+00	.2065E+00	.1347E+00
.050	.1347E+00	.1281E+00	.1309E+00	.1296E+00	.1299E+00	.1316E+00	.1338E+00	.1356E+00	.1401E+00	.1487E+00	.1347E+00
.025	.1347E+00	.7477E-01	.7663E-01	.7611E-01	.7661E-01	.7783E-01	.7929E-01	.8051E-01	.8332E-01	.8869E-01	.1347E+00
0.000	.1347E+00	0.	0.	0.	0.	0.	0.	0.	0.	0.	0.
LENGTH	0.00	5.00	10.00	20.00	40.00	60.00	80.00	100.00	110.00	115.00	120.00

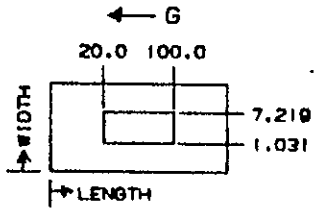

FIGURE 4-7

MOAC-SIL ELECTROPHORESIS DATA REDUCTION
ORIGINATOR: D.W. RICHMAN 12/79

RUN NO. 3, TEST ENGINEER: C.D. WALKER
BUFFER FLOW 20.0 ML/MIN, INLET TEMP 7.7 C
FIELD STRENGTH 20.0 V/CM
BUFFER VERTICAL CENTERLINE VELOCITY

WIDTH										
8.250										
8.225										
8.200										
8.150										
8.050										
7.850										
7.219			.1305E+00	.1272E+00	.1310E+00	.9895E-01	R			
6.188			.1379E+00	.1433E+00	.1128E+00	.1164E+00	R			
5.156			.1538E+00	.1437E+00	.1411E+00	.1390E+00	.1096E+00			
4.125			.1654E+00	.1452E+00	.1583E+00	.1439E+00	.1386E+00			
3.094			.1717E+00	.1428E+00	.1704E+00	.2440E+00	.3339E+00			
2.063			.1717E+00	.2021E+00	.3347E+00	.2633E+00	R			
1.031			.6148E+00	.2936E+00	R	R	R			
.400										
.200										
.100										
.050										
.025										
0.000										
LENGTH	0.00	5.00	10.00	20.00	40.00	60.00	80.00	100.00	110.00	115.00	120.00

HEIGHTS > DATA = R

FIGURE 4-8

MDAC-STL ELECTROPHORESIS ANALYSIS PROGRAM
ORIGINATOR: D.W. RICHMAN 9/78

RUN NO.' 3, TEST ENGINEER: C.D. WALKER
BUFFER FLOW 10.0 ML/MIN, INLET TEMP 7.2 C
FIELD STRENGTH 20.0 V/CM
BUFFER VERTICAL CENTERLINE VELOCITY
WIDTH

8.253	.1347E+00	0.	0.	0.	0.	0.	0.	0.	0.	0.	0.
8.225	.1347E+00	.8561E-01	.9172E-01	.8590E-01	.8384E-01	.8519E-01	.8795E-01	.9009E-01	.9891E-01	.1207E+00	.1347E+00
8.200	.1347E+00	.1507E+00	.1618E+00	.1494E+00	.1444E+00	.1462E+00	.1508E+00	.1543E+00	.1703E+00	.2108E+00	.1347E+00
8.150	.1347E+00	.2177E+00	.2336E+00	.2176E+00	.2100E+00	.2117E+00	.2173E+00	.2214E+00	.2419E+00	.2958E+00	.1347E+00
8.050	.1347E+00	.2220E+00	.2331E+00	.2261E+00	.2227E+00	.2243E+00	.2280E+00	.2309E+00	.2430E+00	.2732E+00	.1347E+00
7.850	.1347E+00	.2071E+00	.2110E+00	.2096E+00	.2089E+00	.2096E+00	.2108E+00	.2119E+00	.2154E+00	.2229E+00	.1347E+00
7.219	.1347E+00	.2031E+00	.2055E+00	.2050E+00	.2048E+00	.2052E+00	.2058E+00	.2064E+00	.2081E+00	.2114E+00	.1347E+00
6.188	.1347E+00	.2023E+00	.2042E+00	.2038E+00	.2037E+00	.2040E+00	.2045E+00	.2050E+00	.2062E+00	.2089E+00	.1347E+00
5.156	.1347E+00	.2023E+00	.2042E+00	.2038E+00	.2037E+00	.2040E+00	.2045E+00	.2050E+00	.2062E+00	.2089E+00	.1347E+00
4.125	.1347E+00	.2023E+00	.2042E+00	.2038E+00	.2037E+00	.2040E+00	.2045E+00	.2050E+00	.2062E+00	.2089E+00	.1347E+00
3.094	.1347E+00	.2023E+00	.2042E+00	.2038E+00	.2037E+00	.2040E+00	.2045E+00	.2050E+00	.2062E+00	.2089E+00	.1347E+00
2.063	.1347E+00	.2023E+00	.2042E+00	.2038E+00	.2037E+00	.2040E+00	.2045E+00	.2050E+00	.2062E+00	.2089E+00	.1347E+00
1.031	.1347E+00	.2031E+00	.2054E+00	.2049E+00	.2047E+00	.2050E+00	.2057E+00	.2063E+00	.2079E+00	.2112E+00	.1347E+00
.400	.1347E+00	.2069E+00	.2108E+00	.2094E+00	.2087E+00	.2094E+00	.2106E+00	.2117E+00	.2152E+00	.2227E+00	.1347E+00
.200	.1347E+00	.2219E+00	.2335E+00	.2271E+00	.2243E+00	.2267E+00	.2314E+00	.2355E+00	.2497E+00	.2853E+00	.1347E+00
.100	.1347E+00	.2271E+00	.2494E+00	.2316E+00	.2249E+00	.2302E+00	.2406E+00	.2491E+00	.2819E+00	.3728E+00	.1347E+00
.050	.1347E+00	.1711E+00	.1917E+00	.1729E+00	.1675E+00	.1736E+00	.1845E+00	.1931E+00	.2268E+00	.3161E+00	.1347E+00
.025	.1347E+00	.1010E+00	.1138E+00	.1032E+00	.1010E+00	.1055E+00	.1127E+00	.1185E+00	.1399E+00	.1947E+00	.1347E+00
0.000	.1347E+00	0.	0.	0.	0.	0.	0.	0.	0.	0.	0.
LENGTH		0.00	5.00	10.00	20.00	40.00	60.00	80.00	100.00	110.00	115.00	120.00

FIGURE 4-9

MDAC-STL ELECTROPHORESIS DATA REDUCTION
ORIGINATOR: D.W. RICHMAN 12/79

RUN NO. 4. TEST ENGINEER: C.C. WALKER
BUFFER FLOW 30.0 ML/MIN. INLET TEMP 6.3 C
FIELD STRENGTH 0.0 V/CM
BUFFER VERTICAL CENTERLINE VELOCITY

WIDTH											
8.250											
8.225											
8.200											
8.150											
8.050											
7.850											
7.219				.2688E+00	.2894E+00	.2847E+00	.2774E+00	.2683E+00			
6.188				.2795E+00	.2796E+00	.2836E+00	.2981E+00	.2689E+00			
5.156				.2929E+00	.2823E+00	.2874E+00	.2922E+00	.2858E+00			
4.125				.3083E+00	.2831E+00	.2912E+00	.2987E+00	.2825E+00			
3.094				.3229E+00	.2785E+00	.2876E+00	.3159E+00	.2829E+00			
2.063				.3474E+00	.2758E+00	.2769E+00	.2998E+00	.2811E+00			
1.031				.2774E+00	.2747E+00	.2731E+00	.2974E+00	.2816E+00			
.400											
.200											
.100											
.050											
.025											
0.000											
LENGTH	0.00	5.00	10.00	20.00	40.00	60.00	80.00	100.00	110.00	115.00	120.00

HEIGHTS > DATA = R

FIGURE 4-10

MDAC-STL ELECTROPHORESIS ANALYSIS PROGRAM
ORIGINATOR: D.W. RICHMAN 9/78

RUN NO. 4, TEST ENGINEER: C.D. WALKER
BUFFER FLOW 15.0 ML/MIN, INLET TEMP 6.3 C
FIELD STRENGTH 0.0 V/CM
BUFFER VERTICAL CENTERLINE VELOCITY

WIDTH												
8.250	.2020E+00	0.	0.	0.	0.	0.	0.	0.	0.	0.	0.	
8.225	.2020E+00	.1050E+00	.1052E+00	.1054E+00	.1058E+00	.1062E+00	.1065E+00	.1069E+00	.1072E+00	.1076E+00	.2020E+00	
8.200	.2020E+00	.1801E+00	.1803E+00	.1806E+00	.1811E+00	.1816E+00	.1821E+00	.1826E+00	.1831E+00	.1837E+00	.2020E+00	
8.150	.2020E+00	.2656E+00	.2660E+00	.2663E+00	.2667E+00	.2671E+00	.2675E+00	.2679E+00	.2683E+00	.2691E+00	.2020E+00	
8.050	.2020E+00	.3036E+00	.3050E+00	.3052E+00	.3054E+00	.3056E+00	.3058E+00	.3061E+00	.3064E+00	.3075E+00	.2020E+00	
7.850	.2020E+00	.3079E+00	.3095E+00	.3097E+00	.3099E+00	.3100E+00	.3102E+00	.3105E+00	.3108E+00	.3120E+00	.2020E+00	
7.219	.2020E+00	.3080E+00	.3096E+00	.3098E+00	.3100E+00	.3101E+00	.3103E+00	.3104E+00	.3109E+00	.3121E+00	.2020E+00	
6.188	.2020E+00	.3079E+00	.3095E+00	.3096E+00	.3098E+00	.3099E+00	.3101E+00	.3103E+00	.3106E+00	.3117E+00	.2020E+00	
5.156	.2020E+00	.3077E+00	.3095E+00	.3096E+00	.3098E+00	.3099E+00	.3101E+00	.3103E+00	.3106E+00	.3117E+00	.2020E+00	
4.125	.2020E+00	.3079E+00	.3095E+00	.3096E+00	.3098E+00	.3099E+00	.3101E+00	.3103E+00	.3106E+00	.3117E+00	.2020E+00	
3.094	.2020E+00	.3079E+00	.3095E+00	.3096E+00	.3098E+00	.3099E+00	.3101E+00	.3103E+00	.3106E+00	.3117E+00	.2020E+00	
2.063	.2020E+00	.3079E+00	.3095E+00	.3096E+00	.3098E+00	.3099E+00	.3101E+00	.3103E+00	.3106E+00	.3117E+00	.2020E+00	
1.031	.2020E+00	.3079E+00	.3096E+00	.3098E+00	.3099E+00	.3101E+00	.3103E+00	.3105E+00	.3108E+00	.3120E+00	.2020E+00	
.400	.2020E+00	.3078E+00	.3095E+00	.3096E+00	.3098E+00	.3100E+00	.3102E+00	.3104E+00	.3107E+00	.3118E+00	.2020E+00	
.200	.2020E+00	.3036E+00	.3050E+00	.3053E+00	.3055E+00	.3057E+00	.3060E+00	.3062E+00	.3066E+00	.3078E+00	.2020E+00	
.100	.2020E+00	.2656E+00	.2662E+00	.2667E+00	.2673E+00	.2679E+00	.2685E+00	.2691E+00	.2696E+00	.2705E+00	.2020E+00	
.050	.2020E+00	.1801E+00	.1806E+00	.1813E+00	.1822E+00	.1830E+00	.1837E+00	.1844E+00	.1850E+00	.1857E+00	.2020E+00	
.025	.2020E+00	.1050E+00	.1054E+00	.1059E+00	.1066E+00	.1073E+00	.1079E+00	.1083E+00	.1087E+00	.1092E+00	.2020E+00	
0.000	.2020E+00	0.	0.	0.	0.	0.	0.	0.	0.	0.	0.	
LENGTH	0.00	5.00	10.00	20.00	40.00	60.00	80.00	100.00	110.00	115.00	120.00	

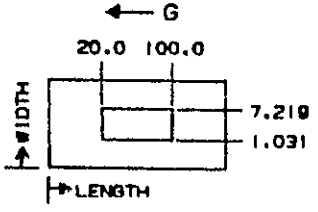

FIGURE 4-11

MCAC-STL ELECTROPHORESIS DATA REDUCTION
ORIGINATOR: D.W. RICHMAN 12/78

RUN NO. 5, TEST ENGINEER: C.O. WALKER
BUFFER FLOW 30.0 ML/MIN, INLET TEMP 6.7 C
FIELD STRENGTH 10.1 V/CM
BUFFER VERTICAL CENTERLINE VELOCITY

WIDTH										
8.250										
8.225										
8.200										
8.150										
8.050										
7.850										
7.219				.2853E+00	.2636E+00	-.1175E+01	.4041E+00	.2974E+00		
6.188				.2930E+00	.2659E+00	.2591E+00	.3279E+00	.3498E+00		
5.156				.3026E+00	.2670E+00	.2615E+00	.3181E+00	.3752E+00		
4.125				.3013E+00	.2647E+00	.2588E+00	.3080E+00	.3680E+00		
3.094				.2945E+00	.2615E+00	.2498E+00	.3014E+00	.3690E+00		
2.063				.2886E+00	.2503E+00	.2492E+00	.3200E+00	.4105E+00		
1.031				R	R	R	R	R		
.400										
.200										
.100										
.050										
.025										
0.000										
LENGTH	.0.00	5.00	10.00	20.00	40.00	60.00	80.00	100.00	110.00	115.00	120.00

HEIGHTS > DATA = R

FIGURE 4-12

MDAC-STL ELECTROPHORESIS ANALYSIS PROGRAM
ORIGINATOR: D.W. RICHMAN 9/78

RUN NO. 5, TEST ENGINEER: C.O. WALKER
BUFFER FLOW 15.0 ML/MIN, INLET TEMP 6.7 C
FIELD STRENGTH 10.1 V/CM
BUFFER VERTICAL CENTERLINE VELOCITY
WIDTH

8.250	.2020E+00	0.	0.	0.	0.	0.	0.	0.	0.	0.	0.
8.225	.2020E+00	.1074E+00	.1085E+00	.1081E+00	.1083E+00	.1089E+00	.1098E+00	.1104E+00	.1119E+00	.1148E+00	.2020E+00
8.200	.2020E+00	.1853E+00	.1869E+00	.1858E+00	.1857E+00	.1865E+00	.1877E+00	.1888E+00	.1914E+00	.1965E+00	.2020E+00
8.150	.2020E+00	.2730E+00	.2756E+00	.2738E+00	.2731E+00	.2738E+00	.2751E+00	.2761E+00	.2794E+00	.2862E+00	.2020E+00
8.050	.2020E+00	.3074E+00	.3107E+00	.3098E+00	.3094E+00	.3099E+00	.3109E+00	.3115E+00	.3138E+00	.3190E+00	.2020E+00
7.850	.2020E+00	.3082E+00	.3106E+00	.3105E+00	.3105E+00	.3108E+00	.3112E+00	.3117E+00	.3127E+00	.3153E+00	.2020E+00
7.219	.2020E+00	.3074E+00	.3095E+00	.3096E+00	.3097E+00	.3099E+00	.3102E+00	.3106E+00	.3112E+00	.3130E+00	.2020E+00
6.188	.2020E+00	.3072E+00	.3091E+00	.3091E+00	.3092E+00	.3094E+00	.3097E+00	.3100E+00	.3105E+00	.3121E+00	.2020E+00
5.156	.2020E+00	.3072E+00	.3091E+00	.3091E+00	.3092E+00	.3094E+00	.3097E+00	.3100E+00	.3105E+00	.3121E+00	.2020E+00
4.125	.2020E+00	.3072E+00	.3091E+00	.3091E+00	.3092E+00	.3094E+00	.3097E+00	.3100E+00	.3105E+00	.3121E+00	.2020E+00
3.094	.2020E+00	.3072E+00	.3091E+00	.3091E+00	.3092E+00	.3094E+00	.3097E+00	.3100E+00	.3105E+00	.3121E+00	.2020E+00
2.063	.2020E+00	.3072E+00	.3091E+00	.3091E+00	.3092E+00	.3094E+00	.3097E+00	.3100E+00	.3105E+00	.3121E+00	.2020E+00
1.031	.2020E+00	.3074E+00	.3095E+00	.3095E+00	.3096E+00	.3098E+00	.3101E+00	.3105E+00	.3111E+00	.3129E+00	.2020E+00
.400	.2020E+00	.3081E+00	.3105E+00	.3104E+00	.3104E+00	.3107E+00	.3111E+00	.3116E+00	.3125E+00	.3150E+00	.2020E+00
.200	.2020E+00	.3072E+00	.3106E+00	.3098E+00	.3095E+00	.3102E+00	.3112E+00	.3122E+00	.3148E+00	.3204E+00	.2020E+00
.100	.2020E+00	.2738E+00	.2773E+00	.2756E+00	.2753E+00	.2767E+00	.2788E+00	.2805E+00	.2852E+00	.2944E+00	.2020E+00
.050	.2020E+00	.1878E+00	.1906E+00	.1894E+00	.1897E+00	.1914E+00	.1936E+00	.1954E+00	.1998E+00	.2082E+00	.2020E+00
.025	.2020E+00	.1096E+00	.1115E+00	.1110E+00	.1115E+00	.1128E+00	.1142E+00	.1155E+00	.1182E+00	.1236E+00	.2020E+00
0.000	.2020E+00	0.	0.	0.	0.	0.	0.	0.	0.	0.	0.
LENGTH	0.00	5.00	10.00	20.00	40.00	60.00	80.00	100.00	110.00	115.00	120.00

FIGURE 4-13

MDAC-STL ELECTROPHORESIS DATA REDUCTION
ORIGINATOR: D.W. RICHMAN 12/78

RUN NO. 6. TEST ENGINEER: C.D. WALKER
BUFFER FLOW 30.0 ML/MIN. INLET TEMP 6.3 C
FIELD STRENGTH 20.2 V/CM
BUFFER VERTICAL CENTERLINE VELOCITY

WIDTH										
8.250										
8.225										
8.200										
8.150										
8.050										
7.850										
7.219			.2341E+00	.2472E+00	.2170E+00	.1965E+00	.1852E+00			
6.188			.2442E+00	.2432E+00	.2166E+00	.2294E+00	.3130E+00			
5.156			.2516E+00	.2433E+00	.2331E+00	.2406E+00	.2798E+00			
4.125			.2552E+00	.2469E+00	.2349E+00	.2430E+00	.3121E+00			
3.094			.2523E+00	.2534E+00	.2359E+00	.2335E+00	.3270E+00			
2.063			.7466E+00	.2604E+00	.3801E+00	.1233E+01	-.3790E+00			
1.031			R	R	R	R	R			
.400										
.200										
.100										
.050										
.025										
0.000										
LENGTH	0.00	5.00	10.00	20.00	40.00	60.00	80.00	100.00	110.00	115.00	120.00

HEIGHTS > DATA = R

FIGURE 4-14

MDAC-STL ELECTROPHORESIS ANALYSIS PROGRAM
ORIGINATOR: D.W. RICHMAN 9/78

RUN NO. 6, TEST ENGINEER: C.D. WALKER
BUFFER FLOW 15.0 ML/MIN, INLET TEMP 6.3 C
FIELD STRENGTH 20.2 V/CM
BUFFER VERTICAL CENTERLINE VELOCITY
WIDTH

8.250	.2020E+00	0.	0.	0.	0.	0.	0.	0.	0.	0.	0.
8.225	.2020E+00	.1195E+00	.1255E+00	.1204E+00	.1166E+00	.1200E+00	.1224E+00	.1246E+00	.1328E+00	.1534E+00	.2020E+00
8.200	.2020E+00	.2089E+00	.2196E+00	.2083E+00	.2038E+00	.2056E+00	.2100E+00	.2133E+00	.2284E+00	.2666E+00	.2020E+00
8.150	.2020E+00	.3029E+00	.3185E+00	.3038E+00	.2969E+00	.2987E+00	.3041E+00	.3079E+00	.3273E+00	.3774E+00	.2020E+00
8.050	.2020E+00	.3206E+00	.3315E+00	.3255E+00	.3224E+00	.3239E+00	.3274E+00	.3302E+00	.3414E+00	.3694E+00	.2020E+00
7.850	.2020E+00	.3091E+00	.3134E+00	.3122E+00	.3116E+00	.3123E+00	.3134E+00	.3144E+00	.3176E+00	.3248E+00	.2020E+00
7.219	.2020E+00	.3058E+00	.3085E+00	.3087E+00	.3080E+00	.3084E+00	.3090E+00	.3096E+00	.3111E+00	.3146E+00	.2020E+00
6.188	.2020E+00	.3052E+00	.3076E+00	.3073E+00	.3072E+00	.3075E+00	.3080E+00	.3085E+00	.3097E+00	.3127E+00	.2020E+00
5.156	.2020E+00	.3052E+00	.3076E+00	.3073E+00	.3072E+00	.3075E+00	.3080E+00	.3085E+00	.3097E+00	.3126E+00	.2020E+00
4.125	.2020E+00	.3052E+00	.3076E+00	.3073E+00	.3072E+00	.3075E+00	.3080E+00	.3085E+00	.3097E+00	.3126E+00	.2020E+00
3.094	.2020E+00	.3052E+00	.3076E+00	.3073E+00	.3072E+00	.3075E+00	.3080E+00	.3085E+00	.3097E+00	.3126E+00	.2020E+00
2.063	.2020E+00	.3052E+00	.3076E+00	.3073E+00	.3072E+00	.3075E+00	.3080E+00	.3085E+00	.3097E+00	.3127E+00	.2020E+00
1.031	.2020E+00	.3057E+00	.3085E+00	.3081E+00	.3079E+00	.3083E+00	.3089E+00	.3094E+00	.3109E+00	.3144E+00	.2020E+00
.400	.2020E+00	.3093E+00	.3132E+00	.3120E+00	.3114E+00	.3121E+00	.3132E+00	.3143E+00	.3174E+00	.3246E+00	.2020E+00
.200	.2020E+00	.3207E+00	.3322E+00	.3265E+00	.3240E+00	.3263E+00	.3307E+00	.3345E+00	.3476E+00	.3804E+00	.2020E+00
.100	.2020E+00	.3125E+00	.3341E+00	.3175E+00	.3110E+00	.3161E+00	.3261E+00	.3344E+00	.3655E+00	.4492E+00	.2020E+00
.050	.2020E+00	.2303E+00	.2500E+00	.2317E+00	.2264E+00	.2323E+00	.2429E+00	.2514E+00	.2838E+00	.3683E+00	.2020E+00
.025	.2020E+00	.1359E+00	.1484E+00	.1379E+00	.1357E+00	.1401E+00	.1471E+00	.1529E+00	.1737E+00	.2264E+00	.2020E+00
0.000	.2020E+00	0.	0.	0.	0.	0.	0.	0.	0.	0.	0.
LENGTH	0.00	5.00	10.00	20.00	40.00	60.00	80.00	100.00	110.00	115.00	120.00

FIGURE 4-15

MDAC-STL ELECTROPHORESIS DATA REDUCTION
ORIGINATOR: D.W. RICHMAN 12/79

RUN NO. 7, TEST ENGINEER: C.D. WALKER
BUFFER FLOW 40.0 ML/MIN, INLET TEMP 6.9 C
FIELD STRENGTH 0.0 V/CM
BUFFER VERTICAL CENTERLINE VELOCITY

WIDTH										
8.250										
8.225										
8.200										
8.150										
8.050										
7.850										
7.219			-.1972E+00	.4239E+00	.3788E+00	.3812E+00	.3943E+00			
6.188			.3558E+00	.3708E+00	.3966E+00	.3999E+00	.3899E+00			
5.156			.3669E+00	.3791E+00	.3841E+00	.3977E+00	.3796E+00			
4.125			.3699E+00	.3843E+00	.3954E+00	.4171E+00	.3938E+00			
3.094			.3680E+00	.3799E+00	.3868E+00	.4105E+00	.3961E+00			
2.063			.3557E+00	.3604E+00	.3904E+00	.3914E+00	.3953E+00			
1.031			.3462E+00	.3540E+00	.4032E+00	.3818E+00	.4033E+00			
.490										
.200										
.100										
.050										
.025										
0.000										
LENGTH	0.00	5.00	10.00	20.00	40.00	60.00	80.00	100.00	110.00	115.00	120.00

HEIGHTS > DATA = R

FIGURE 4-16

MDAC-STL ELECTROPHORESIS ANALYSIS PROGRAM
ORIGINATOR: D.W. RICHMAN 9/78

RUN NO. 7, TEST ENGINEER: C.D. WALKER
BUFFER FLOW 20.0 ML/MIN, INLET TEMP 6.9 C
FIELD STRENGTH 0.0 V/CM
BUFFER VERTICAL CENTERLINE VELOCITY
WIDTH

8.250	.2694E+00	0.	0.	0.	0.	0.	0.	0.	0.	0.	0.
8.225	.2694E+00	.1398E+00	.1399E+00	.1401E+00	.1405E+00	.1409E+00	.1414E+00	.1418E+00	.1421E+00	.1427E+00	.2694E+00
8.200	.2694E+00	.2398E+00	.2400E+00	.2402E+00	.2408E+00	.2414E+00	.2419E+00	.2425E+00	.2430E+00	.2438E+00	.2694E+00
8.150	.2694E+00	.3541E+00	.3547E+00	.3549E+00	.3553E+00	.3557E+00	.3561E+00	.3566E+00	.3570E+00	.3581E+00	.2694E+00
8.050	.2694E+00	.4047E+00	.4070E+00	.4073E+00	.4075E+00	.4077E+00	.4079E+00	.4082E+00	.4086E+00	.4106E+00	.2694E+00
7.950	.2694E+00	.4102E+00	.4130E+00	.4133E+00	.4135E+00	.4137E+00	.4139E+00	.4143E+00	.4148E+00	.4169E+00	.2694E+00
7.719	.2694E+00	.4104E+00	.4132E+00	.4134E+00	.4136E+00	.4139E+00	.4141E+00	.4144E+00	.4149E+00	.4170E+00	.2694E+00
6.188	.2694E+00	.4101E+00	.4128E+00	.4130E+00	.4131E+00	.4133E+00	.4135E+00	.4138E+00	.4141E+00	.4161E+00	.2694E+00
5.156	.2694E+00	.4101E+00	.4128E+00	.4130E+00	.4131E+00	.4132E+00	.4135E+00	.4137E+00	.4141E+00	.4161E+00	.2694E+00
4.125	.2694E+00	.4101E+00	.4128E+00	.4130E+00	.4131E+00	.4132E+00	.4135E+00	.4137E+00	.4141E+00	.4161E+00	.2694E+00
3.094	.2694E+00	.4101E+00	.4128E+00	.4130E+00	.4131E+00	.4132E+00	.4135E+00	.4137E+00	.4141E+00	.4161E+00	.2694E+00
2.063	.2694E+00	.4101E+00	.4128E+00	.4130E+00	.4131E+00	.4133E+00	.4135E+00	.4139E+00	.4141E+00	.4161E+00	.2694E+00
1.031	.2694E+00	.4103E+00	.4131E+00	.4134E+00	.4136E+00	.4137E+00	.4140E+00	.4143E+00	.4148E+00	.4168E+00	.2694E+00
.400	.2694E+00	.4101E+00	.4129E+00	.4132E+00	.4133E+00	.4135E+00	.4138E+00	.4141E+00	.4146E+00	.4166E+00	.2694E+00
.200	.2694E+00	.4046E+00	.4070E+00	.4073E+00	.4075E+00	.4077E+00	.4080E+00	.4084E+00	.4088E+00	.4108E+00	.2694E+00
.100	.2694E+00	.3541E+00	.3549E+00	.3554E+00	.3561E+00	.3569E+00	.3574E+00	.3581E+00	.3587E+00	.3600E+00	.2694E+00
.050	.2694E+00	.2398E+00	.2403E+00	.2410E+00	.2421E+00	.2431E+00	.2440E+00	.2448E+00	.2455E+00	.2465E+00	.2694E+00
.025	.2694E+00	.1397E+00	.1401E+00	.1407E+00	.1415E+00	.1423E+00	.1430E+00	.1435E+00	.1440E+00	.1448E+00	.2694E+00
0.000	.2694E+00	0.	0.	0.	0.	0.	0.	0.	0.	0.	0.
LENGTH		0.00	5.00	10.00	20.00	40.00	60.00	80.00	100.00	110.00	115.00	120.00

FIGURE 4-17

NOAC-STL ELECTROPHORESIS DATA REDUCTION
ORIGINATOR: D.W. RICHMAN 12/78

RUN NO. 8, TEST ENGINEER: C.D. WALKER
BUFFER FLOW 40.0 ML/MIN, INLET TEMP 6.9 C
FIELD STRENGTH 10.2 V/CM
BUFFER VERTICAL CENTERLINE VELOCITY

WIDTH											
8.250											
8.225											
8.200											
8.150											
8.050											
7.850											
7.219				.3470E+00	.3636E+00	.3785E+00	.5119E+00	.2293E+00			
6.188				.3534E+00	.3774E+00	.3852E+00	.4056E+00	.3276E+00			
5.156				.3654E+00	.3801E+00	.3853E+00	.4125E+00	.3569E+00			
4.125				.3691E+00	.3770E+00	.3832E+00	.4094E+00	.3589E+00			
3.094				.3618E+00	.3742E+00	.3800E+00	.4079E+00	.3454E+00			
2.063				.3445E+00	.3675E+00	.3435E+00	.5220E+00	.3807E+00			
1.031				.3585E+00	.3501E+00	.1635E+01	.2194E+00	.5653E+00			
.400											
.200											
.100											
.050											
.025											
0.000											
LENGTH	0.00	5.00	10.00	20.00	40.00	60.00	80.00	100.00	110.00	115.00	120.00

HEIGHTS > DATA = R

FIGURE 4-18

MDAC-STL ELECTROPHORESIS ANALYSIS PROGRAM
ORIGINATOR: D.W. RICHMAN 9/78

RUN NO. 8. TEST ENGINEER: C.D. WALKER
BUFFER FLOW 20.0 ML/MIN. INLET TEMP 6.9 C
FIELD STRENGTH 10.2 V/CM
BUFFER VERTICAL CENTERLINE VELOCITY

WIDTH											
8.250	.2694E+00	0.	0.	0.	0.	0.	0.	0.	0.	0.	0.
8.225	.2694E+00	.1428E+00	.1440E+00	.1436E+00	.1440E+00	.1448E+00	.1457E+00	.1466E+00	.1483E+00	.1517E+00	.2694E+00
8.200	.2694E+00	.2460E+00	.2480E+00	.2468E+00	.2469E+00	.2478E+00	.2493E+00	.2506E+00	.2536E+00	.2596E+00	.2694E+00
8.150	.2694E+00	.3626E+00	.3659E+00	.3639E+00	.3641E+00	.3640E+00	.3655E+00	.3668E+00	.3706E+00	.3786E+00	.2694E+00
8.050	.2694E+00	.4088E+00	.4134E+00	.4125E+00	.4120E+00	.4125E+00	.4136E+00	.4145E+00	.4172E+00	.4239E+00	.2694E+00
7.950	.2694E+00	.4104E+00	.4140E+00	.4140E+00	.4139E+00	.4143E+00	.4148E+00	.4154E+00	.4167E+00	.4203E+00	.2694E+00
7.219	.2694E+00	.4096E+00	.4123E+00	.4129E+00	.4130E+00	.4133E+00	.4136E+00	.4141E+00	.4149E+00	.4177E+00	.2694E+00
6.188	.2694E+00	.4092E+00	.4123E+00	.4123E+00	.4124E+00	.4127E+00	.4130E+00	.4134E+00	.4141E+00	.4166E+00	.2694E+00
5.156	.2694E+00	.4092E+00	.4123E+00	.4123E+00	.4124E+00	.4126E+00	.4130E+00	.4134E+00	.4141E+00	.4166E+00	.2694E+00
4.125	.2694E+00	.4092E+00	.4123E+00	.4123E+00	.4124E+00	.4126E+00	.4130E+00	.4134E+00	.4141E+00	.4166E+00	.2694E+00
3.094	.2694E+00	.4092E+00	.4123E+00	.4123E+00	.4124E+00	.4126E+00	.4130E+00	.4134E+00	.4141E+00	.4166E+00	.2694E+00
2.063	.2694E+00	.4092E+00	.4123E+00	.4123E+00	.4124E+00	.4127E+00	.4130E+00	.4134E+00	.4141E+00	.4166E+00	.2694E+00
1.031	.2694E+00	.4095E+00	.4127E+00	.4128E+00	.4129E+00	.4132E+00	.4135E+00	.4140E+00	.4148E+00	.4175E+00	.2694E+00
.400	.2694E+00	.4103E+00	.4139E+00	.4138E+00	.4139E+00	.4141E+00	.4146E+00	.4152E+00	.4164E+00	.4200E+00	.2694E+00
.200	.2694E+00	.4095E+00	.4132E+00	.4124E+00	.4121E+00	.4128E+00	.4141E+00	.4152E+00	.4182E+00	.4254E+00	.2694E+00
.100	.2694E+00	.3635E+00	.3679E+00	.3660E+00	.3659E+00	.3675E+00	.3699E+00	.3719E+00	.3772E+00	.3879E+00	.2694E+00
.050	.2694E+00	.2491E+00	.2529E+00	.2513E+00	.2518E+00	.2539E+00	.2563E+00	.2585E+00	.2635E+00	.2732E+00	.2694E+00
.025	.2694E+00	.1454E+00	.1477E+00	.1472E+00	.1480E+00	.1495E+00	.1512E+00	.1526E+00	.1558E+00	.1620E+00	.2694E+00
0.000	.2694E+00	0.	0.	0.	0.	0.	0.	0.	0.	0.	0.
LENGTH	0.00	5.00	10.00	20.00	40.00	60.00	80.00	100.00	110.00	115.00	120.00

FIGURE 4-19

MDAC-STL ELECTROPHORESIS DATA REDUCTION
ORIGINATOR: D.W. RICHMAN 12/79

RUN NO. 9, TEST ENGINEER: C.D. WALKER
BUFFER FLOW 40.0 ML/MIN, INLET TEMP 6.8 C
FIELD STRENGTH 20.2 V/CM
BUFFER VERTICAL CENTERLINE VELOCITY

WIDTH											
8.250											
8.225											
8.200											
8.150											
8.050											
7.850											
7.219				.3166E+00	.3700E+00	.3347E+00	.3633E+00	.2361E+00			
6.188				.3701E+00	.3556E+00	.3538E+00	.3590E+00	.3191E+00			
5.156				.3862E+00	.3626E+00	.3670E+00	.3478E+00	.3447E+00			
4.125				.3861E+00	.3624E+00	.3655E+00	.3524E+00	.3484E+00			
3.094				.3803E+00	.3512E+00	.3467E+00	.3590E+00	.3341E+00			
2.063				.3834E+00	.3544E+00	.3441E+00	.3716E+00	.3780E+00			
1.031				.4185E+00	R	R	R	R			
.400											
.200											
.100											
.050											
.025											
0.000											
LENGTH	0.00	5.00	10.00	20.00	40.00	60.00	80.00	100.00	110.00	115.00	120.00

HEIGHTS > DATA = R

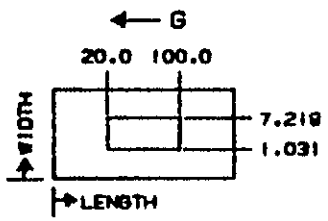

FIGURE 4-20

MDAC-STL ELECTROPHORESIS ANALYSIS PROGRAM
ORIGINATOR: D.W. RICHMAN 9/78

RUN NO. 9, TEST ENGINEER: C.D. WALKER
BUFFER FLOW 20.0 ML/MIN, INLET TEMP 6.8 C
FIELD STRENGTH 20.2 V/CM
BUFFER VERTICAL CENTERLINE VELOCITY

WIDTH											
8.250	.2694E+00	0.	0.	0.	0.	0.	0.	0.	0.	0.	0.
8.225	.2694E+00	.1957E+00	.1625E+00	.1573E+00	.1559E+00	.1579E+00	.1612E+00	.1638E+00	.1733E+00	.1965E+00	.2694E+00
8.200	.2694E+00	.2723E+00	.2844E+00	.2724E+00	.2680E+00	.2706E+00	.2760E+00	.2801E+00	.2975E+00	.3402E+00	.2694E+00
8.150	.2694E+00	.3972E+00	.4152E+00	.3991E+00	.3914E+00	.3937E+00	.4001E+00	.4047E+00	.4268E+00	.4829E+00	.2694E+00
8.050	.2694E+00	.4243E+00	.4382E+00	.4315E+00	.4280E+00	.4297E+00	.4338E+00	.4372E+00	.4504E+00	.4833E+00	.2694E+00
7.850	.2694E+00	.4115E+00	.4175E+00	.4162E+00	.4156E+00	.4163E+00	.4177E+00	.4191E+00	.4230E+00	.4324E+00	.2694E+00
7.219	.2694E+00	.4075E+00	.4117E+00	.4113E+00	.4111E+00	.4116E+00	.4123E+00	.4131E+00	.4150E+00	.4200E+00	.2694E+00
6.188	.2694E+00	.4067E+00	.4104E+00	.4101E+00	.4100E+00	.4104E+00	.4110E+00	.4116E+00	.4132E+00	.4173E+00	.2694E+00
5.156	.2694E+00	.4067E+00	.4104E+00	.4101E+00	.4100E+00	.4104E+00	.4110E+00	.4116E+00	.4131E+00	.4173E+00	.2694E+00
4.125	.2694E+00	.4067E+00	.4104E+00	.4101E+00	.4100E+00	.4104E+00	.4110E+00	.4116E+00	.4131E+00	.4173E+00	.2694E+00
3.094	.2694E+00	.4067E+00	.4104E+00	.4101E+00	.4100E+00	.4104E+00	.4110E+00	.4116E+00	.4131E+00	.4173E+00	.2694E+00
2.063	.2694E+00	.4067E+00	.4104E+00	.4101E+00	.4100E+00	.4104E+00	.4110E+00	.4116E+00	.4132E+00	.4173E+00	.2694E+00
1.031	.2694E+00	.4074E+00	.4114E+00	.4112E+00	.4110E+00	.4114E+00	.4122E+00	.4129E+00	.4148E+00	.4197E+00	.2694E+00
.400	.2694E+00	.4113E+00	.4173E+00	.4160E+00	.4153E+00	.4161E+00	.4175E+00	.4188E+00	.4227E+00	.4320E+00	.2694E+00
.200	.2694E+00	.4244E+00	.4389E+00	.4329E+00	.4300E+00	.4327E+00	.4379E+00	.4425E+00	.4579E+00	.4964E+00	.2694E+00
.100	.2694E+00	.4085E+00	.4334E+00	.4165E+00	.4096E+00	.4159E+00	.4277E+00	.4373E+00	.4728E+00	.5674E+00	.2694E+00
.050	.2694E+00	.2975E+00	.3216E+00	.3030E+00	.2979E+00	.3053E+00	.3176E+00	.3275E+00	.3650E+00	.4604E+00	.2694E+00
.025	.2694E+00	.1755E+00	.1909E+00	.1807E+00	.1789E+00	.1843E+00	.1926E+00	.1992E+00	.2235E+00	.2840E+00	.2694E+00
0.000	.2694E+00	0.	0.	0.	0.	0.	0.	0.	0.	0.	0.
LENGTH		0.00	5.00	10.00	20.00	40.00	60.00	80.00	100.00	110.00	115.00	120.00

FIGURE 4-21

The second nine tests given in the Figure 4-3 Task 1.0 Test Matrix used dye streams to determine horizontal centerline velocity. The reduced data for horizontal centerline velocity at 0 volts/cm and 20 ml/min is presented in Figure 4-22. The expected value of horizontal centerline velocity with no field applied is 0.0 cm/sec. From the reduced data, the predominant order of magnitude of the data is 10^{-4} cm/sec. This is larger than the analytically predicted values found in Figure 4-23. It is apparent from the test data that the magnitude of the values represent the limit of accuracy for the test method. Similar results are shown in the 0 volt/cm data presented in Figures 4-28 and 4-29 for a buffer flowrate of 30 ml/min and in Figures 4-34 and 4-35 for a buffer flowrate of 40 ml/min.

The reduced data for horizontal centerline velocity at 10 volts/cm and 20 ml/min buffer flowrate is presented in Figure 4-24. Here the horizontal centerline velocities appear to be grouped about a value of about 2×10^{-3} cm/sec. With voltage applied, the electrophoretic mobility and the electroosmotic return flow cause the dye streams to deflect toward the anode. This deflection is pictured at a buffer flowrate of 40 ml/min in Figure 1-7. The deflection causes all of the points at 1.031 cm and three of the points at 2.063 cm are outside of the first dye stream near the cathode, as indicated by the "0.'s" in the reduced data. The points were zeroed instead of extrapolating the test data, which would have been unreliable. The corresponding analytical predictions are presented in Figure 4-25. Here the horizontal centerline velocities within the reduced data field are nearly constant about 2×10^{-3} cm/sec toward the anode and the velocities decrease to zero at the membranes. Because of the magnitude of the measurement errors, as indicated by the scatter with no applied field as shown in Figure 4-22, no conclusions can be drawn with respect to trends of the data. Similar results are shown in Figures 4-30 and 4-31 for a buffer flowrate of 30 ml/min and by Figures 4-36 and 4-37 for a buffer flowrate of 40 ml/min.

The reduced data for horizontal centerline velocity at 20 volts/cm and 20 ml/min buffer flowrate is presented in Figure 4-26 and the corresponding analytical prediction in Figure 4-27. Here the analytical predictions show increased horizontal velocities, as would be expected at the higher voltage level. Similar results are shown by Figures 4-32 and 4-33 for a buffer flowrate of 30 ml/min and by Figures 4-38 and 4-39 for a buffer flowrate of 40 ml/min.

MOAC-SIL ELECTROPHORESIS DATA REDUCTION
ORIGINATOR: D.W. RICHMAN 12/78

RUN NO. 10, TEST ENGINEER: C.O. WALKER
BUFFER FLOW 20.0 ML/MIN. INLET TEMP 6.2 C
FIELD STRENGTH 0.0 V/CM
BUFFER HORIZONTAL CENTER.INE VELOCITY

WIDTH											
8.250											
8.225											
8.200											
8.150											
8.050											
7.850											
7.219				0.	.4050E-03	0.	0.	.1110E-02			
6.188				.2763E-02	.4543E-03	-.5498E-03	-.1192E-03	.4056E-03			
5.156				.2832E-02	.4012E-03	-.6554E-03	-.4404E-03	-.3011E-03			
4.125				.2711E-02	.3458E-03	-.6564E-03	-.5041E-03	-.5074E-03			
3.094				.1745E-02	.2571E-03	-.5347E-03	-.5038E-03	-.3015E-03			
2.063				.1471E-02	.3449E-03	-.1915E-03	-.3959E-03	-.8094E-03			
1.031				.7587E-03	0.	0.	0.	-.1530E-03			
.400											
.200											
.100											
.050											
.025											
0.000											
LENGTH	0.00	5.00	10.00	20.00	40.00	60.00	80.00	100.00	110.00	115.00	120.00

WIDTHS OUTSIDE DATA = 0

FIGURE 4-22

MDAC-STL ELECTROPHORESIS ANALYSIS PROGRAM
ORIGINATOR: D.W. RICHMAN 9/78

RUN NO. 10, TEST ENGINEER: C.D. WALKER
BUFFER FLOW 10.0 ML/MIN, INLET TEMP 8.2 C
FIELD STRENGTH 0.0 V/CM
BUFFER HORIZONTAL CENTERLINE VELOCITY

WIDTH											
8.250	0.	0.	0.	0.	0.	0.	0.	0.	0.	0.	0.
8.225	0.	-.4496E-03	-.1056E-05	.5171E-06	.4446E-06	0.	-.3220E-05	.2462E-04	.2472E-04	.4716E-03	0.
8.200	0.	-.7820E-03	-.3050E-05	.1031E-05	-.7037E-07	0.	.1667E-04	.6797E-05	.7685E-04	.7770E-03	0.
8.150	0.	-.1203E-02	-.4478E-05	.8154E-06	.2780E-05	0.	.3212E-04	.3741E-04	.5993E-04	.1159E-02	0.
8.050	0.	-.7928E-03	.2145E-05	.4916E-06	.3688E-05	0.	.6067E-04	.1683E-03	.2712E-03	.2820E-03	0.
7.850	0.	.1365E-03	.1569E-05	.1888E-06	.1111E-05	0.	-.5658E-05	-.1265E-04	-.1573E-04	-.1507E-03	0.
7.219	0.	.9273E-04	.1000E-05	.1117E-06	.9430E-06	0.	-.6578E-05	-.9687E-05	-.1844E-04	-.9662E-04	0.
6.188	0.	.9085E-04	.8759E-06	.9416E-07	.4490E-07	0.	-.4367E-05	-.9481E-05	-.1524E-04	-.9482E-04	0.
5.156	0.	.9076E-04	.8755E-06	.9349E-07	.4345E-07	0.	-.4353E-05	-.9466E-05	-.1521E-04	-.9472E-04	0.
4.125	0.	-.1311E-09	.6224E-08	-.1143E-10	.1630E-10	0.	.2880E-10	-.6948E-10	.1806E-09	.1397E-09	0.
3.094	0.	-.9076E-04	-.8755E-06	-.9349E-07	-.4345E-07	0.	.4353E-05	.9466E-05	.1521E-04	.9472E-04	0.
2.063	0.	-.9085E-04	-.9134E-06	-.9409E-07	-.4500E-07	0.	.4366E-05	.9481E-05	.1524E-04	.9482E-04	0.
1.031	0.	-.9258E-04	-.1902E-04	-.1286E-06	-.9433E-06	0.	.6576E-05	.9683E-05	.1844E-04	.9652E-04	0.
.400	0.	-.1462E-03	-.1735E-04	-.2229E-06	-.1133E-05	0.	.5668E-05	.1265E-04	.1700E-04	.1508E-03	0.
.200	0.	.2837E-03	-.3886E-04	-.1011E-05	-.2672E-05	0.	-.6028E-04	-.1680E-03	-.2391E-03	-.2767E-03	0.
.100	0.	.1193E-02	.3762E-04	-.3061E-05	-.2425E-05	0.	-.3210E-04	-.3573E-04	-.1182E-03	-.1124E-02	0.
.050	0.	.7746E-03	.7473E-06	-.3422E-05	-.9473E-06	0.	-.1889E-04	-.5463E-05	-.4825E-04	-.7547E-03	0.
.025	0.	.4523E-03	-.1029E-05	-.1683E-05	.1297E-06	0.	-.1048E-05	-.2433E-04	.3861E-06	-.4656E-03	0.
0.000	0.	0.	0.	0.	0.	0.	0.	0.	0.	0.	0.
LENGTH		0.00	5.00	10.00	20.00	40.00	60.00	80.00	100.00	110.00	115.00	120.00

FIGURE 4-23

MDAC-STL ELECTROPHORESIS DATA REDUCTION
ORIGINATOR: D.W. RICHMAN 12/79

RUN NO. 11, TEST ENGINEER: C.D. WALKER
BUFFER FLOW 20.0 ML/MIN, INLET TEMP 8.4 C
FIELD STRENGTH 9.9 V/CM
BUFFER HORIZONTAL CENTERLINE VELOCITY

WIDTH											
8.250											
8.225											
8.200											
8.150											
8.050											
7.850											
7.219				.3951E-02	.3452E-02	.4284E-02	.4551E-02	.1809E-02			
6.188				.3672E-02	.2752E-02	.2152E-02	.1757E-02	.1256E-03			
5.156				.4897E-02	.2333E-02	.1890E-02	.1700E-02	.1902E-03			
4.125				.4687E-02	.2325E-02	.1728E-02	.1385E-02	.3127E-03			
3.094				.4318E-02	.2586E-02	.2005E-02	.1533E-02	.6430E-03			
2.063				.3900E-02	.2872E-02	0.	0.	0.			
1.031				0.	0.	0.	0.	0.			
.400											
.200											
.100											
.050											
.025											
0.000											
LENGTH	0.00	5.00	10.00	20.00	40.00	60.00	80.00	100.00	110.00	115.00	120.00

WIDTHS OUTSIDE DATA = 0

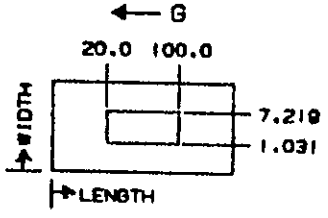

FIGURE 4-24

MOAC-STL ELECTROPHORESIS ANALYSIS PROGRAM
ORIGINATOR: D.W. RICHMAN 9/79

RUN NO. 11: [illegible]
BUFFER FLOW 10.0 ML/MIN, INLET TEMP 8.4 C
FIELD STRENGTH 9.9 V/CM
BUFFER HORIZONTAL CENTERLINE VELOCITY

WIDTH											
8.250	0.	0.	0.	0.	0.	0.	0.	0.	0.	0.	0.
8.225	0.	-.7747E-04	.3192E-03	.3624E-03	.3588E-03	.3568E-03	.3639E-03	.3876E-03	.3689E-03	.8215E-03	0.
8.200	0.	-.2858E-04	.6822E-03	.6786E-03	.6933E-03	.7045E-03	.7135E-03	.7216E-03	.7540E-03	.1378E-02	0.
8.150	0.	.7492E-04	.1127E-02	.1113E-02	.1106E-02	.1110E-02	.1136E-02	.1195E-02	.1271E-02	.2057E-02	0.
8.050	0.	.1215E-02	.1407E-02	.1386E-02	.1425E-02	.1453E-02	.1465E-02	.1459E-02	.1604E-02	.1570E-02	0.
7.850	0.	.2084E-02	.2007E-02	.1998E-02	.1979E-02	.1973E-02	.1975E-02	.1979E-02	.1963E-02	.1843E-02	0.
7.719	0.	.2073E-02	.1993E-02	.2003E-02	.2012E-02	.2012E-02	.2008E-02	.2009E-02	.1996E-02	.1946E-02	0.
6.184	0.	.2079E-02	.2017E-02	.2016E-02	.2012E-02	.2012E-02	.2009E-02	.1997E-02	.1986E-02	.1957E-02	0.
5.196	0.	.2071E-02	.2010E-02	.2009E-02	.2010E-02	.2009E-02	.2007E-02	.2005E-02	.2005E-02	.1944E-02	0.
4.125	0.	.1976E-02	.2014E-02	.2030E-02	.2010E-02	.2012E-02	.2011E-02	.2014E-02	.2026E-02	.2019E-02	0.
3.094	0.	.1924E-02	.2017E-02	.2002E-02	.2011E-02	.2014E-02	.2015E-02	.2020E-02	.2036E-02	.2100E-02	0.
2.063	0.	.1925E-02	.2004E-02	.2029E-02	.2011E-02	.2011E-02	.2016E-02	.2016E-02	.2017E-02	.2104E-02	0.
1.031	0.	.1923E-02	.2002E-02	.2009E-02	.2011E-02	.2011E-02	.2017E-02	.2036E-02	.2032E-02	.2114E-02	0.
.400	0.	.1930E-02	.1965E-02	.1961E-02	.1978E-02	.1987E-02	.1986E-02	.1972E-02	.2017E-02	.2129E-02	0.
.200	0.	.1650E-02	.1426E-02	.1435E-02	.1429E-02	.1417E-02	.1396E-02	.1396E-02	.1312E-02	.1306E-02	0.
.100	0.	.2072E-02	.1093E-02	.1097E-02	.1107E-02	.1107E-02	.1078E-02	.1002E-02	.9412E-03	.2444E-03	0.
.050	0.	.1437E-02	.6693E-03	.7165E-03	.6949E-03	.6880E-03	.6820E-03	.6622E-03	.6487E-03	.3239E-04	0.
.025	0.	.8740E-03	.3797E-03	.3211E-03	.3605E-03	.3659E-03	.3570E-03	.3534E-03	.3206E-03	-.7406E-04	0.
0.000	0.	0.	0.	0.	0.	0.	0.	0.	0.	0.	0.
LENGTH		0.00	5.00	10.00	20.00	40.00	60.00	80.00	100.00	110.00	115.00	120.00

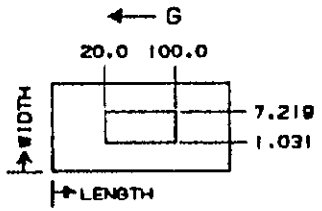

FIGURE 4-25

MDAC-STL ELECTROPHORESIS DATA REDUCTION
ORIGINATOR: D.W. RICHMAN 12/78

RUN NO. 12, TEST ENGINEER: C.D. WALKER
BUFFER FLOW 20.0 ML/MIN, INLET TEMP 8.2 C
FIELD STRENGTH 20.0 V/CM
BUFFER HORIZONTAL CENTERLINE VELOCITY

WIDTH										
8.250										
8.225										
8.200										
8.150										
8.050										
7.850										
7.219			.1315E-01	.4475E-02	.4207E-02	.4396E-02	.6404E-02			
6.188			.4833E-02	.4223E-02	.3546E-02	.4095E-02	.5429E-02			
5.156			.5204E-02	.4321E-02	.2664E-02	.3373E-02	.5767E-02			
4.125			.6652E-02	.4343E-02	.3118E-02	.4558E-02	0.			
3.094			.7779E-02	.5083E-02	0.	0.	0.			
2.063			.6661E-02	0.	0.	0.	0.			
1.031			0.	0.	0.	0.	0.			
.400										
.200										
.100										
.050										
.025										
0.000										
LENGTH	0.00	5.00	10.00	20.00	40.00	60.00	80.00	100.00	110.00	115.00	120.00

WIDTHS OUTSIDE DATA = 0

FIGURE 4-26

MDAC-STL ELECTROPHORESIS ANALYSIS PROGRAM
ORIGINATOR: D.W. RICHMAN 9/78

RUN NO. 12, TEST ENGINEER: C.D. WALKER
BUFFER FLOW 10.0 ML/MIN, INLET TEMP 8.2 C
FIELD STRENGTH 20.0 V/CM
BUFFER HORIZONTAL CENTERLINE VELOCITY

WIDTH											
8.250	0.	0.	0.	0.	0.	0.	0.	0.	0.	0.	0.
8.225	0.	.3420E-03	.7933E-03	.7911E-03	.7587E-03	.7580E-03	.7757E-03	.7995E-03	.8954E-03	.1250E-02	0.
8.200	0.	.9423E-03	.1620E-02	.1520E-02	.1491E-02	.1482E-02	.1521E-02	.1593E-02	.1781E-02	.2044E-02	0.
8.150	0.	.1905E-02	.2769E-02	.2345E-02	.2372E-02	.2390E-02	.2444E-02	.2535E-02	.3020E-02	.2538E-02	0.
8.050	0.	.3090E-02	.3216E-02	.2967E-02	.3003E-02	.3024E-02	.3059E-02	.3138E-02	.3266E-02	.2061E-02	0.
7.850	0.	.4159E-02	.4077E-02	.4029E-02	.4033E-02	.4038E-02	.4049E-02	.4049E-02	.4053E-02	.3862E-02	0.
7.219	0.	.4097E-02	.4074E-02	.4037E-02	.4075E-02	.4074E-02	.4073E-02	.4059E-02	.4085E-02	.4071E-02	0.
6.188	0.	.4117E-02	.4071E-02	.4057E-02	.4068E-02	.4074E-02	.4077E-02	.4078E-02	.4068E-02	.4035E-02	0.
5.156	0.	.4108E-02	.4080E-02	.4071E-02	.4067E-02	.4068E-02	.4071E-02	.4072E-02	.4074E-02	.4040E-02	0.
4.125	0.	.4039E-02	.4073E-02	.4079E-02	.4064E-02	.4067E-02	.4073E-02	.4079E-02	.4096E-02	.4121E-02	0.
3.094	0.	.3972E-02	.4073E-02	.4078E-02	.4068E-02	.4069E-02	.4077E-02	.4086E-02	.4109E-02	.4206E-02	0.
2.063	0.	.3965E-02	.4073E-02	.4073E-02	.4075E-02	.4075E-02	.4078E-02	.4085E-02	.4087E-02	.4209E-02	0.
1.031	0.	.3963E-02	.4071E-02	.4073E-02	.4071E-02	.4077E-02	.4085E-02	.4097E-02	.4124E-02	.4234E-02	0.
.400	0.	.3951E-02	.3999E-02	.4033E-02	.4042E-02	.4054E-02	.4064E-02	.4066E-02	.4120E-02	.4467E-02	0.
.200	0.	.2698E-02	.2804E-02	.3075E-02	.3030E-02	.3048E-02	.3090E-02	.3117E-02	.2976E-02	.5131E-02	0.
.100	0.	.2927E-02	.2319E-02	.2622E-02	.2439E-02	.2514E-02	.2523E-02	.2381E-02	.1974E-02	.4512E-02	0.
.050	0.	.1979E-02	.1582E-02	.1680E-02	.1582E-02	.1585E-02	.1618E-02	.1612E-02	.1391E-02	.2398E-02	0.
.025	0.	.1190E-02	.8405E-03	.8692E-03	.8259E-03	.8306E-03	.8451E-03	.8320E-03	.7813E-03	.1035E-02	0.
0.000	0.	0.	0.	0.	0.	0.	0.	0.	0.	0.	0.
LENGTH		0.00	5.00	10.00	20.00	40.00	60.00	80.00	100.00	110.00	115.00	120.00

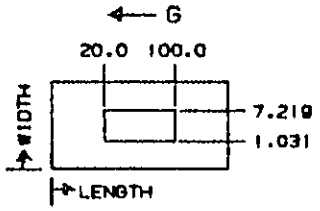

FIGURE 4-27

MOAC-STL ELECTROPHORESIS DATA REDUCTION
ORIGINATOR: D.W. RICHMAN 12/79

RUN NO. 13, TEST ENGINEER: C.D. WALKER
BUFFER FLOW 30.0 ML/MIN, INLET TEMP 6.7 C
FIELD STRENGTH 0.0 V/CM
BUFFER HORIZONTAL CENTERLINE VELOCITY

WIDTH					
8.250					
8.225					
8.200					
8.150					
8.050					
7.850					
7.219	0.	.6922E-03	0.	0.	0.
6.188	.5761E-02	.8343E-03	-.9036E-03	-.7416E-03	-.1874E-02
5.156	.5355E-02	.7588E-03	-.8342E-03	-.8295E-03	-.2167E-02
4.125	.5238E-02	.8323E-03	-.8357E-03	-.1061E-02	-.2568E-02
3.094	.5001E-02	.7044E-03	-.9778E-03	-.1127E-02	-.2198E-02
2.063	.4785E-02	.3541E-03	-.6667E-03	-.5841E-03	-.2718E-02
1.031	.2958E-02	0.	0.	0.	-.2581E-02
.400					
.200					
.100					
.050					
.025					
0.000					

LENGTH	0.00	5.00	10.00	20.00	40.00	60.00	80.00	100.00	110.00	115.00	120.00
WIDTHS OUTSIDE DATA	0										

FIGURE 4-28

MDAC-STL ELECTROPHORESIS ANALYSIS PROGRAM
ORIGINATOR: D.W. RICHMAN 9/78

RUN NO. 13, TEST ENGINEER C.P. WALKER
BUFFER FLOW 15.0 ML/MIN, INLET TEMP 7.9 C
FIELD STRENGTH 0.0 V/CM
BUFFER HORIZONTAL CENTERLINE VELOCITY

WIDTH											
8.250	0.	0.	0.	0.	0.	0.	0.	0.	0.	0.	0.
8.225	0.	-.6872E-03	-.1273E-05	.4619E-06	.5930E-06	0.	.3166E-04	.6320E-05	.1034E-04	.6691E-03	0.
8.200	0.	-.1167E-02	-.3855E-05	.9092E-06	.1223E-05	0.	.5021E-04	.3904E-04	.1322E-03	.1161E-02	0.
8.150	0.	-.1696E-02	-.2907E-04	.6892E-06	.1096E-05	0.	.7971E-04	.8988E-04	.2017E-03	.1730E-02	0.
8.050	0.	-.5319E-03	.5586E-05	.5094E-06	.3885E-06	0.	.6062E-04	.1570E-03	.4218E-03	.4338E-03	0.
7.850	0.	.2093E-03	.4173E-05	.2039E-06	.1033E-06	0.	-.9836E-05	-.1009E-04	-.2568E-04	-.2207E-03	0.
7.219	0.	.1357E-03	.2551E-05	.1217E-06	.5889E-07	0.	-.7283E-05	-.1110E-04	-.3372E-04	-.1424E-03	0.
6.188	0.	.1342E-03	.2428E-05	.5591E-07	.4357E-07	0.	-.7162E-05	-.1095E-04	-.3335E-04	-.1397E-03	0.
5.156	0.	.1341E-03	.2427E-05	.5558E-07	.4320E-07	0.	-.7151E-05	-.1094E-04	-.3330E-04	-.1396E-03	0.
4.125	0.	-.2609E-09	.1508E-09	.8802E-11	-.1900E-10	0.	.2449E-10	-.1734E-10	.1209E-09	.2267E-09	0.
3.094	0.	-.1341E-03	-.2427E-05	-.5558E-07	-.4320E-07	0.	.7151E-05	.1094E-04	.3330E-04	.1396E-03	0.
2.063	0.	-.1342E-03	-.2429E-05	-.5596E-07	-.4346E-07	0.	.7162E-05	.1095E-04	.3335E-04	.1397E-03	0.
1.031	0.	-.1355E-03	-.2489E-05	-.1233E-06	-.5960E-07	0.	.7279E-05	.1110E-04	.3371E-04	.1423E-03	0.
.400	0.	-.2037E-03	-.4719E-05	-.2247E-06	-.1125E-06	0.	.9841E-05	.1008E-04	.2569E-04	.2213E-03	0.
.200	0.	.5333E-03	-.9890E-05	-.1308E-05	-.6599E-06	0.	-.5999E-04	-.1567E-03	-.4211E-03	-.4071E-03	0.
.100	0.	.1696E-02	-.1465E-05	-.3058E-05	-.2374E-05	0.	-.7689E-04	-.9834E-04	-.1984E-03	-.1670E-02	0.
.050	0.	.1167E-02	.2193E-04	-.3397E-05	-.2574E-05	0.	-.5009E-04	-.3794E-04	-.1302E-03	-.1151E-02	0.
.025	0.	.6869E-03	.2844E-04	-.1673E-05	-.1260E-05	0.	-.3181E-04	-.5753E-05	-.8955E-05	-.7207E-03	0.
0.000	0.	0.	0.	0.	0.	0.	0.	0.	0.	0.	0.
LENGTH		1.00	5.00	10.00	20.00	40.00	60.00	80.00	100.00	110.00	115.00	120.00

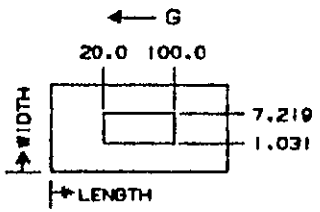

FIGURE 4-29

MDAC-STL ELECTROPHORESIS DATA REDUCTION
ORIGINATOR: D.W. RICHMAN 12/76

RUN NO. 14, TEST ENGINEER: C.D. WALKER
BUFFER FLOW 30.0 ML/MIN, INLET TEMP 6.8 C
FIELD STRENGTH 10.1 V/CM
BUFFER HORIZONTAL CENTERLINE VELOCITY

WIDTH											
8.250											
8.225											
8.200											
8.150											
8.050											
7.850											
7.219				.4930E-02	.2985E-02	.3121E-02	.2692E-02	.1597E-02			
6.188				.5540E-02	.2713E-02	.1660E-02	.1903E-02	.5917E-05			
5.156				.6218E-02	.2463E-02	.1375E-02	.6664E-03	-.6349E-03			
4.125				.4987E-02	.2625E-02	.9488E-03	.4930E-03	.1324E-04			
3.094				.6064E-02	.2684E-02	.1580E-02	.7186E-02	.5229E-03			
2.063				.5650E-02	.2843E-02	.2716E-02	0.	0.			
1.031				0.	0.	0.	0.	0.			
.400											
.200											
.100											
.050											
.025											
0.000											
LENGTH	0.00	5.00	10.00	20.00	40.00	60.00	80.00	100.00	110.00	115.00	120.00

WIDTHS OUTSIDE DATA = 0

FIGURE 4-30

MDAC-STL ELECTROPHORESIS ANALYSIS PROGRAM
ORIGINATOR: D.W. RICHMAN 9/78

RUN NO. 14, TEST ENGINEER: C.C. WALKER
BUFFER FLOW 15.0 ML/MIN, INLET TEMP 5.8 C
FIELD STRENGTH 10.1 V/CM
BUFFER HORIZONTAL CENTERLINE VELOCITY

WIDTH											
8.250	0.	0.	0.	0.	0.	0.	0.	0.	0.	0.	0.
8.225	0.	-.3151E-03	.3392E-03	.3284E-03	.3564E-03	.3474E-03	.3456E-03	.3954E-03	.4138E-03	.1061E-02	0.
8.200	0.	-.4181E-03	.6784E-03	.6526E-03	.6885E-03	.6909E-03	.6984E-03	.7502E-03	.8158E-03	.1764E-02	0.
8.150	0.	-.3683E-03	.1096E-02	.1109E-02	.1146E-02	.1136E-02	.1141E-02	.1221E-02	.1353E-02	.2456E-02	0.
8.050	0.	.1099E-02	.1441E-02	.1396E-02	.1371E-02	.1426E-02	.1481E-02	.1457E-02	.1630E-02	.1562E-02	0.
7.850	0.	.2197E-02	.1943E-02	.1933E-02	.1944E-02	.1936E-02	.1923E-02	.1920E-02	.1900E-02	.1763E-02	0.
7.219	0.	.2061E-02	.1945E-02	.1965E-02	.1947E-02	.1955E-02	.1964E-02	.1960E-02	.1953E-02	.1862E-02	0.
6.188	0.	.2053E-02	.1971E-02	.1960E-02	.1971E-02	.1973E-02	.1963E-02	.1940E-02	.1947E-02	.1861E-02	0.
5.156	0.	.2054E-02	.1959E-02	.1963E-02	.1961E-02	.1957E-02	.1957E-02	.1960E-02	.1941E-02	.1871E-02	0.
4.125	0.	.1941E-02	.1954E-02	.1971E-02	.1953E-02	.1951E-02	.1959E-02	.1974E-02	.1963E-02	.1995E-02	0.
3.094	0.	.1929E-02	.1956E-02	.1972E-02	.1957E-02	.1957E-02	.1966E-02	.1981E-02	.1989E-02	.2110E-02	0.
2.063	0.	.1925E-02	.1944E-02	.1957E-02	.1979E-02	.1979E-02	.1974E-02	.1978E-02	.1996E-02	.2098E-02	0.
1.031	0.	.1829E-02	.1958E-02	.1961E-02	.1957E-02	.1971E-02	.1983E-02	.1971E-02	.1979E-02	.2121E-02	0.
.400	0.	.1751E-02	.1906E-02	.1948E-02	.1944E-02	.1938E-02	.1937E-02	.1950E-02	.1963E-02	.2174E-02	0.
.200	0.	.1637E-02	.1366E-02	.1392E-02	.1424E-02	.1393E-02	.1347E-02	.1332E-02	.1239E-02	.1417E-02	0.
.100	0.	.2490E-02	.1076E-02	.1103E-02	.1051E-02	.1085E-02	.1094E-02	.9692E-03	.8433E-03	-.5070E-04	0.
.050	0.	.1791E-02	.6956E-03	.6755E-03	.6852E-03	.6917E-03	.6981E-03	.7075E-03	.5790E-03	-.2550E-03	0.
.025	0.	.1012E-02	.3537E-03	.3790E-03	.3804E-03	.3626E-03	.3553E-03	.3882E-03	.3055E-03	-.2428E-03	0.
0.000	0.	0.	0.	0.	0.	0.	0.	0.	0.	0.	0.
LENGTH		0.00	5.00	10.00	20.00	40.00	60.00	80.00	100.00	110.00	115.00	120.00

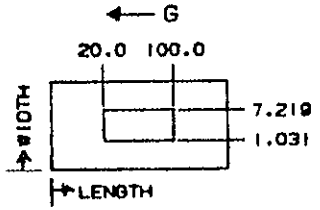

FIGURE 4-31

MDAC-STL ELECTROPHORESIS DATA REDUCTION
ORIGINATOR: D.W. RICHMAN 12/79

RUN NO. 15, TEST ENGINEER: C.D. WALKER
BUFFER FLOW 30.0 ML/MIN, INLET TEMP 7.7 C
FIELD STRENGTH 29.3 V/CM
BUFFER HORIZONTAL CENTERLINE VELOCITY

WIDTH											
8.250											
8.225											
8.200											
8.150											
8.050											
7.850											
7.219				.4138E-02	.4583E-02	.6301E-02	.3399E-02	-.5853E-02			
6.188				.5991E-02	.3522E-02	.3385E-02	.7683E-03	-.2227E-02			
5.156				.6175E-02	.3870E-02	.2862E-02	.1201E-02	-.2263E-02			
4.125				.5907E-02	.4293E-02	.3534E-02	.2291E-02	-.1219E-02			
3.094				.6141E-02	.4665E-02	.4475E-02	.2467E-02	0.			
2.063				.5472E-02	.4942E-02	0.	0.	0.			
1.031			0.	0.	0.	0.	0.				
.400											
.200											
.100											
.050											
.025											
0.000											
LENGTH	0.00	5.00	10.00	20.00	40.00	60.00	80.00	100.00	110.00	115.00	120.00

WIDTHS OUTSIDE DATA = 0

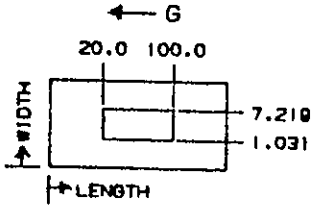

FIGURE 4-32

MDAC-STL ELECTROPHORESIS ANALYSIS PROGRAM
ORIGINATOR: D.W. RICHMAN 9/78

RUN NO. 15, TEST ENGINEER: C.D. WALKER
BUFFER FLOW 15.0 ML/MIN, INLET TEMP 7.7 C
FIELD STRENGTH 20.0 V/CM
BUFFER HORIZONTAL CENTERLINE VELOCITY

WIDTH											
8.250	0.	0.	0.	0.	0.	0.	0.	0.	0.	0.	0.
8.225	0.	.1004E-03	.7962E-03	.7495E-03	.7493E-03	.7541E-03	.7666E-03	.7894E-03	.8931E-03	.1413E-02	0.
8.200	0.	.5323E-03	.1609E-02	.1496E-02	.1454E-02	.1478E-02	.1533E-02	.1579E-02	.1794E-02	.2450E-02	0.
8.150	0.	.1399E-02	.2703E-02	.2301E-02	.2350E-02	.2379E-02	.2435E-02	.2567E-02	.2976E-02	.3109E-02	0.
8.050	0.	.2865E-02	.3704E-02	.2905E-02	.2954E-02	.2981E-02	.3016E-02	.3089E-02	.3294E-02	.2191E-02	0.
7.850	0.	.4127E-02	.3999E-02	.3968E-02	.3950E-02	.3953E-02	.3961E-02	.3956E-02	.3962E-02	.3709E-02	0.
7.219	0.	.4064E-02	.3973E-02	.3999E-02	.3997E-02	.4005E-02	.4013E-02	.4011E-02	.3999E-02	.3942E-02	0.
6.188	0.	.4048E-02	.4012E-02	.3992E-02	.3998E-02	.3990E-02	.3977E-02	.3978E-02	.3996E-02	.3928E-02	0.
5.156	0.	.4055E-02	.4000E-02	.3994E-02	.4006E-02	.4000E-02	.3997E-02	.3994E-02	.3994E-02	.3939E-02	0.
4.125	0.	.3951E-02	.3987E-02	.3998E-02	.4001E-02	.4005E-02	.4009E-02	.4014E-02	.4017E-02	.4067E-02	0.
3.094	0.	.3843E-02	.3983E-02	.3995E-02	.3998E-02	.4003E-02	.4011E-02	.4023E-02	.4040E-02	.4186E-02	0.
2.063	0.	.3839E-02	.3996E-02	.3986E-02	.3987E-02	.3993E-02	.4009E-02	.4007E-02	.4039E-02	.4169E-02	0.
1.031	0.	.3835E-02	.3996E-02	.4010E-02	.3997E-02	.3999E-02	.4012E-02	.4030E-02	.4044E-02	.4225E-02	0.
.400	0.	.3717E-02	.3924E-02	.3976E-02	.3956E-02	.3963E-02	.3980E-02	.3990E-02	.4053E-02	.4449E-02	0.
.200	0.	.2774E-02	.2696E-02	.2964E-02	.2993E-02	.3039E-02	.3070E-02	.3053E-02	.2862E-02	.4863E-02	0.
.100	0.	.3379E-02	.2206E-02	.2648E-02	.2464E-02	.2424E-02	.2409E-02	.2296E-02	.1857E-02	.3952E-02	0.
.050	0.	.2334E-02	.1554E-02	.1665E-02	.1601E-02	.1602E-02	.1588E-02	.1479E-02	.1318E-02	.1966E-02	0.
.025	0.	.1389E-02	.8330E-03	.8559E-03	.8191E-03	.8237E-03	.8260E-03	.7820E-03	.7429E-03	.7244E-03	0.
0.000	0.	0.	0.	0.	0.	0.	0.	0.	0.	0.	0.
LENGTH		0.00	5.00	10.00	20.00	40.00	60.00	80.00	100.00	110.00	115.00	120.00

FIGURE 4-33

MDAC-STL ELECTROPHORESIS DATA REDUCTION
ORIGINATOR: D.W. RICHMAN 12/78

RUN NO. 16, TEST ENGINFER: C.O. WALKER
BUFFER FLOW 40.0 ML/MIN, INLET TEMP 7.4 C
FIELD STRENGTH 0.0 V/CM
BUFFER HORIZONTAL CENTERLINE VELOCITY

WIDTH											
8.250											
8.225											
8.200											
8.150											
8.050											
7.850											
7.219				0.	0.	.2929E-03	0.	0.			
6.188				.2155E-02	.1327E-02	-.2967E-03	-.1092E-02	-.3514E-03			
5.156				.2550E-02	.1112E-02	-.2021E-03	-.1197E-02	-.1896E-02			
4.125				.1848E-02	.1312E-02	-.3247E-03	-.1704E-02	-.1977E-02			
3.094				.4641E-02	.1365E-02	-.1047E-02	-.1904E-02	-.2124E-02			
2.063				.4447E-02	.7821E-03	-.8932E-03	-.1097E-02	-.1737E-02			
1.031				0.	0.	0.	0.	-.9203E-03			
.400											
.200											
.100											
.050											
.025											
0.000											
LENGTH	0.00	5.00	10.00	20.00	40.00	60.00	80.00	100.00	110.00	115.00	120.00

WIDTHS OUTSIDE DATA = 0

FIGURE 4-34

MDAC-STL ELECTROPHORESIS ANALYSIS PROGRAM
ORIGINATOR: D.W. RICHMAN 9/78

RUN NO. 16, TEST ENGINEER: C.D. WALKER
BUFFER FLOW 20.0 ML/MIN, INLET TEMP 7.4 C
FIELD STRENGTH 0.0 V/CM
BUFFER HORIZONTAL CENTERLINE VELOCITY

WIDTH											
8.250	0.	0.	0.	0.	0.	0.	0.	0.	0.	0.	0.
8.225	0.	-.9244E-03	-.5310E-06	.7435E-06	.7772E-06	0.	.1903E-04	-.5088E-05	.6735E-05	.9441E-03	0.
8.200	0.	-.1503E-02	-.2454E-05	.1528E-05	.1623E-05	0.	.6117E-04	.8704E-04	.1616E-03	.1517E-02	0.
8.150	0.	-.2327E-02	-.4617E-05	.1402E-05	.1535E-05	0.	.8139E-04	.1249E-03	.2268E-03	.2272E-02	0.
8.050	0.	-.6201E-03	.1116E-04	.7419E-06	.5657E-06	0.	.1662E-03	.2846E-03	.5747E-03	.6095E-03	0.
7.850	0.	.2674E-03	.4215E-05	.2287E-06	.1134E-06	0.	-.7865E-05	-.2646E-04	-.6215E-04	-.2876E-03	0.
7.219	0.	.1779E-03	.2943E-05	.1361E-06	.6313E-07	0.	-.7981E-05	-.2458E-04	-.3321E-04	-.1958E-03	0.
6.188	0.	.1727E-03	.2867E-05	.7965E-07	.5222E-07	0.	-.7959E-05	-.2153E-04	-.3259E-04	-.1935E-03	0.
5.156	0.	.1726E-03	.2865E-05	.7919E-07	.5215E-07	0.	-.7846E-05	-.2150E-04	-.3255E-04	-.1934E-03	0.
4.125	0.	-.2425E-09	.1742E-09	.1038E-10	.2689E-11	0.	.2294E-10	.2698E-10	-.2469E-10	-.2245E-09	0.
3.094	0.	-.1726E-03	-.2865E-05	-.7919E-07	-.5215E-07	0.	.7846E-05	.2150E-04	.3255E-04	.1934E-03	0.
2.063	0.	-.1727E-03	-.2868E-05	-.7971E-07	-.5223E-07	0.	.7859E-05	.2153E-04	.3259E-04	.1935E-03	0.
1.031	0.	-.1747E-03	-.3153E-05	-.1397E-06	-.6406E-07	0.	.7956E-05	.2457E-04	.3320E-04	.1956E-03	0.
.400	0.	-.2661E-03	-.5508E-05	-.2583E-06	-.1240E-06	0.	.7471E-05	.2634E-04	.6223E-04	.2873E-03	0.
.200	0.	.5223E-03	-.9764E-05	-.1276E-05	-.7782E-06	0.	-.1635E-03	-.2887E-03	-.5732E-03	-.5986E-03	0.
.100	0.	.2327E-02	-.2122E-05	-.3983E-05	-.2813E-05	0.	-.9848E-04	-.1374E-03	-.2263E-03	-.2233E-02	0.
.050	0.	.1509E-02	-.3633E-05	-.4282E-05	-.2982E-05	0.	-.5883E-04	-.1078E-03	-.1367E-03	-.1460E-02	0.
.025	0.	.9242E-03	-.2295E-05	-.2091E-05	-.1453E-05	0.	-.1891E-04	-.3837E-05	.2477E-04	-.8856E-03	0.
0.000	0.	0.	0.	0.	0.	0.	0.	0.	0.	0.	0.
LENGTH		0.00	5.00	10.00	20.00	40.00	60.00	80.00	100.00	110.00	115.00	120.00

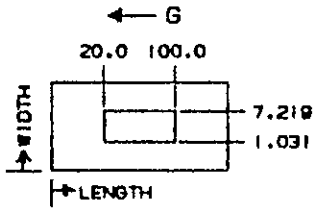

FIGURE 4-35

MDAC-STL ELECTROPHORESIS DATA REDUCTION
ORIGINATOR: D.W. RICHMAN 12/79

RUN NO. 17, TEST ENGINEER: C.D. WALKER
BUFFER FLOW 40.0 ML/MIN, INLET TEMP 6.9 C
FIELD STRENGTH 10.0 V/CM
BUFFER HORIZONTAL CENTERLINE VELOCITY

WIDTH											
8.250											
8.225											
8.200											
8.150											
8.050											
7.850											
7.219					0.	.3196E-02	.1877E-02	.2792E-02	.4134E-02		
6.188					.6866E-02	.3609E-02	.1473E-02	.1607E-02	.2269E-02		
5.156					.7117E-02	.2964E-02	.8660E-03	.1240E-02	.2141E-02		
4.125					.6525E-02	.2884E-02	.1083E-02	.9015E-03	.1349E-03		
3.094					.5587E-02	.2962E-02	.1351E-02	.9499E-03	.2644E-03		
2.063					.6000E-02	.3071E-02	.1654E-02	.1080E-02	.2764E-03		
1.031					0.	0.	0.	0.	0.		
.403											
.230											
.130											
.059											
.025											
0.000											
LENGTH	0.00	5.00	10.00	20.00	40.00	60.00	80.00	100.00	110.00	115.00	120.00

WIDTHS OUTSIDE DATA = 0

FIGURE 4-36

MDAC-STL ELECTROPHORESIS ANALYSIS PROGRAM
ORIGINATOR: D.W. RICHMAN 9/78

RUN NO. 17, TEST ENGINEER C.D. WALKER
BUFFER FLOW 20.0 ML/MIN, INLET TEMP 5.9 C
FIELD STRENGTH 10.0 V/CM
BUFFER HORIZONTAL CENTERLINE VELOCITY

WIDTH											
8.250	0.	0.	0.	0.	0.	0.	0.	0.	0.	0.	0.
8.225	0.	-.5955E-03	.3534E-03	.3470E-03	.3725E-03	.3409E-03	.3202E-03	.3833E-03	.4039E-03	.1244E-02	0.
8.200	0.	-.7955E-03	.6779E-03	.6804E-03	.7165E-03	.7110E-03	.7156E-03	.7581E-03	.8481E-03	.2131E-02	0.
8.150	0.	-.8820E-03	.1047E-02	.1029E-02	.1068E-02	.1097E-02	.1143E-02	.1234E-02	.1453E-02	.2970E-02	0.
8.050	0.	.1012E-02	.1487E-02	.1410E-02	.1410E-02	.1416E-02	.1449E-02	.1537E-02	.1688E-02	.1654E-02	0.
7.850	0.	.2107E-02	.1897E-02	.1900E-02	.1891E-02	.1900E-02	.1905E-02	.1884E-02	.1874E-02	.1651E-02	0.
7.219	0.	.2062E-02	.1950E-02	.1936E-02	.1948E-02	.1945E-02	.1930E-02	.1908E-02	.1914E-02	.1813E-02	0.
6.188	0.	.2060E-02	.1934E-02	.1929E-02	.1918E-02	.1921E-02	.1921E-02	.1928E-02	.1899E-02	.1801E-02	0.
5.156	0.	.2049E-02	.1931E-02	.1943E-02	.1934E-02	.1932E-02	.1931E-02	.1927E-02	.1914E-02	.1799E-02	0.
4.125	0.	.1803E-02	.1928E-02	.1945E-02	.1938E-02	.1937E-02	.1934E-02	.1940E-02	.1954E-02	.1957E-02	0.
3.094	0.	.1754E-02	.1929E-02	.1937E-02	.1937E-02	.1938E-02	.1942E-02	.1954E-02	.1983E-02	.2118E-02	0.
2.063	0.	.1760E-02	.1940E-02	.1922E-02	.1937E-02	.1936E-02	.1937E-02	.1957E-02	.1966E-02	.2120E-02	0.
1.031	0.	.1763E-02	.1922E-02	.1929E-02	.1934E-02	.1934E-02	.1936E-02	.1949E-02	.1972E-02	.2129E-02	0.
.400	0.	.1641E-02	.1931E-02	.1919E-02	.1910E-02	.1919E-02	.1933E-02	.1938E-02	.1954E-02	.2225E-02	0.
.200	0.	.1764E-02	.1933E-02	.1423E-02	.1347E-02	.1322E-02	.1311E-02	.1279E-02	.1153E-02	.1296E-02	0.
.100	0.	.3003E-02	.1050E-02	.1001E-02	.1110E-02	.1102E-02	.1020E-02	.9120E-03	.7621E-03	-.4924E-03	0.
.050	0.	.2132E-02	.6906E-03	.6583E-03	.7126E-03	.6901E-03	.6395E-03	.6055E-03	.5254E-03	-.5943E-03	0.
.025	0.	.1762E-02	.4071E-03	.3470E-03	.3410E-03	.3263E-03	.3207E-03	.3421E-03	.2901E-03	-.4506E-03	0.
0.000	0.	0.	0.	0.	0.	0.	0.	0.	0.	0.	0.
LENGTH		0.00	5.00	10.00	20.00	40.00	60.00	80.00	100.00	110.00	115.00	120.00

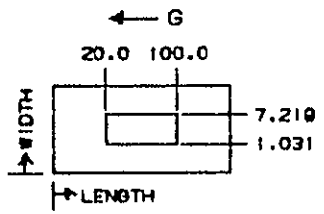

FIGURE 4-37

MDAC-STL ELECTROPHORESIS DATA REDUCTION
ORIGINATOR: D.W. RICHMAN 12/79

RUN NO. 18, TEST ENGINEER: C.D. WALKER
BUFFER FLOW 40.0 ML/MIN, INLET TEMP 7.2 C
FIELD STRENGTH 20.0 V/CM
BUFFER HORIZONTAL CENTERLINE VELOCITY

WIDTH											
8.250											
8.225											
8.200											
8.150											
8.050											
7.850											
7.219				-.1103E-01	.9090E-02	.4577E-02	.8098E-03	-.4101E-02			
6.188				.8292E-02	.5363E-02	.4230E-02	.2754E-02	-.1439E-02			
5.156				.1004E-01	.4951E-02	.3022E-02	.2037E-02	.3746E-03			
4.125				.9960E-02	.5125E-02	.2699E-02	.1834E-02	.1045E-02			
3.094				.8800E-02	.5330E-02	.3823E-02	.2342E-02	.1564E-02			
2.063				.8529E-02	.6896E-02	0.	0.	0.			
1.031				0.	0.	0.	0.	0.			
.403											
.200											
.100											
.050											
.025											
0.000											
LENGTH	1.00	5.00	10.00	20.00	40.00	60.00	80.00	100.00	110.00	115.00	120.00

WIDTHS OUTSIDE DATA = 0

FIGURE 4-38

MDAC-STL ELECTROPHORESIS ANALYSIS PROGRAM
ORIGINATOR: D.W. RICHMAN 9/78

RUN NO. 18, TEST ENGINEER: C.C. WALKER
BUFFER FLOW 20.0 ML/MIN, INLET TEMP 7.2 C
FIELD STRENGTH 20.0 V/CM
BUFFER HORIZONTAL CENTERLINE VELOCITY
WIDTH

8.250	0.	0.	0.	0.	0.	0.	0.	0.	0.	0.	0.
8.225	0.	-.1133E-03	.7739E-03	.7026E-03	.7662E-03	.7930E-03	.7965E-03	.7902E-03	.8823E-03	.1646E-02	0.
8.200	0.	.1223E-03	.1523E-02	.1412E-02	.1439E-02	.1452E-02	.1493E-02	.1589E-02	.1762E-02	.2764E-02	0.
8.150	0.	.7652E-03	.2562E-02	.2302E-02	.2327E-02	.2363E-02	.2431E-02	.2549E-02	.3015E-02	.3599E-02	0.
8.050	0.	.2721E-02	.3185E-02	.2933E-02	.2924E-02	.2935E-02	.2969E-02	.3077E-02	.3337E-02	.2309E-02	0.
7.850	0.	.4107E-02	.3944E-02	.3909E-02	.3900E-02	.3905E-02	.3913E-02	.3911E-02	.3911E-02	.3625E-02	0.
7.219	0.	.4031E-02	.3971E-02	.3954E-02	.3957E-02	.3963E-02	.3963E-02	.3949E-02	.3944E-02	.3875E-02	0.
6.188	0.	.4045E-02	.3939E-02	.3941E-02	.3953E-02	.3949E-02	.3942E-02	.3942E-02	.3939E-02	.3863E-02	0.
5.156	0.	.4031E-02	.3957E-02	.3953E-02	.3948E-02	.3938E-02	.3936E-02	.3957E-02	.3949E-02	.3863E-02	0.
4.125	0.	.3994E-02	.3957E-02	.3956E-02	.3941E-02	.3938E-02	.3949E-02	.3971E-02	.3976E-02	.4019E-02	0.
3.094	0.	.3745E-02	.3949E-02	.3953E-02	.3939E-02	.3947E-02	.3965E-02	.3978E-02	.3999E-02	.4178E-02	0.
2.063	0.	.3754E-02	.3938E-02	.3942E-02	.3950E-02	.3960E-02	.3948E-02	.3969E-02	.3998E-02	.4183E-02	0.
1.031	0.	.3749E-02	.3956E-02	.3954E-02	.3960E-02	.3964E-02	.3972E-02	.3993E-02	.4002E-02	.4223E-02	0.
.400	0.	.3590E-02	.3867E-02	.3923E-02	.3902E-02	.3925E-02	.3955E-02	.3952E-02	.4017E-02	.4449E-02	0.
.200	0.	.2884E-02	.3451E-02	.2989E-02	.2963E-02	.2940E-02	.2930E-02	.2939E-02	.2765E-02	.4664E-02	0.
.100	0.	.3933E-02	.2321E-02	.2545E-02	.2424E-02	.2424E-02	.2413E-02	.2755E-02	.1820E-02	.3252E-02	0.
.050	0.	.2717E-02	.1935E-02	.1635E-02	.1502E-02	.1520E-02	.1556E-02	.1475E-02	.1226E-02	.1557E-02	0.
.025	0.	.1469E-02	.9216E-03	.8744E-03	.8294E-03	.8197E-03	.8108E-03	.7680E-03	.7095E-03	.4172E-03	0.
0.000	0.	0.	0.	0.	0.	0.	0.	0.	0.	0.	0.
LENGTH		0.00	5.00	10.00	20.00	40.00	60.00	80.00	100.00	110.00	115.00	120.00

FIGURE 4-39

5.0 PROTEIN GRAVITY EFFECTS

The purpose of the tests described in this section was to demonstrate the effects of gravity on protein particle streams during electrophoresis. The two proteins used for these tests, both singly and as mixtures, were human fibrinogen and human albumin. First, tests were run on single proteins varying electrical field strength and buffer flowrates The proteins were then mixed and processed at varying flowrates and concentrations. Data collection is described in Section 5.1, while the rationale for buffer selection and assay methods are described in Sections 5.2 and 5.3, respectively. The data reduction and mathematical correlations are discussed in Section 5.4.

5.1 TEST DATA COLLECTION

Electrophoresis chamber flow, electrical field and temperature conditions during the protein runs were established as closely as possible to the conditions during the analagous Task 1.0 runs with comparable time to reach stability. With the repeatability of the chamber proven during the Task 1.0 runs, dye streams were not used to demonstrate laminar flow of the carrier buffer. Dye in very dilute form (0.01 mg/ml) was mixed with small samples of protein to demonstrate that a specific concentration would not "fall-back".

A fixed ratio of sample to carrier buffer flow rates was applied to all protein runs. The intended ratio was 1:200; however, due to inherent limitations of the sample syringe pump utilized, it actually varied $\pm$ 9%.

Protein runs 19 through 36 for albumin and fibrinogen separately (Figures 5-1 and 5-2), and 37 through 48 (Figure 5-3) for the mixture, were conducted in the same general manner as the dye stream runs of Task 1.0. The main protocol differences being control of sample handling. Protein stock was prepared and assayed to assure proper concentration. Concentrations of 0.6 mg/ml were sought for the single protein runs and actual assayed concentrations of the pre-run samples were 0.60 $\pm$ 0.03 mg/ml albumin and 0.64 $\pm$ 0.03 mg/ml fibrinogen. Mixed protein concentrations were 1.2, 0.34 and 0.18 mg/ml. In the case of the mixed concentrations, the fewer scheduled runs allowed all runs at each concentration to be completed during one day from a single assayed stock.

Sample injection into the chamber was from a syringe by means of a commercially available syringe pump. Collection of sample and buffer at the chamber outlet

TASK 2.0

TEST MATRIX, RUNS 19-27

BUFFER FLOW ML/MIN \ FIELD VOLTS/CM	0	10	20
20	19	20	21
30	22	23	24
40	25	26	27

- SINGLE PROTEIN, HUMAN ALBUMIN
- 1 MM DIAMETER SAMPLE STREAMS
- PROTEIN ASSAY FOR OUTLET DISTRIBUTION
- GRAVITY INDUCED CHANGES ARE DEPENDENT ON BUFFER FLOW RATE

Figure 5–1

TASK 2.0

TEST MATRIX, RUNS 28-36

BUFFER FLOW ML/MIN \ FIELD VOLTS/CM	0	10	20
20	28	29	30
30	31	32	33
40	34	35	36

- o SINGLE PROTEIN, HUMAN FIBRINOGEN
- o 1 MM DIAMETER SAMPLE STREAMS
- o PROTEIN ASSAY FOR OUTLET DISTRIBUTION
- o GRAVITY INDUCED CHANGES ARE DEPENDENT ON BUFFER FLOW RATE

Figure 5–2

TASK 2.0

TEST MATRIX, RUNS 37-48

MIXED SPECIES CONCENTRATION TESTS

SAMPLE CONCENTRATION \ BUFFER FLOW ML/MIN	20	40
0.120%	37 / 38	39 / 40
0.034%	41 / 42	43 / 44
0.018%	45 / 46	47 / 48

- MIXED PROTEIN 1 MM DIAMETER SAMPLE STREAM
- PROTEIN ASSAY OF OUTLET DISTRIBUTION
- GRAVITY INDUCED CHANGES ARE CONCENTRATION AND BUFFER FLOW RATE DEPENDENT

0 VOLTS/CM \ 20 VOLTS/CM

FIELD STRENGTH

Figure 5–3

tubes for assay and distribution determination was typically timed to collect $\geq$ 2ml at each tube. Assaying was generally done the same day as the run and included collected sample from tubes as far as fifteen (15) either side of the expected protein peak or peaks. Protein samples not assayed on the same day were capped and stored at the $4^{o}C$ for about 16 hours and assayed the following morning. In order to prevent sample stream smearing in the chamber because of electrical field variations immediately following voltage application or voltage setting adjustment, the protein sample was not introduced into the chamber with field until readings showed the field had stabilized. The sample was then allowed to flow for at least 2.5 residence times before sample collection to allow the outlet distributions to show any crescent distortion present in the sample stream.

5.2 BUFFER SELECTION

Sodium barbital buffer was used throughout the protein tests as the carrier and electrolyte fluids and for dissolving the protein samples. This buffer has been used widely for protein electrophoresis and at pH 8.3 provides a sufficient menstrum for separation of fibrinogen from albumin. The basic difference in this buffer from those used for traditional electrophoresis (i.e., cellulose acetate, agar and polyacrylamide) studies is ionic strength. Traditionally the ionic strength ranges from about 0.01 to 0.05 whereas for our studies the ionic strength was much lower (about 0.0025) to minimize Joule heating. It was prepared as follows: Two stock solutions, one acidic and one alkaline,were prepared by dissolving 4.6 grams of diethylbarbituric acid in 1000 ml of deionized water (acidic solution) and 103.0 grams of diethylbarbituric acid-sodium salt in a separate 1000 ml of deionized water (alkaline solution). These solutions were stored at 4°C and were kept up to five days before being discarded. Carrier buffer and buffer used to dissolve the protein test solutions were prepared daily by mixing 409 ml of the acidic solution with 100 ml of the alkaline solution and then diluting the resultant solution to 20 liters with deionized, deaerated water. Deaeration was attained by exposing the water to about 0.001 ATM for 16 hours to obtain an oxygen partial pressure of 100 mm of mercury. The 20 liter solution was tested for pH and adjusted to pH 8.3 with the required amounts of either acidic or alkaline solution. The final pH of the buffer was 8.3 and its conductivity was 1.005×10^{-4} mho/cm to 1.020×10^{-4} mho/cm at $20^{o}C$. The ionic strength of the buffer was approximately 0.0025 and its specific gravity was approximately 1.0012 gm/cc at $20^{o}C$. Variations in osmolarity and conductivity

were due to slight variations in the day-to-day preparation of the buffer. We chose to prepare buffers fresh daily to minimize the possibility of both microbial and chemical deterioration and to avoid addition of preservatives which would affect cell viability. Constant pH values were maintained from day to day by minor additions to the fresh daily buffer of appropriate amounts of either acidic or alkaline solution.

Buffer used as the electrolyte solution was prepared similarly except that the mixture of 409 ml acidic solution and 100 ml alkaline solution was diluted to four liters to provide a concentration five times that of the carrier buffer. Similar day to day pH adjustments were made as with the carrier and sample buffer to assure constant pH values throughout the tests. The final pH of the electrolyte buffer was 8.3 and its conductivity was 7.21×10^{-4} mho to 7.41×10^{-4} mho. The ionic strength was approximately 0.0125. Both the diethylbarbituric acid and its sodium salt were obtained from Sigma Chemical Company, St. Louis, Missouri.

5.3 ASSAY METHODS

The two proteins used during these tests, human albumin and fibrinogen, were obtained from Sigma Chemical Company in St. Louis and are the most highly purified forms found commercially available. Both are reactive to the Folin and Ciocalteu reagent described by Lowry (7), and a modification of his method was used to conduct all the protein assays during these tests. This modified procedure was conducted as follows:

REAGENTS

Source of Reagents

Sodium carbonate, sodium hydroxide and cupric sulfate penthydrate were obtained from Mallinkrodt Chemical Company in St. Louis. Sodium potassium tartrate and the Folin and Ciocalteu Reagent (2N) were obtained from Sigma Chemical Company in St. Louis.

Composition of Reagents

Reagent 1 - 20 grams of sodium carbonate and 4 grams of sodium hydroxide dissolved in 1000 ml of deionized water.

Reagent 2 - 20 grams of sodium potassium tartrate dissolved in 1000 ml of deionized water.

Reagent 3 - 10 grams of cupric sulfate pentahydrate dissolved in 1000 ml of deionized water.

Reagent 4 - Folin and Ciocalteu Reagent (2N).

Assay Procedure

1. Just prior to use, 50 ml of Reagent 1 was mixed with 0.5 ml of Reagent 2. This solution was mixed thoroughly and then 0.5 ml of Reagent 3 was added. After thorough mixing, this solution was labeled Reagent A. This reagent was prepared fresh daily.
2. Samples to be assayed were pipetted into 16 x 100 mm plastic test tubes in 1.0 ml aliquots. To the 1.0 ml of sample was added 2.0 ml of Reagent A. After mixing, these solutions were allowed to stand at room temperature for 10 minutes.
3. After 10 minutes 0.1 ml of the Folin and Ciocalteu Reagent (2N) was added and the solutions again mixed thoroughly. These final test solutions were allowed to stand at room temperature for 30 minutes. After this time their optical densities were determined at 700 nm in a Coleman Spectronic 70 Colorimeter using as a blank the 0.0025 ionic strength diethylbarbituric acid buffer described in Section 4.1.
4. Standard curves were prepared daily using human albumin as the standard at concentrations ranging from 400 to 3.125 µg/ml in the same 0.0025 ionic strength barbituric acid.

5.4 DATA REDUCTION AND CORRELATION

The results of the single protein runs of human albumin at 0 volts/cm and buffer flowrates of 20, 30 and 40 ml/min are shown in Figure 5-4. The dashed lines in each case are for the corresponding analytical predictions. What is immediately apparent from this comparison is that the test results show some widening of the sample stream even with no voltage applied. Since the analytical predictions included modeling of the effects of diffusion, some of this widening must be attributed to the test hardware. The corresponding results and comparisons for the single protein runs of fibrinogen at 0 volts/cm and buffer flowrates of 20, 30, and 40 ml/min are shown in Figure 5-7. Here again, the same widening of the sample streams at zero applied voltage is evident.

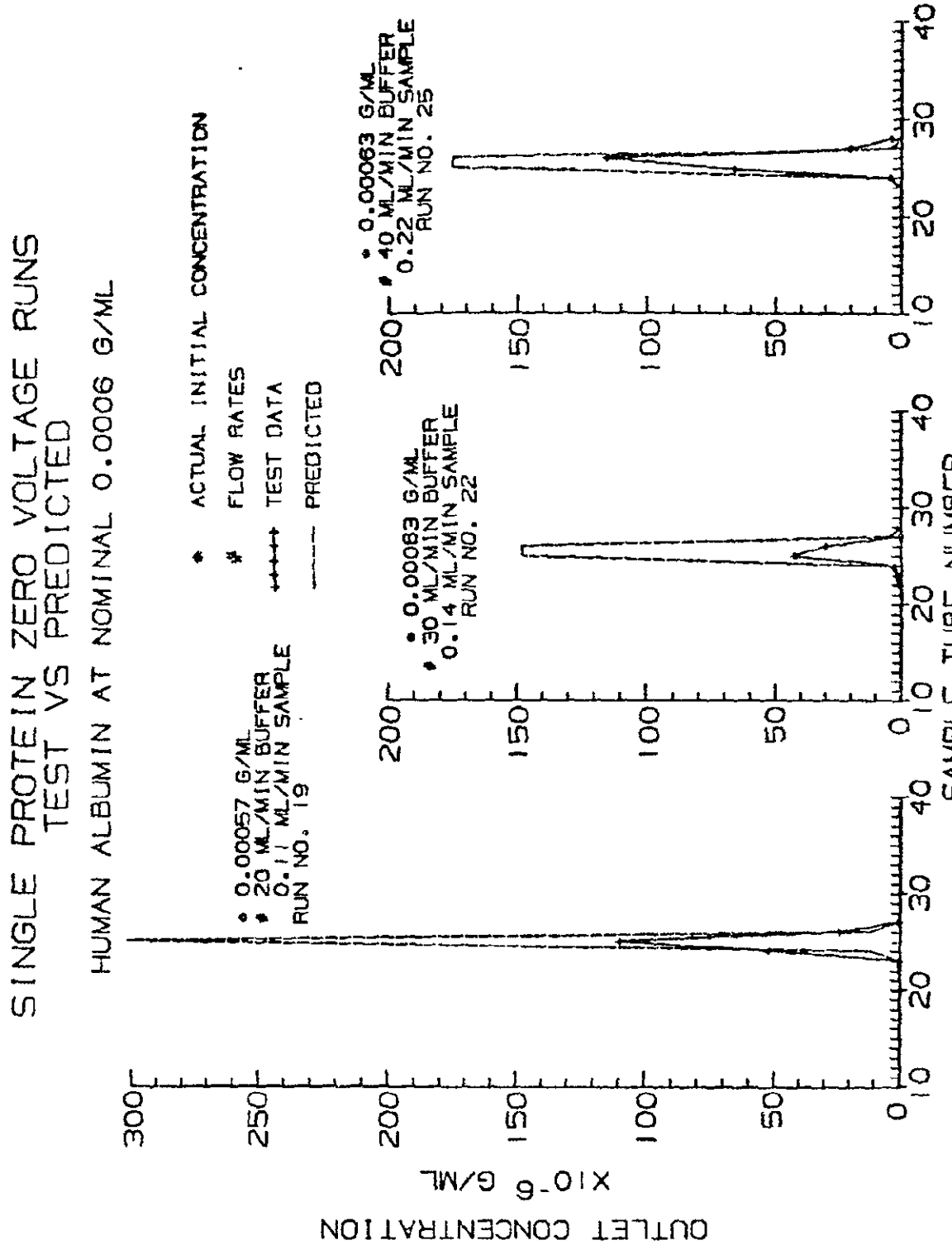
SINGLE PROTEIN ZERO VOLTAGE RUNS
TEST VS PREDICTED
HUMAN ALBUMIN AT NOMINAL 0.0006 G/ML
* ACTUAL INITIAL CONCENTRATION
# FLOW RATES
+++++ TEST DATA
—— PREDICTED
* 0.00057 G/ML
# 20 ML/MIN BUFFER
0.11 ML/MIN SAMPLE
RUN NO. 19
* 0.00083 G/ML
# 30 ML/MIN BUFFER
0.14 ML/MIN SAMPLE
RUN NO. 22
* 0.00063 G/ML
# 40 ML/MIN BUFFER
0.22 ML/MIN SAMPLE
RUN NO. 25
OUTLET CONCENTRATION
X 10⁻⁶ G/ML
SAMPLE TUBE NUMBER

FIGURE 5-4

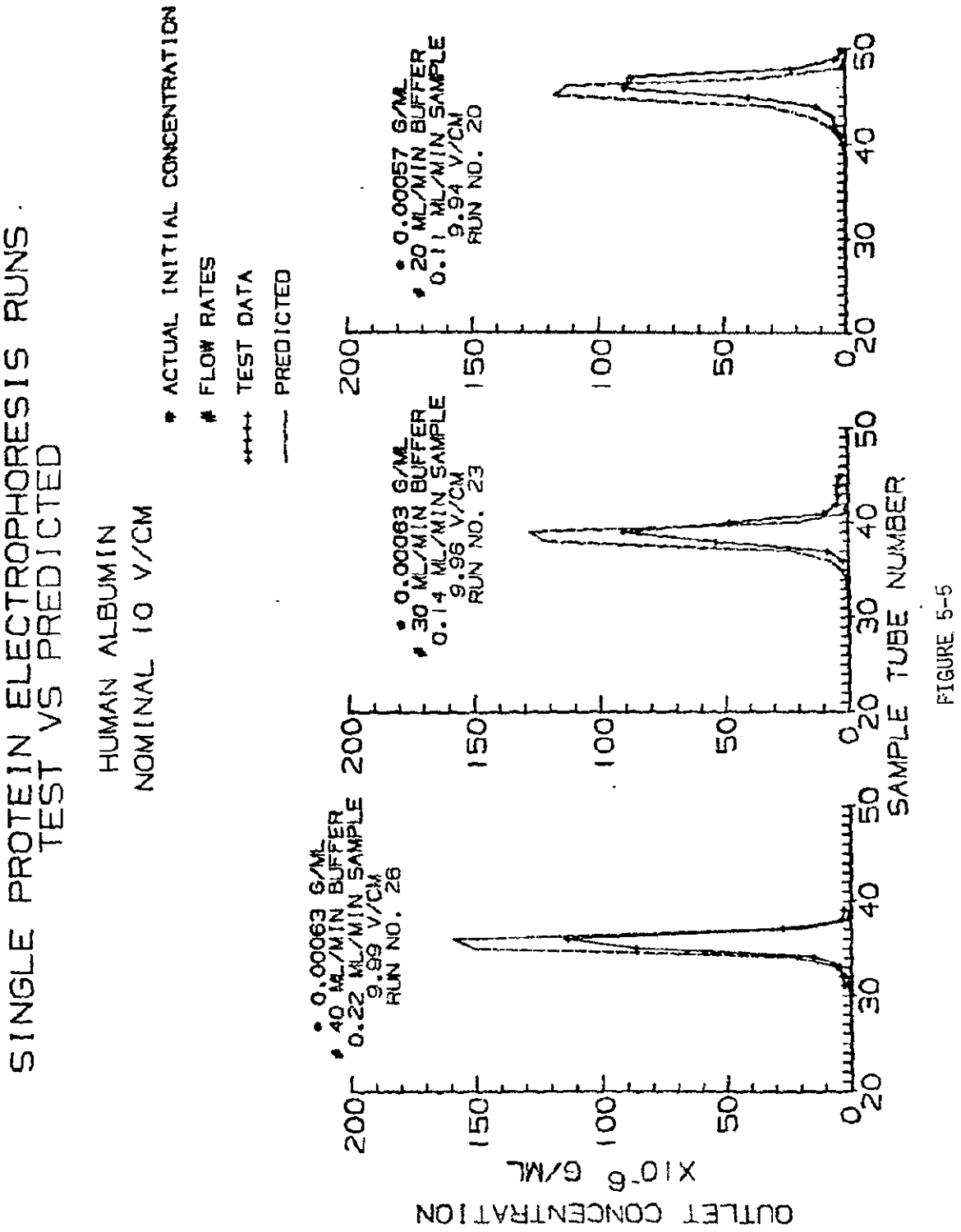
SINGLE PROTEIN ELECTROPHORESIS RUNS
TEST VS PREDICTED
HUMAN ALBUMIN
NOMINAL 10 V/CM
* ACTUAL INITIAL CONCENTRATION
# FLOW RATES
++++ TEST DATA
—— PREDICTED
* 0.00063 G/ML
# 40 ML/MIN BUFFER
0.22 ML/MIN SAMPLE
9.99 V/CM
RUN NO. 26
* 0.00063 G/ML
# 30 ML/MIN BUFFER
0.14 ML/MIN SAMPLE
9.96 V/CM
RUN NO. 23
* 0.00057 G/ML
# 20 ML/MIN BUFFER
0.11 ML/MIN SAMPLE
9.94 V/CM
RUN NO. 20
OUTLET CONCENTRATION
X10⁻⁶ G/ML
SAMPLE TUBE NUMBER

FIGURE 5-5

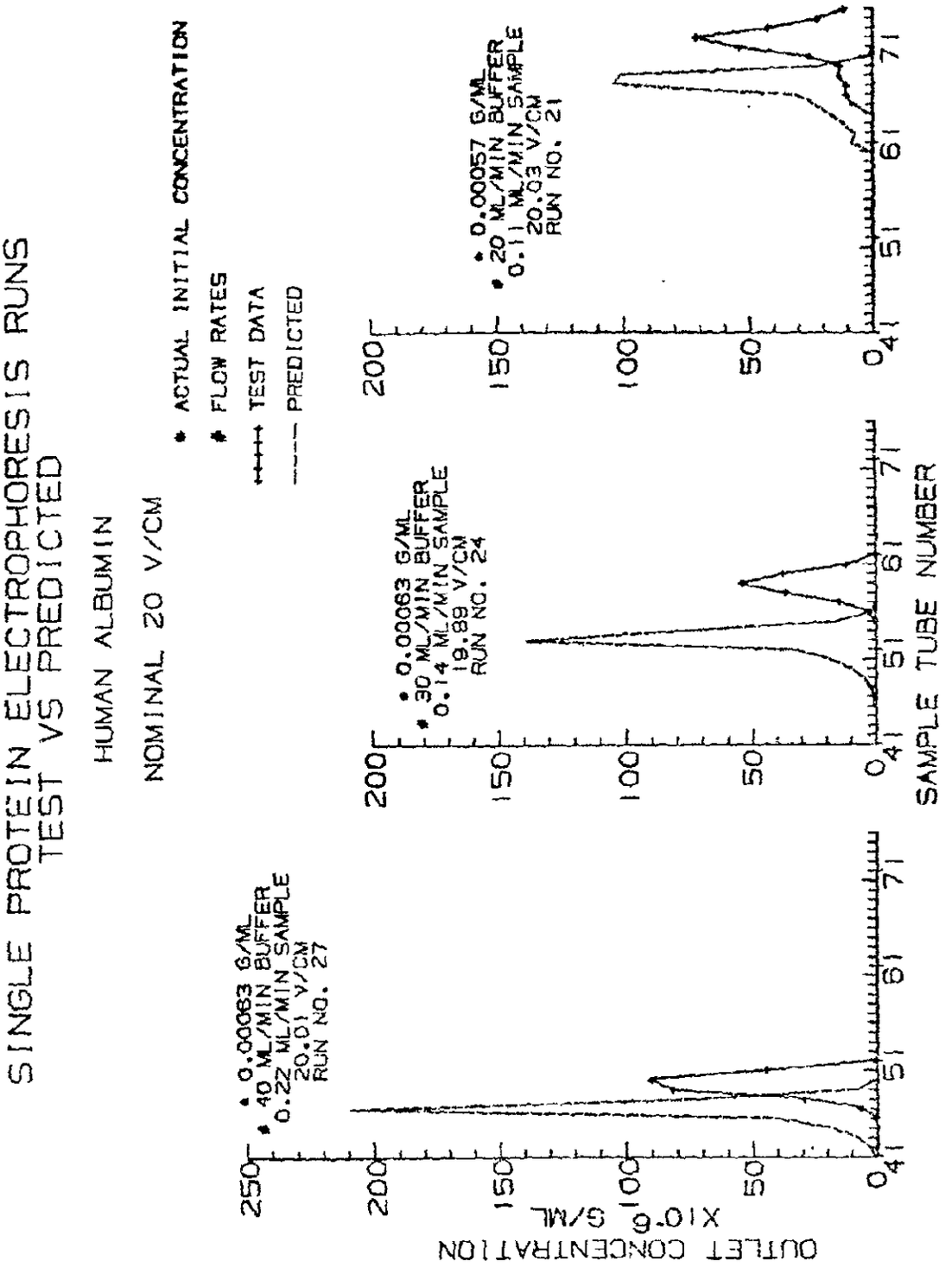
SINGLE PROTEIN ELECTROPHORESIS RUNS
TEST VS PREDICTED
HUMAN ALBUMIN
NOMINAL 20 V/CM
* ACTUAL INITIAL CONCENTRATION
# FLOW RATES
+++ TEST DATA
---- PREDICTED
* 0.00063 G/ML
# 40 ML/MIN BUFFER
0.22 ML/MIN SAMPLE
20.01 V/CM
RUN NO. 27
* 0.00063 G/ML
# 30 ML/MIN BUFFER
0.14 ML/MIN SAMPLE
19.89 V/CM
RUN NO. 24
* 0.00057 G/ML
# 20 ML/MIN BUFFER
0.11 ML/MIN SAMPLE
20.03 V/CM
RUN NO. 21
OUTLET CONCENTRATION
X10^6 G/ML
SAMPLE TUBE NUMBER

FIGURE 5-6

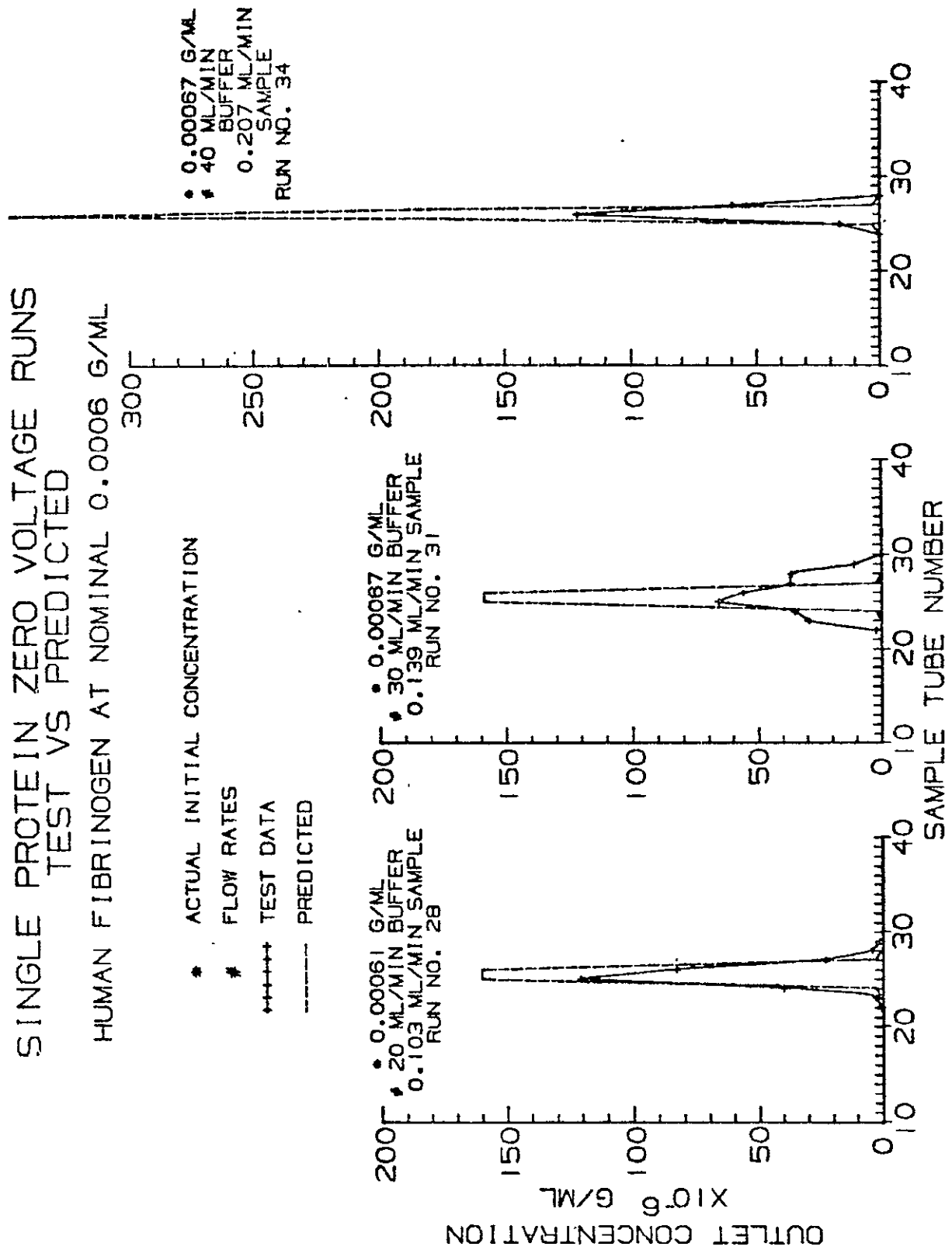
SINGLE PROTEIN ZERO VOLTAGE RUNS
TEST VS PREDICTED
HUMAN FIBRINOGEN AT NOMINAL 0.0006 G/ML
* ACTUAL INITIAL CONCENTRATION
# FLOW RATES
TEST DATA
PREDICTED
* 0.00061 G/ML
# 20 ML/MIN BUFFER
0.103 ML/MIN SAMPLE
RUN NO. 28
* 0.00087 G/ML
# 30 ML/MIN BUFFER
0.139 ML/MIN SAMPLE
RUN NO. 31
* 0.00067 G/ML
# 40 ML/MIN
BUFFER
0.207 ML/MIN
SAMPLE
RUN NO. 34
OUTLET CONCENTRATION
X10^6 G/ML
SAMPLE TUBE NUMBER

FIGURE 5-7

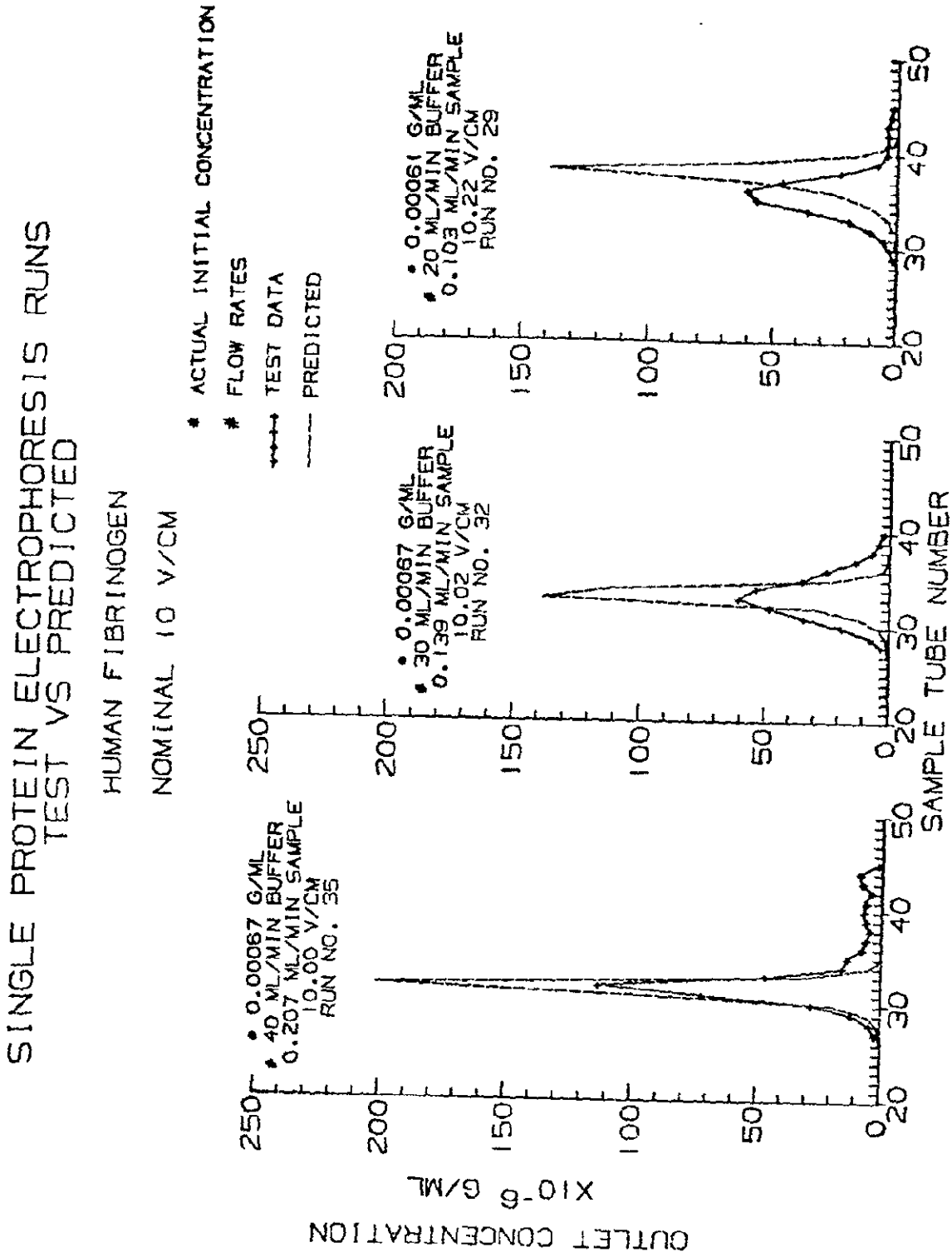
SINGLE PROTEIN ELECTROPHORESIS RUNS
TEST VS PREDICTED
HUMAN FIBRINOGEN
NOMINAL 10 V/CM
* ACTUAL INITIAL CONCENTRATION
# FLOW RATES
TEST DATA
PREDICTED
* 0.00067 G/ML
# 40 ML/MIN BUFFER
0.207 ML/MIN SAMPLE
10.00 V/CM
RUN NO. 35
* 0.00067 G/ML
# 30 ML/MIN BUFFER
0.139 ML/MIN SAMPLE
10.02 V/CM
RUN NO. 32
* 0.00061 G/ML
# 20 ML/MIN BUFFER
0.103 ML/MIN SAMPLE
10.22 V/CM
RUN NO. 29
OUTLET CONCENTRATION
X10-6 G/ML
SAMPLE TUBE NUMBER

FIGURE 5-8

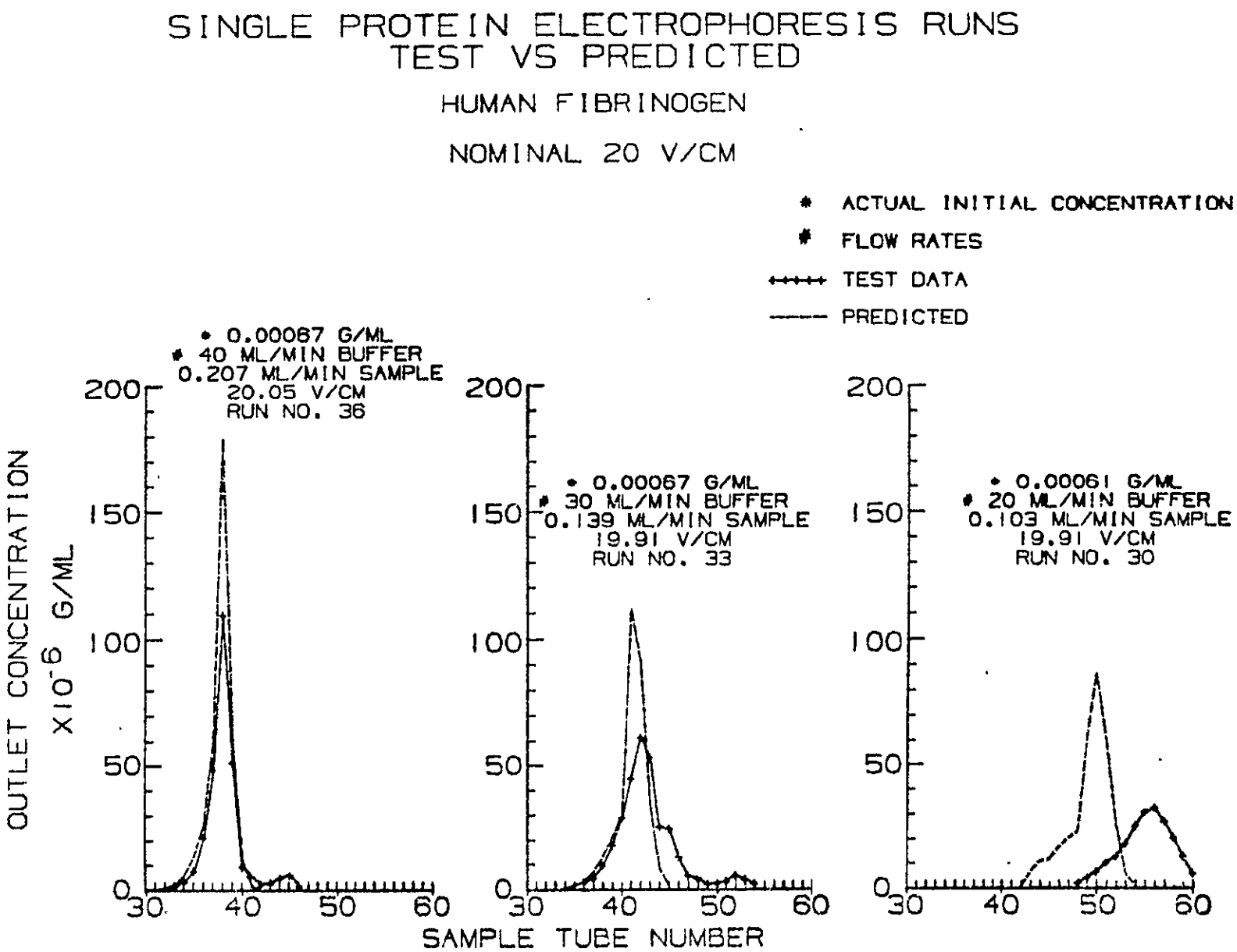
SINGLE PROTEIN ELECTROPHORESIS RUNS
TEST VS PREDICTED
HUMAN FIBRINOGEN
NOMINAL 20 V/CM
* ACTUAL INITIAL CONCENTRATION
# FLOW RATES
TEST DATA
PREDICTED
* 0.00087 G/ML
# 40 ML/MIN BUFFER
0.207 ML/MIN SAMPLE
20.05 V/CM
RUN NO. 36
* 0.00067 G/ML
# 30 ML/MIN BUFFER
0.139 ML/MIN SAMPLE
19.91 V/CM
RUN NO. 33
* 0.00061 G/ML
# 20 ML/MIN BUFFER
0.103 ML/MIN SAMPLE
19.91 V/CM
RUN NO. 30
OUTLET CONCENTRATION
X10-6 G/ML
0
50
100
150
200
30
40
50
60
SAMPLE TUBE NUMBER

FIGURE 5-9

The results of the single protein runs of human albumin at 10 volts/cm and buffer flowrates of 20, 30, and 40 ml/min are shown in Figure 5-5. The dashed lines in each case are for the corresponding analytical predictions. These runs, particularly at the higher flowrates, show the effects of the widening of the sample stream that was evident in the runs with no applied voltage. If it is assumed that the zero voltage widening also applies to cases with voltage, as it would if it were associated with the system, then the analytical predictions show very good correlation with the test results. The corresponding distributions for human albumin at 20 volts/cm and 40, 30 and 20 ml/min buffer flowrate are presented in Figure 5-6. Here again, the difference between the predicted distributions and the test results can be explained in terms of the zero voltage widening of the sample streams and is not attributable to the application of voltage. The underprediction of sample movement in the analysis can be attributed to the actual residence times being greater than the predicted residence times as evidenced by the buffer flow gravity effects test data correlation.

The results of the single protein runs of human fibrinogen at field strengths of 10 and 20 volts per cm are presented in Figures 5-8 and 5-9 respectively. Here, both the general widening of the sample streams characteristic of the zero voltage cases and the increased movement for the test peaks relative to the predicted peaks at higher voltages is evident.

The output concentration distributions for the mixed protein separations are presented in Figures 5-10 through 5-16. The results for the highest concentration, 0.12% protein by weight per unit volume, and the lowest buffer flowrate, 20 ml/min are presented in Figure 5-10. The results show generally good correlation, once the widening of the sample stream for the no voltage case is accounted for. The question in interpreting the results is how much of the widening of the sample stream can be attributed to gravity. This was determined analytically by predicting the distribution with and without the gravity body force in the - $\bar{z}$ direction (Figure 5-11). The peak shift, due to gravity, is about one tube of additional movement. Of course, this widening would increase at higher concentration or lower buffer flowrates. Corresponding data at lower concentrations 0.034% and 0.018% protein by weight per unit volume is presented in Figures 5-13 and 5-15.

The results of mixed protein concentration distributions at a higher buffer flowrate of 40 ml/min are presented in Figures 5-12, 5-14, and 5-16. These results are consistent with those for the 20 ml/min buffer flowrate, except that the peaks are sharper and the distance moved is less due to the shorter residence time. Figure 5-16, which has the outlet concentration distribution for the lowest concentration, 0.018%, and the highest buffer flowrate, 40 ml/min, should have a minimum of gravity effects.

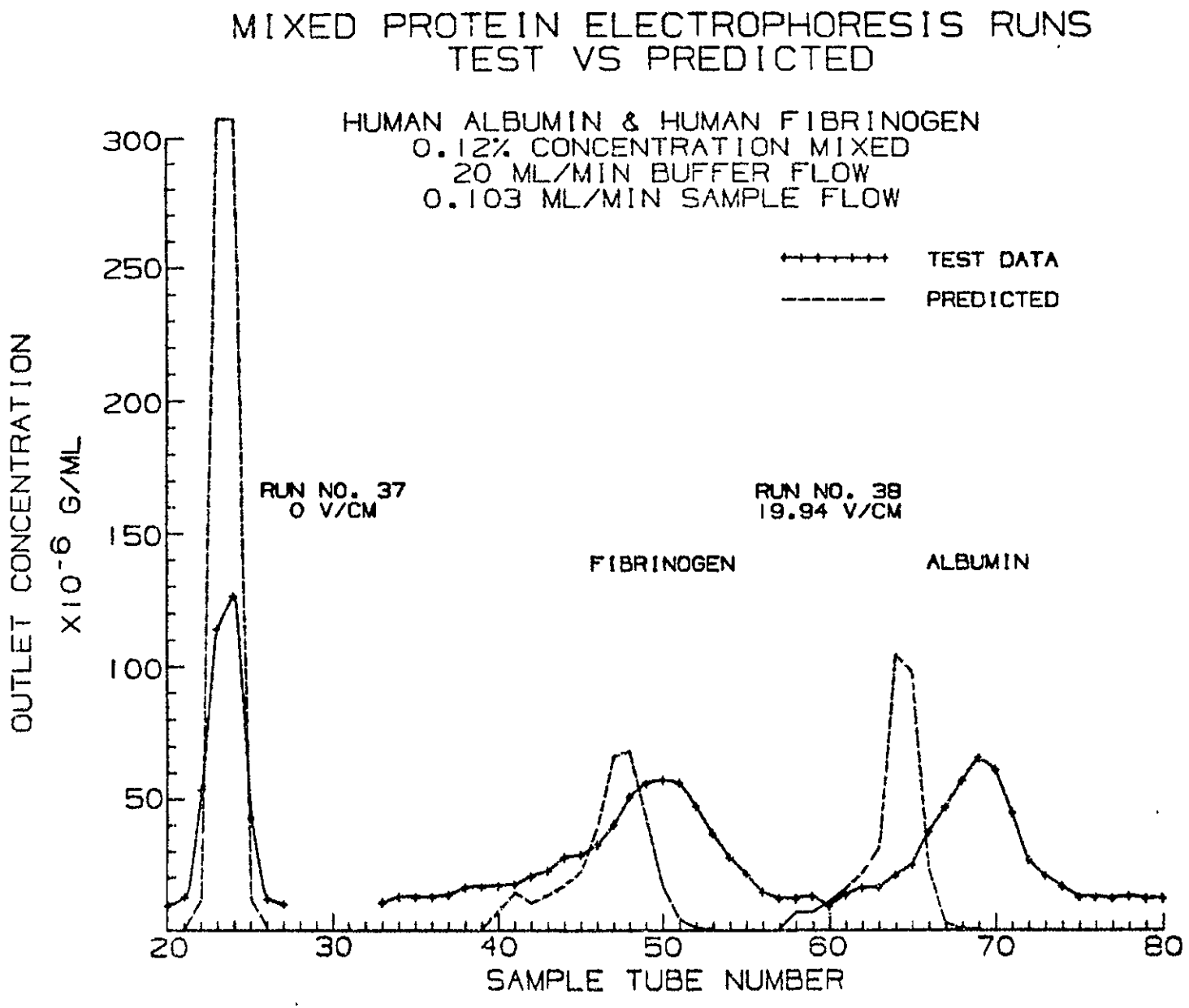
MIXED PROTEIN ELECTROPHORESIS RUNS
TEST VS PREDICTED
HUMAN ALBUMIN & HUMAN FIBRINOGEN
0.12% CONCENTRATION MIXED
20 ML/MIN BUFFER FLOW
0.103 ML/MIN SAMPLE FLOW
TEST DATA
PREDICTED
OUTLET CONCENTRATION
X10-6 G/ML
300
250
200
150
100
50
RUN NO. 37
0 V/CM
RUN NO. 38
19.94 V/CM
FIBRINOGEN
ALBUMIN
20
30
40
50
60
70
80
SAMPLE TUBE NUMBER

FIGURE 5-10

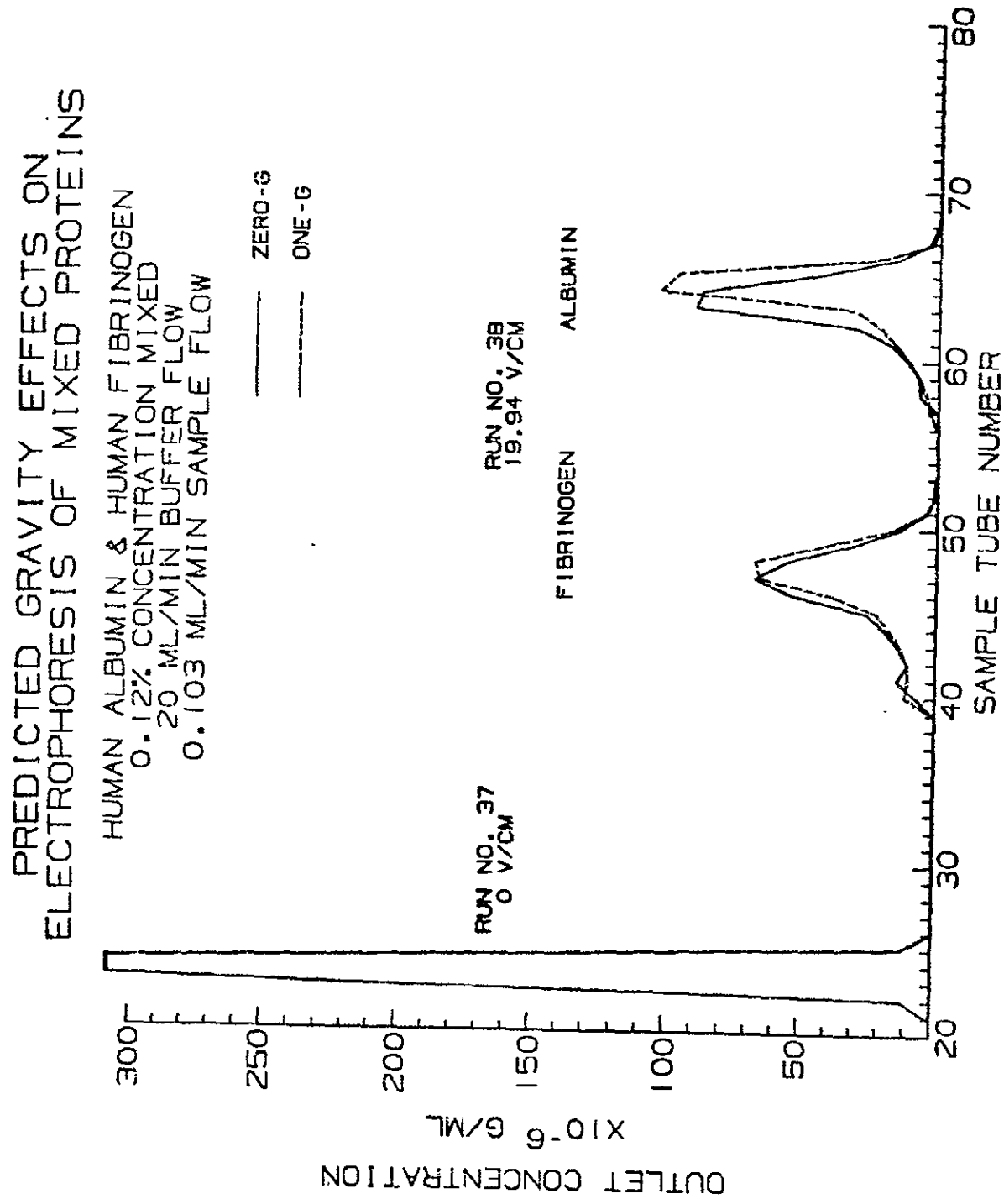
PREDICTED GRAVITY EFFECTS ON
ELECTROPHORESIS OF MIXED PROTEINS
HUMAN ALBUMIN & HUMAN FIBRINOGEN
0.12% CONCENTRATION MIXED
20 ML/MIN BUFFER FLOW
0.103 ML/MIN SAMPLE FLOW
ZERO-G
ONE-G
RUN NO. 38
19.94 V/CM
RUN NO. 37
0 V/CM
FIBRINOGEN
ALBUMIN
OUTLET CONCENTRATION
X10^-6 G/ML
SAMPLE TUBE NUMBER
300
250
200
150
100
50
20
30
40
50
60
70
80

FIGURE 5-11

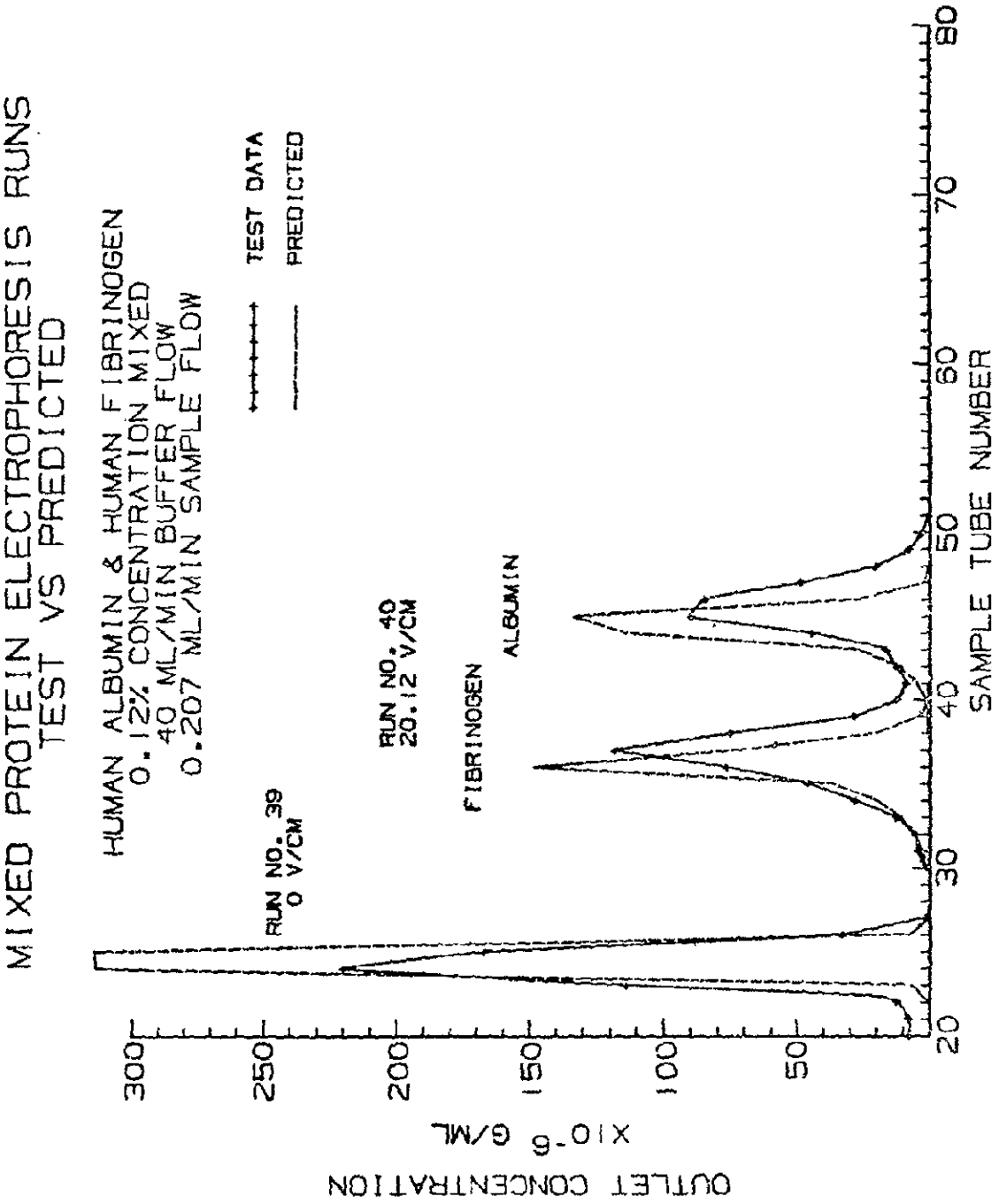
MIXED PROTEIN ELECTROPHORESIS RUNS
TEST VS PREDICTED
HUMAN ALBUMIN & HUMAN FIBRINOGEN
0.12% CONCENTRATION MIXED
40 ML/MIN BUFFER FLOW
0.207 ML/MIN SAMPLE FLOW
TEST DATA
PREDICTED
RUN NO. 39
0 V/CM
RUN NO. 40
20.12 V/CM
FIBRINOGEN
ALBUMIN
OUTLET CONCENTRATION
X10⁻⁶ G/ML
SAMPLE TUBE NUMBER
300
250
200
150
100
50
20
30
40
50
60
70
80

FIGURE 5-12

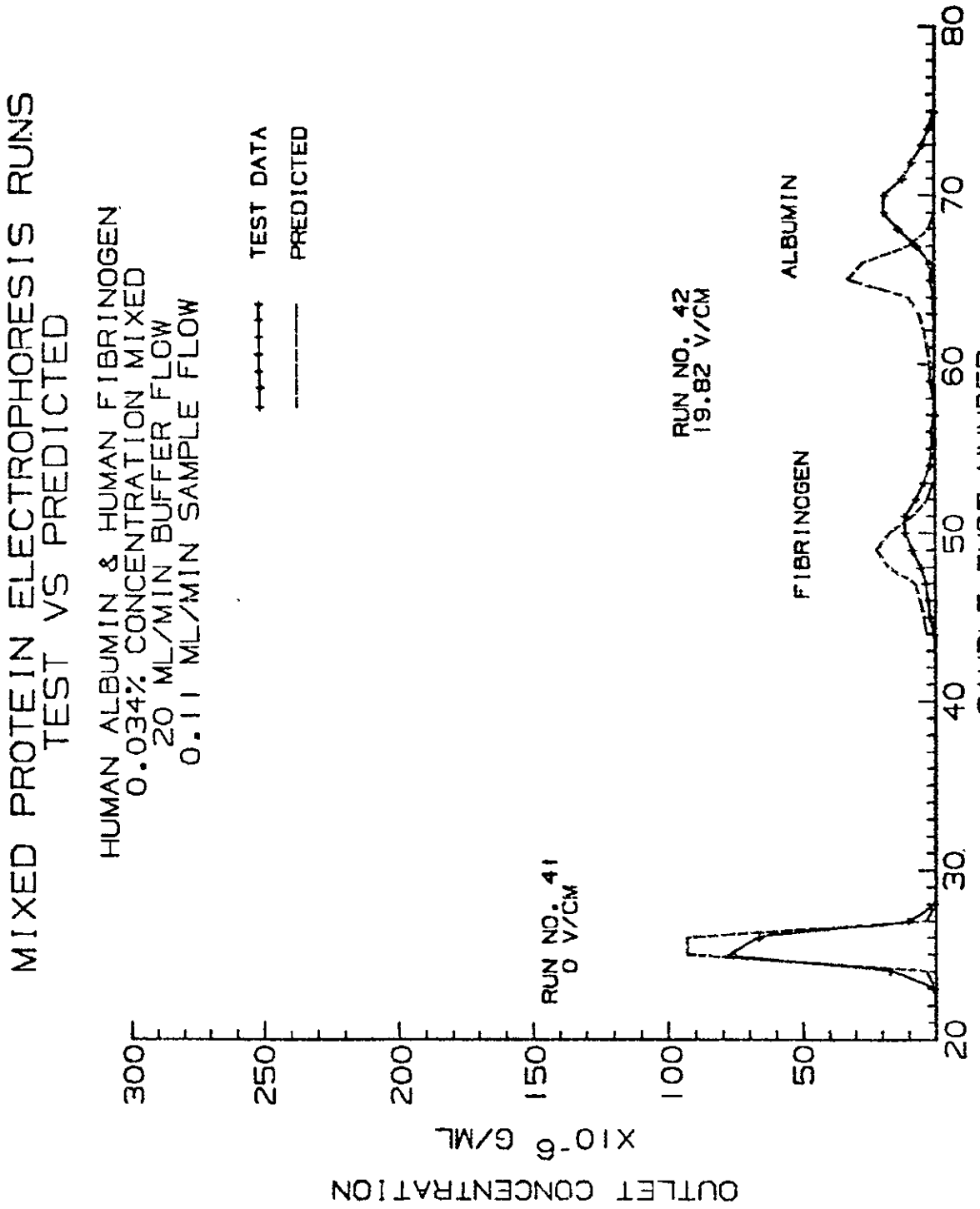
MIXED PROTEIN ELECTROPHORESIS RUNS
TEST VS PREDICTED
HUMAN ALBUMIN & HUMAN FIBRINOGEN
0.034% CONCENTRATION MIXED
20 ML/MIN BUFFER FLOW
0.11 ML/MIN SAMPLE FLOW
TEST DATA
PREDICTED
RUN NO. 41
0 V/CM
RUN NO. 42
19.82 V/CM
ALBUMIN
FIBRINOGEN
OUTLET CONCENTRATION
X10⁻⁶ G/ML
SAMPLE TUBE NUMBER
300
250
200
150
100
50
20
30
40
50
60
70
80

FIGURE 5-13

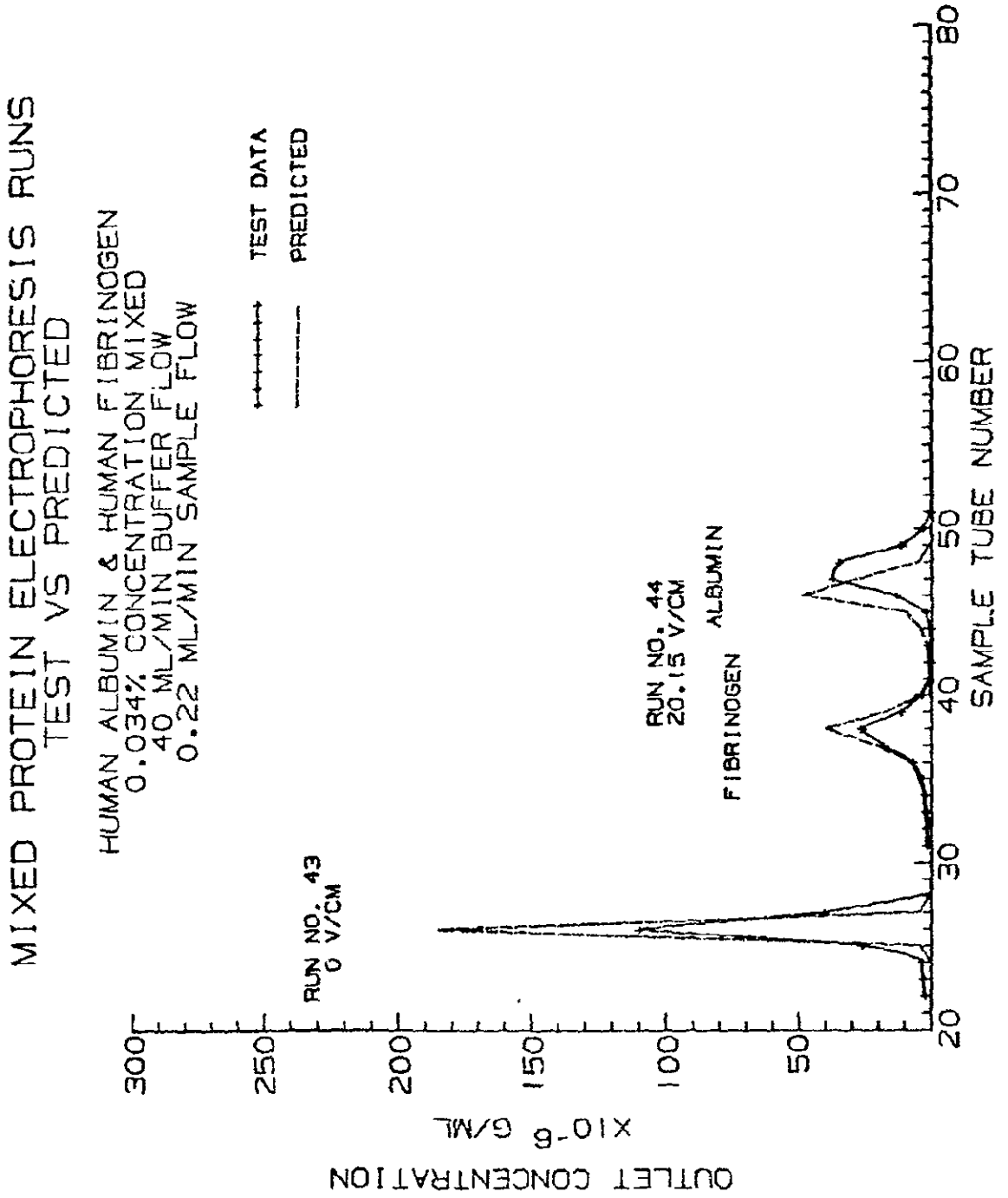
MIXED PROTEIN ELECTROPHORESIS RUNS
TEST VS PREDICTED
HUMAN ALBUMIN & HUMAN FIBRINOGEN
0.034% CONCENTRATION MIXED
40 ML/MIN BUFFER FLOW
0.22 ML/MIN SAMPLE FLOW
TEST DATA
PREDICTED
RUN NO. 43
0 V/CM
RUN NO. 44
20.15 V/CM
FIBRINOGEN
ALBUMIN
OUTLET CONCENTRATION
X10⁻⁶ G/ML
SAMPLE TUBE NUMBER
300
250
200
150
100
50
20
30
40
50
60
70
80

FIGURE 5-14

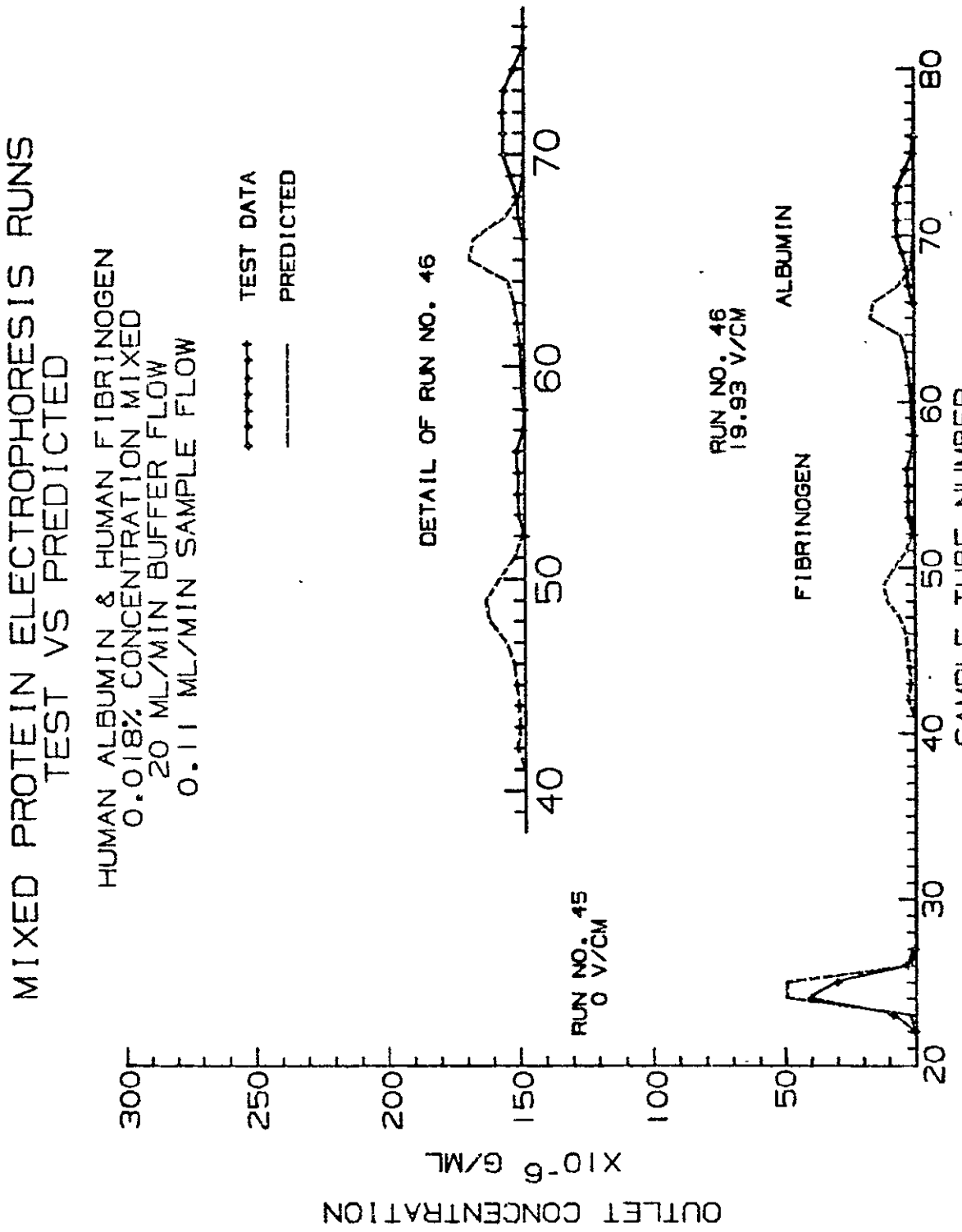
MIXED PROTEIN ELECTROPHORESIS RUNS
TEST VS PREDICTED
HUMAN ALBUMIN & HUMAN FIBRINOGEN
0.018% CONCENTRATION MIXED
20 ML/MIN BUFFER FLOW
0.11 ML/MIN SAMPLE FLOW
TEST DATA
PREDICTED
DETAIL OF RUN NO. 46
RUN NO. 45
0 V/CM
RUN NO. 46
19.93 V/CM
ALBUMIN
FIBRINOGEN
OUTLET CONCENTRATION
X10⁻⁶ G/ML
SAMPLE TUBE NUMBER
300
250
200
150
100
50
40
50
60
70
20
30
40
50
60
70
80

FIGURE 5-15

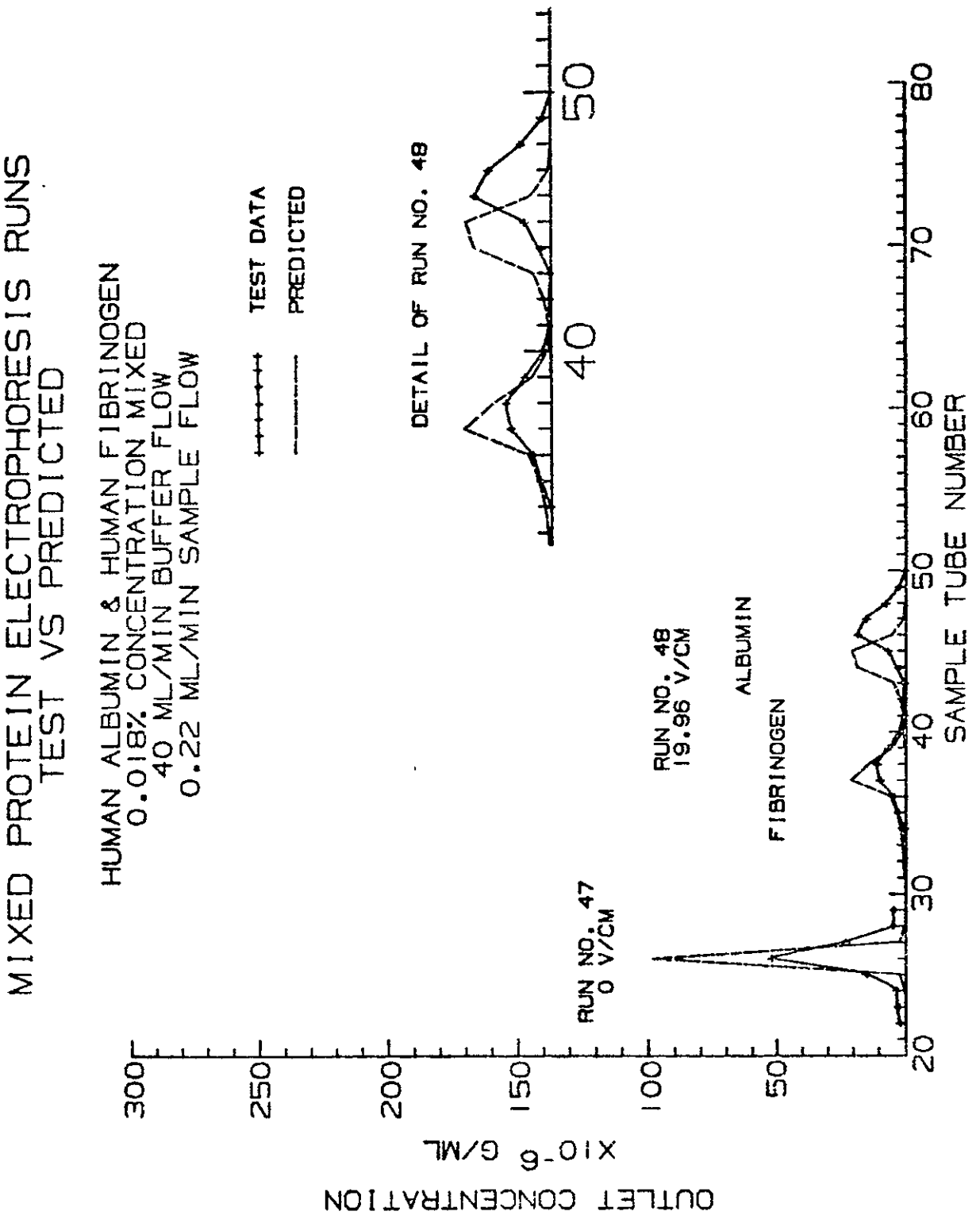
MIXED PROTEIN ELECTROPHORESIS RUNS
TEST VS PREDICTED
HUMAN ALBUMIN & HUMAN FIBRINOGEN
0.018% CONCENTRATION MIXED
40 ML/MIN BUFFER FLOW
0.22 ML/MIN SAMPLE FLOW
TEST DATA
PREDICTED
DETAIL OF RUN NO. 48
RUN NO. 47
0 V/CM
RUN NO. 48
19.96 V/CM
ALBUMIN
FIBRINOGEN
OUTLET CONCENTRATION
X10⁻⁶ G/ML
SAMPLE TUBE NUMBER

FIGURE 5-16

6.0 CELL GRAVITY EFFECTS

The purpose of the tests described in this section was to demonstrate the effects of gravity on sample streams of cells. The cells used for these tests shown in Figure 6-1 were 33H human lymphocytes. The movement of the lymphocytes during electrophoresis was experimentally found at flowrates of 20 and 40 ml/min and concentrations of 1×10^7, 5×10^6, and 2.7×10^5 cells/ml. Test data collectionis described in Section 6.1 and the data reduction and correlation in Section 6.2.

6.1 TEST DATA COLLECTION

Continuity of test conditions previously run with proteins was maintained by establishing chamber conditions as close as possible to those of the Task 1.0 runs. As with the protein test runs, dye was used only for initial verification that a cell density would flow within the chamber. This method was used to determine the upper limit for cell densities at the stated carrier buffer flow rates and for the trypsinized buffer used. The lower density limit was set by the assay technique. Sample to carrier buffer ratios of 1:200 $\pm$ 9% were again maintained.

Cells were harvested, washed, counted and diluted as required on a daily basis. Because of an expected tendency for cells in the sample syringe to settle with time, thereby effecting outlet distribution, the syringe was slowly and continuously agitated to control settling. Because of some syringe and connected feed tube movement due to the agitation, a slight, short period (1-2 CPS) pulse of the sample stream as it left the capillary tube in the chamber was noted. This pulse caused some of the spread in the collected sample distribution.

Only two cell runs, one at zero-voltage and one electrophoresis could be conducted each day and this required a new sample of cells be counted the next test day. These day-to-day harvestings, suspensions, and dilutions resulted only in about 3% deviation in initial cell counts. Sample injection and collection procedures were generally the same as for the protein runs. In the assay, cell counting was performed on all collected samples and included sample from tubes as far as twenty (20) on either side of the expected peak count.

Cell concentrations in units of g/ml were calculated from the cell counts and

TASK 2.0

TEST MATRIX, RUNS 49-60

CELL DENSITY EFFECTS

CELL DENSITY \ BUFFER FLOW ML/MIN	20	40
1.0×10^7	50 / 49	52 / 51
5.0×10^6	54 / 53	56 / 55
2.7×10^5	58 / 57	60 / 59

0 VOLTS/CM \ 10 VOLTS/CM

FIELD STRENGTH

- SINGLE CELL TYPE, LYMPHOCYTES
- 1 MM DIAMETER SAMPLE STREAM
- CELL COUNT FOR OUTLET DISTRIBUTION
- GRAVITY INDUCED CHANGES ARE CONCENTRATION AND BUFFER FLOW RATE DEPENDENT

Figure 6—1

an experimentally determined mass of 1.235×10^{-9} g/cell and density of 1.060 g/cm^3.

6.2 CELL SELECTION

Cells used for these tests were a continuous human lymphocyte line designated 33H by the American Type Tissue Culture Collection. They are a vigorously proliferating cell which grows in suspension culture, and range in diameter from 8.5 to about 15 microns. Since lymphocytes produce a wide variety of materials which may become candidates for space bioprocessing, these cells represented an ideal source of material for the conduct of these tests.

6.3 CELL PREPARATION

Cells used for these tests were grown in RPMI medium (Grand Island Biological Company (GIBCO), Buffalo, New York) which contained 0.03% glutamine and 0.2% sodium carbonate. Prior to use the medium was supplemented with 20% fetal calf serum, also obtained from GIBCO. Starter cultures consisted of 100 ml spinner flasks containing 100 ml of medium inoculated with 3×10^7 cells to provide a starter culture containing 3×10^5 cells/ml. During incubation, cells were exposed to an atmosphere of 5% CO_2, 95% air. After three to four days incubation at 37^oC, the starter cultures were used to inoculate 500 ml spinner flasks at a concentration of 3×10^5 cells/ml. After three to four days, the cultures were similarly inoculated into 1000 ml flasks from which test samples were harvested. Cells for electrophoretic tests were harvested by centrifugation at 200g for 20 minutes. Harvested cells were washed once in approximately 100 volumes of buffer (described in Section 5.3), resuspended in the same buffer, enumerated for total and viable cells, adjusted to the concentration desired for testing, and stored at 4^oC until ready for processing.

Generally speaking, cells were harvested at 9:00 a.m., processing was initiated at 11:00 a.m. and completed by 3:00 p.m. Assays of the processed samples were generally completed by 4:00 p.m. In all cases, cells were harvested and prepared fresh daily.

6.4 BUFFER SELECTION

The buffer used for washing, resuspending and processing the human lymphocytes in the electrophoresis unit was prepared as follows: Triethanolamine (2.4 gm), glycine (20.7 gm), potassium acetate (0.4 gm), and glacial acetic acid (0.6 ml) were dissolved in 100 ml of deionized water. When these materials were completely dissolved, calcium chloride dihydrate (0.044 gm) and magnesium chloride hexahydrate (0.061 gm) were added. For use as the carrier buffer and for washing and suspending the test cells, the 1000 ml solution was diluted to 20 liters and 1.0 ml of 2.5% trypsin in .85% sodium chloride (GIBCO) was added and mixed well. For use as electrolyte fluid, another 1000 ml solution was diluted to eight liters and no trypsin was added.

The final pH of the buffer was 7.4, its osmolarity was 294 to 301 m OSM and its conductivity was 1.21×19^{-4} mho/cm to 1.45×10^{-4} mho/cm. The specific gravity was approximately 1.00982 gm/cc at 20°C. Variations in osmolarity and conductivity were due to slight variations in the day to day preparation of the buffer. We chose to prepare buffers fresh daily to minimize the possibility of both microbial and chemical deterioration of the buffer and to avoid addition of preservatives which would affect cell viability. Constant pH values were maintained from day to day by minor additions to the fresh daily buffer of appropriate amounts of either acetic acid or triethanolamine. This buffer provided viability recoveries of up to 90% over the course of the day's testing and assaying, and prevented agglutination of the cells which would have interfered with the tests.

6.5 ASSAY METHOD

Lymphocytes were enumerated in a standard laboratory hemocytometer using Erythrosin B (Fisher Scientific Company, St. Louis, Missouri) dissolved in saline to differentiate viable from nonviable cells. Viable cells exclude the dye and appear clear, while the nonviable cells take up the dye and stain pink.

Depending on the total cell population in the samples, either 0.05% Erythrosin B or 0.4% Erythrosin B was used. If the cell population was between one million and three million cells per ml (100 to 300 cells actually counted in the hemocytometer), the sample was prepared by adding 0.1 ml of the sample to 0.9 ml of 0.05% Erythrosin B. If the cell population was between 40,000 and 100,000 cells per ml (48 to

120 actually counted in the hemocytometer), the sample was prepared by adding 0.5 ml of sample to 0.1 ml of 0.4% Erythrosin B. After adding the dye, cells were allowed to stand at room temperature for 5 minutes before placing them in the hemocytometer for counting. In all cases, prior to dye addition, a preliminary cell count was made to estimate the cell population and to make initial dilutions to bring the total cell population into one of the proper ranges for counting.

6.6 DATA REDUCTION AND CORRELATION

Test versus predicted outlet concentration distributions for the electrophoresis of 33H human lymphocytes are shown in Figures 6-2 through 6-8. The concentration distributions shown in Figure 6-2 are for the lowest buffer flowrate, 20 ml/min and the highest cell density, the case where gravity effects should be most apparent. In general, the predicted spreading of the sample is less than for the test data, both with and without applied electrical field, so some of this spreading is a characteristic of the MDAC-St. Louis test hardware.

In addition, the smaller predicted movement of the cells with the field applied is caused by the actual residence times being greater than predicted, as evidenced by the buffer gravity effects data correlation.

Predicted gravity effects on the electrophoresis of cells are shown in Figure 6-3. The greater movement under electrophoresis in one-g is caused by the increased residence times due to the particle streams slipping with respect to the surrounding buffer. Widening of the particle streams is not evident for this case, but would probably become evident at higher concentrations or greater electrophoretic movement. Test versus predicted concentration distributions for the lower cell densities of 5×10^6 and 2.7×10^5 cells/ml at a buffer flowrate of 20 ml/min are presented in Figures 6-5 and 6-7.

The results of cell electrophoresis at a higher buffer flowrate of 40 ml/min are presented in Figures 6-4, 6-6, and 6-8. These results are consistent with those for the 20 ml/min buffer flowrate, except that the peaks are sharper and the distance moved is less due to the shorter residence times. Figure 6-8, which is the outlet concentration distribution for the lowest cell density, 2.7×10^5 cells/ml, and the highest buffer flowrate, 40 ml/min, would have a minimum of gravity effects.

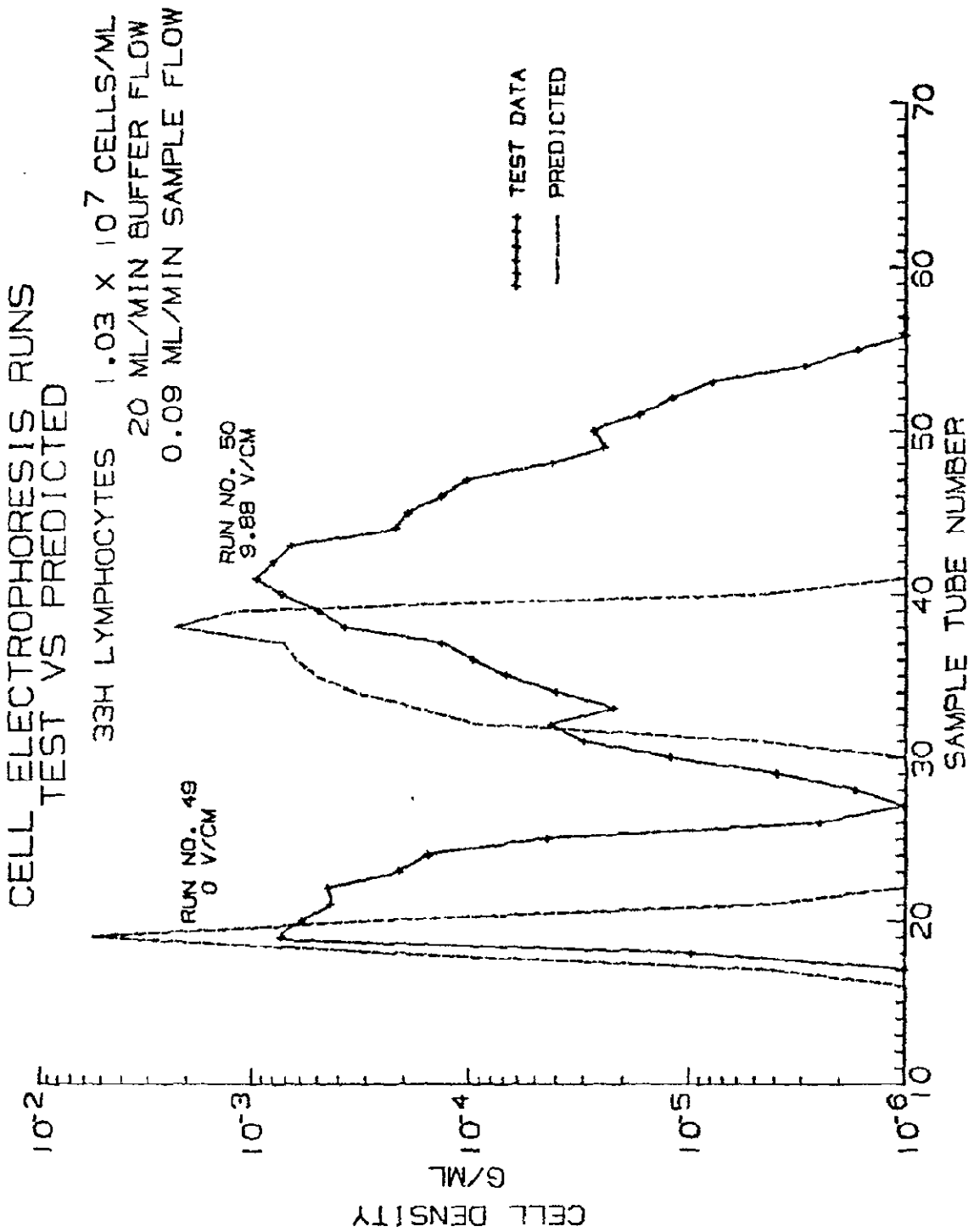
CELL ELECTROPHORESIS RUNS
TEST VS PREDICTED
33H LYMPHOCYTES 1.03 X 10^7 CELLS/ML
20 ML/MIN BUFFER FLOW
0.09 ML/MIN SAMPLE FLOW
TEST DATA
PREDICTED
RUN NO. 49
0 V/CM
RUN NO. 50
9.88 V/CM
CELL DENSITY
G/ML
10^-2
10^-3
10^-4
10^-5
10^-6
10
20
30
40
50
60
70
SAMPLE TUBE NUMBER

FIGURE 6-2

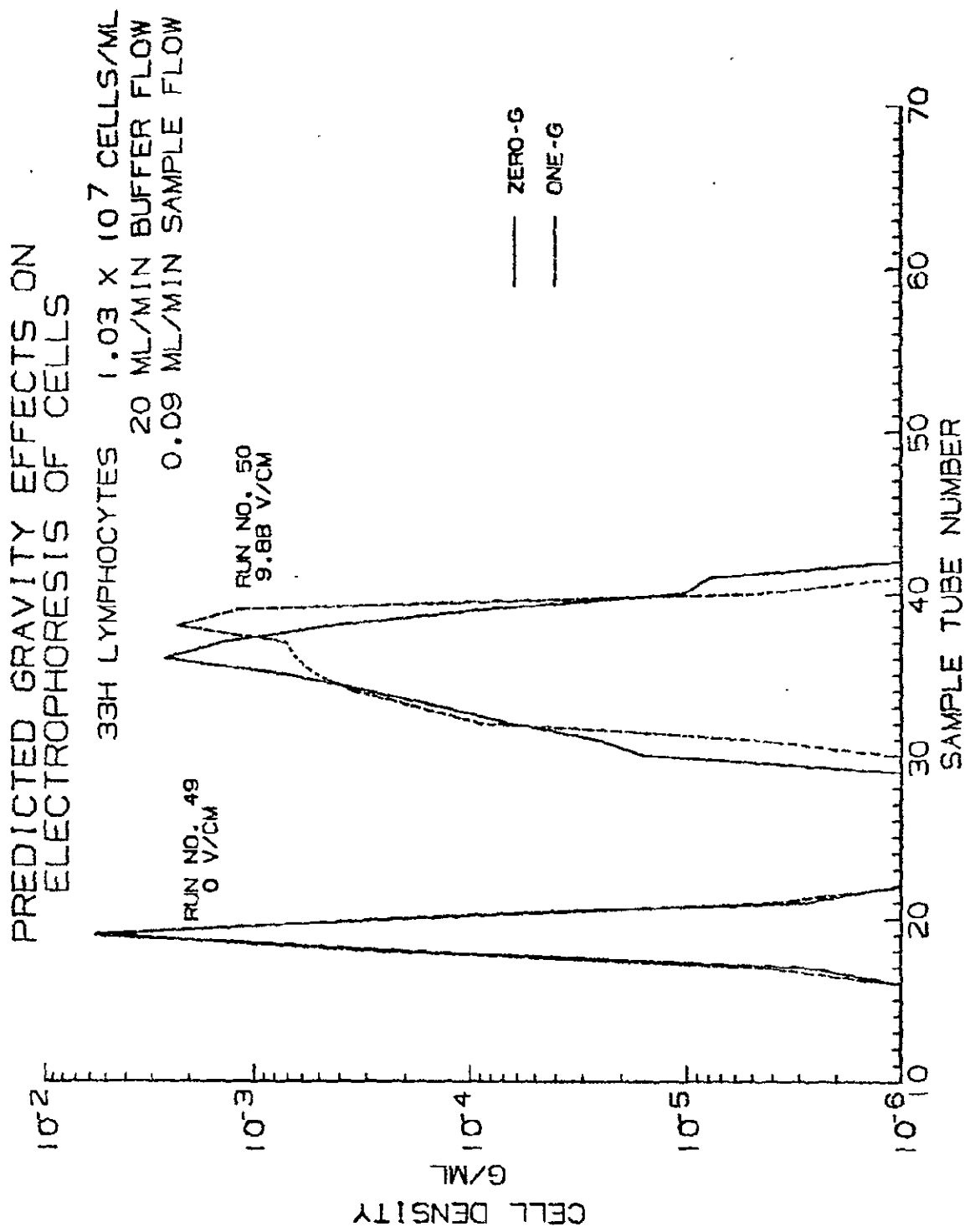
PREDICTED GRAVITY EFFECTS ON
ELECTROPHORESIS OF CELLS
33H LYMPHOCYTES 1.03 X 10^7 CELLS/ML
20 ML/MIN BUFFER FLOW
0.09 ML/MIN SAMPLE FLOW
ZERO-G
ONE-G
RUN NO. 50
9.88 V/CM
RUN NO. 49
0 V/CM
CELL DENSITY
G/ML
SAMPLE TUBE NUMBER

FIGURE 6-3

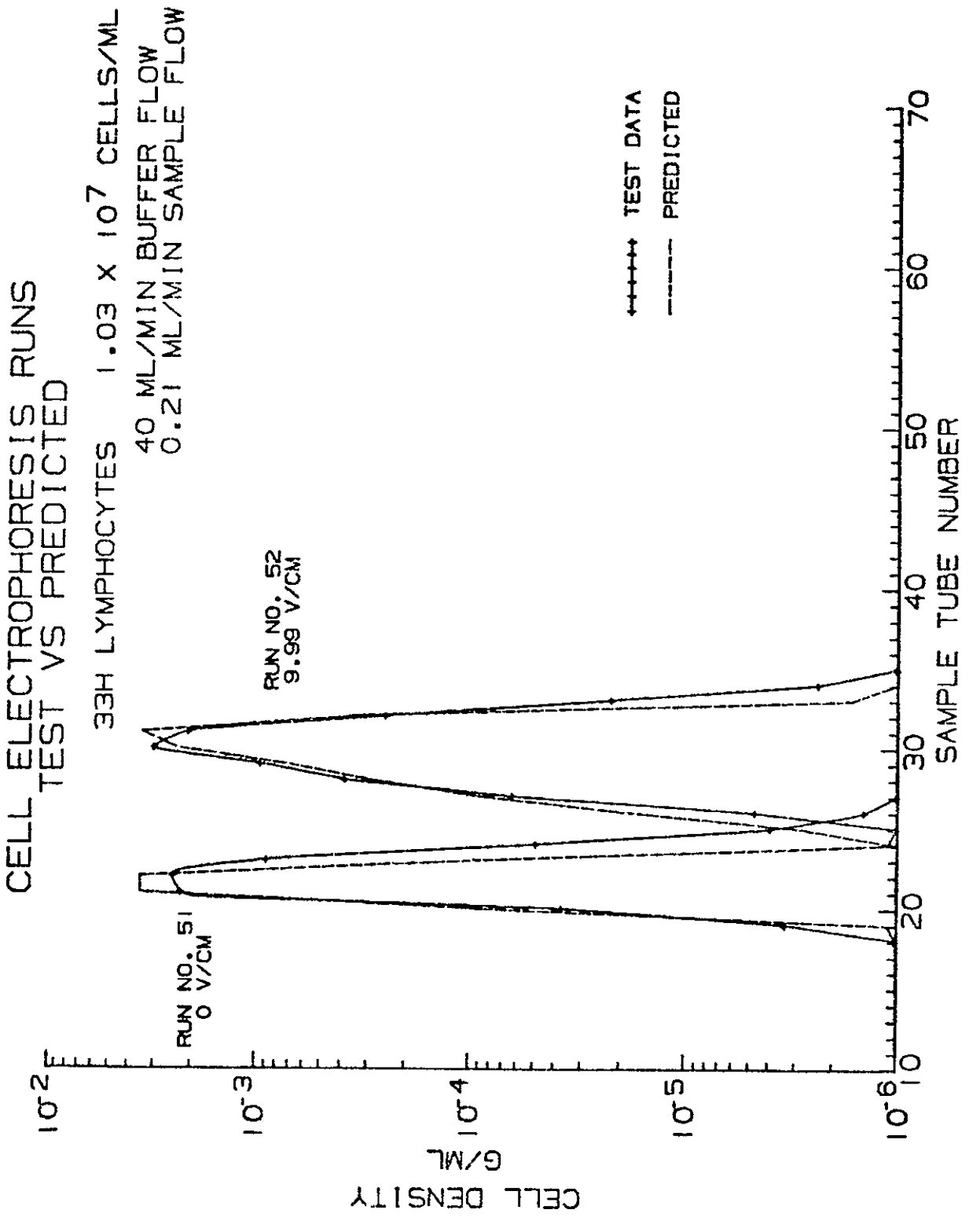
CELL ELECTROPHORESIS RUNS
TEST VS PREDICTED
33H LYMPHOCYTES 1.03 X 10^7 CELLS/ML
40 ML/MIN BUFFER FLOW
0.21 ML/MIN SAMPLE FLOW
TEST DATA
PREDICTED
RUN NO. 52
9.98 V/CM
RUN NO. 51
0 V/CM
CELL DENSITY
G/ML
SAMPLE TUBE NUMBER

FIGURE 6-4

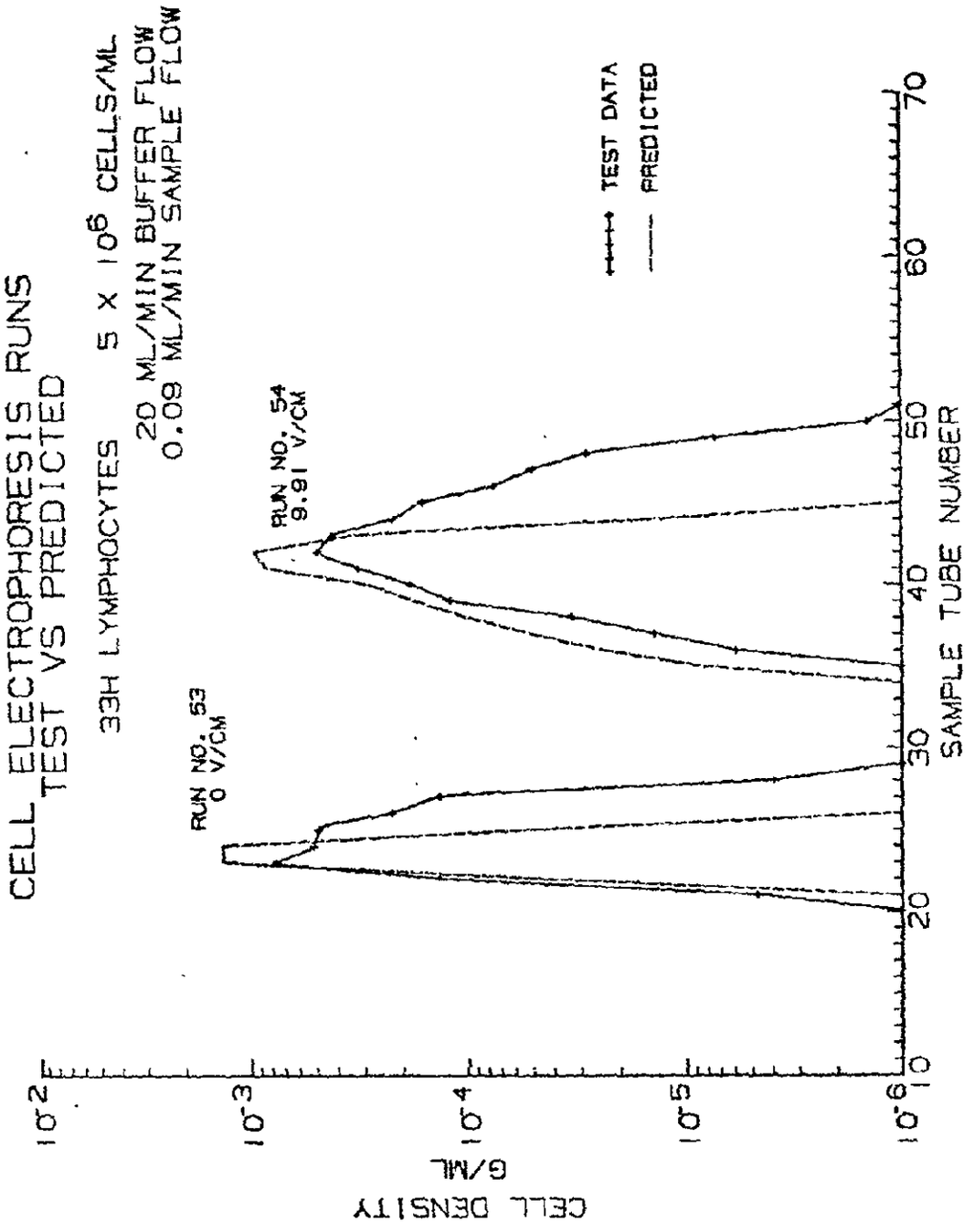
CELL ELECTROPHORESIS RUNS
TEST VS PREDICTED
33H LYMPHOCYTES 5 X 10⁶ CELLS/ML
20 ML/MIN BUFFER FLOW
0.09 ML/MIN SAMPLE FLOW
TEST DATA
PREDICTED
RUN NO. 53
0 V/CM
RUN NO. 54
9.91 V/CM
CELL DENSITY
G/ML
10⁻²
10⁻³
10⁻⁴
10⁻⁵
10⁻⁶
10
20
30
40
50
60
70
SAMPLE TUBE NUMBER

FIGURE 6-5

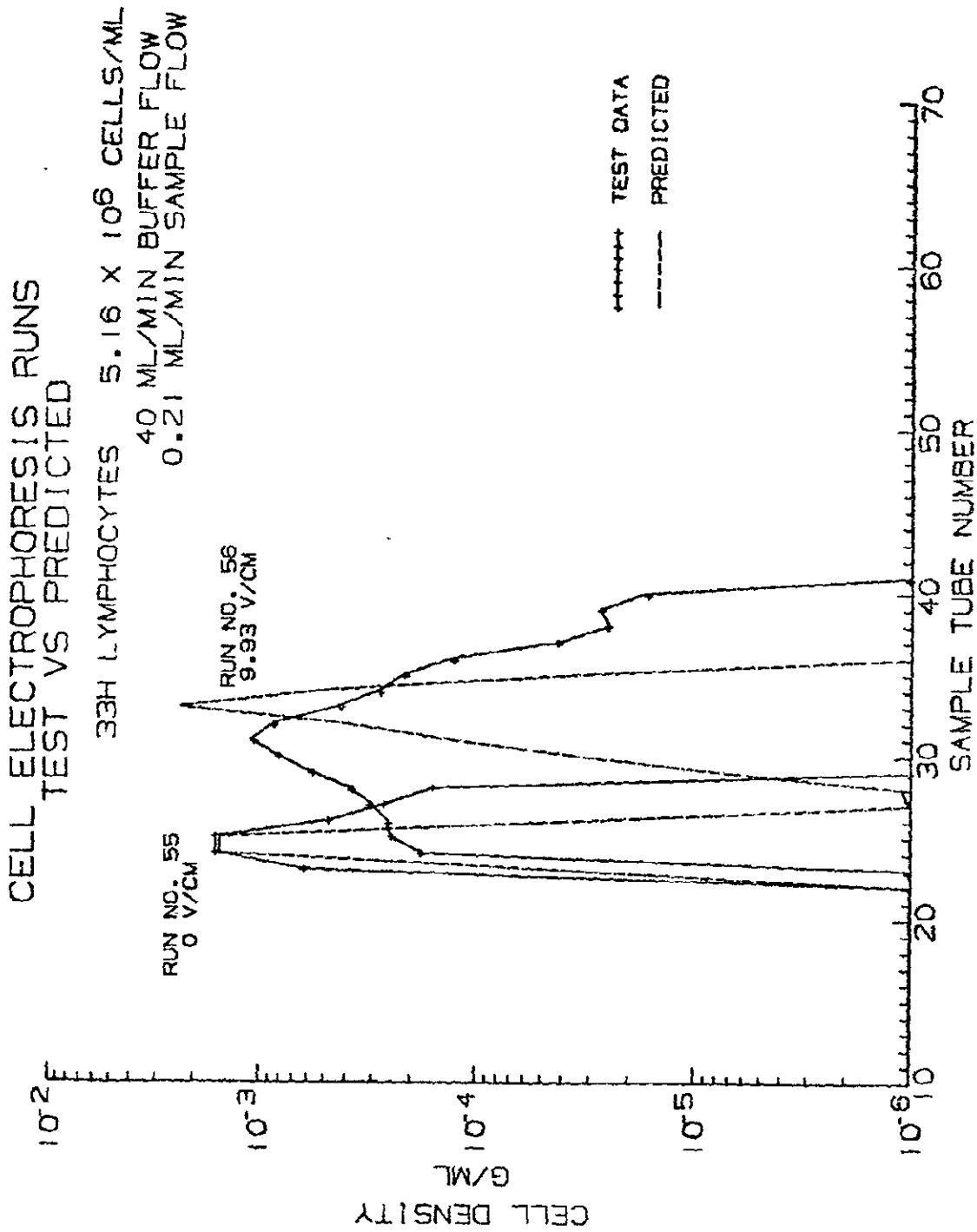
CELL ELECTROPHORESIS RUNS
TEST VS PREDICTED
33H LYMPHOCYTES 5.16 X 10⁶ CELLS/ML
40 ML/MIN BUFFER FLOW
0.21 ML/MIN SAMPLE FLOW
TEST DATA
PREDICTED
RUN NO. 56
9.93 V/CM
RUN NO. 55
0 V/CM
CELL DENSITY
G/ML
10⁻²
10⁻³
10⁻⁴
10⁻⁵
10⁻⁶
10
20
30
40
50
60
70
SAMPLE TUBE NUMBER

FIGURE 6-6

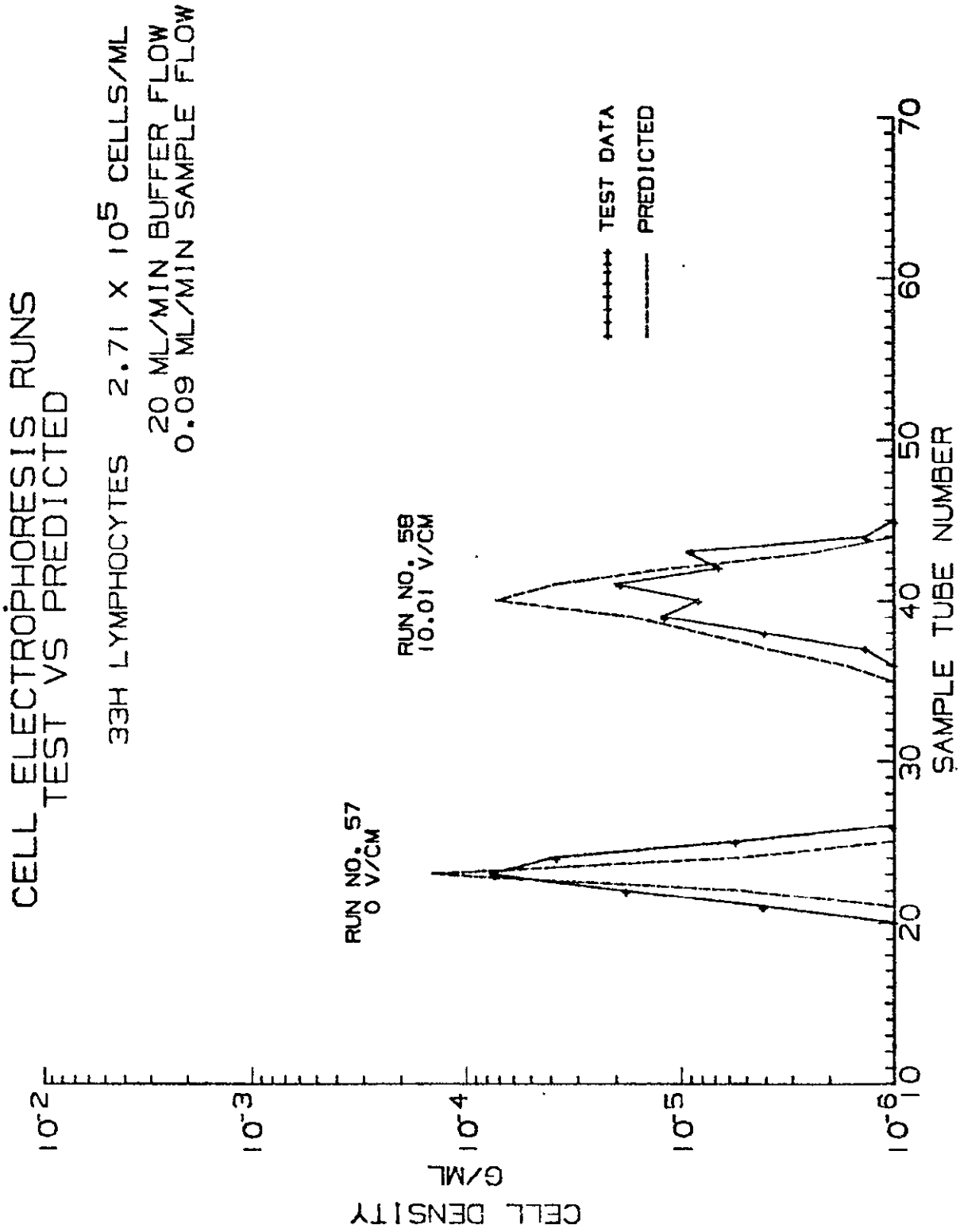
CELL ELECTROPHORESIS RUNS
TEST VS PREDICTED
33H LYMPHOCYTES 2.71 X 10^5 CELLS/ML
20 ML/MIN BUFFER FLOW
0.09 ML/MIN SAMPLE FLOW
TEST DATA
PREDICTED
RUN NO. 57
0 V/CM
RUN NO. 58
10.01 V/CM
CELL DENSITY
G/ML
SAMPLE TUBE NUMBER

FIGURE 6-7

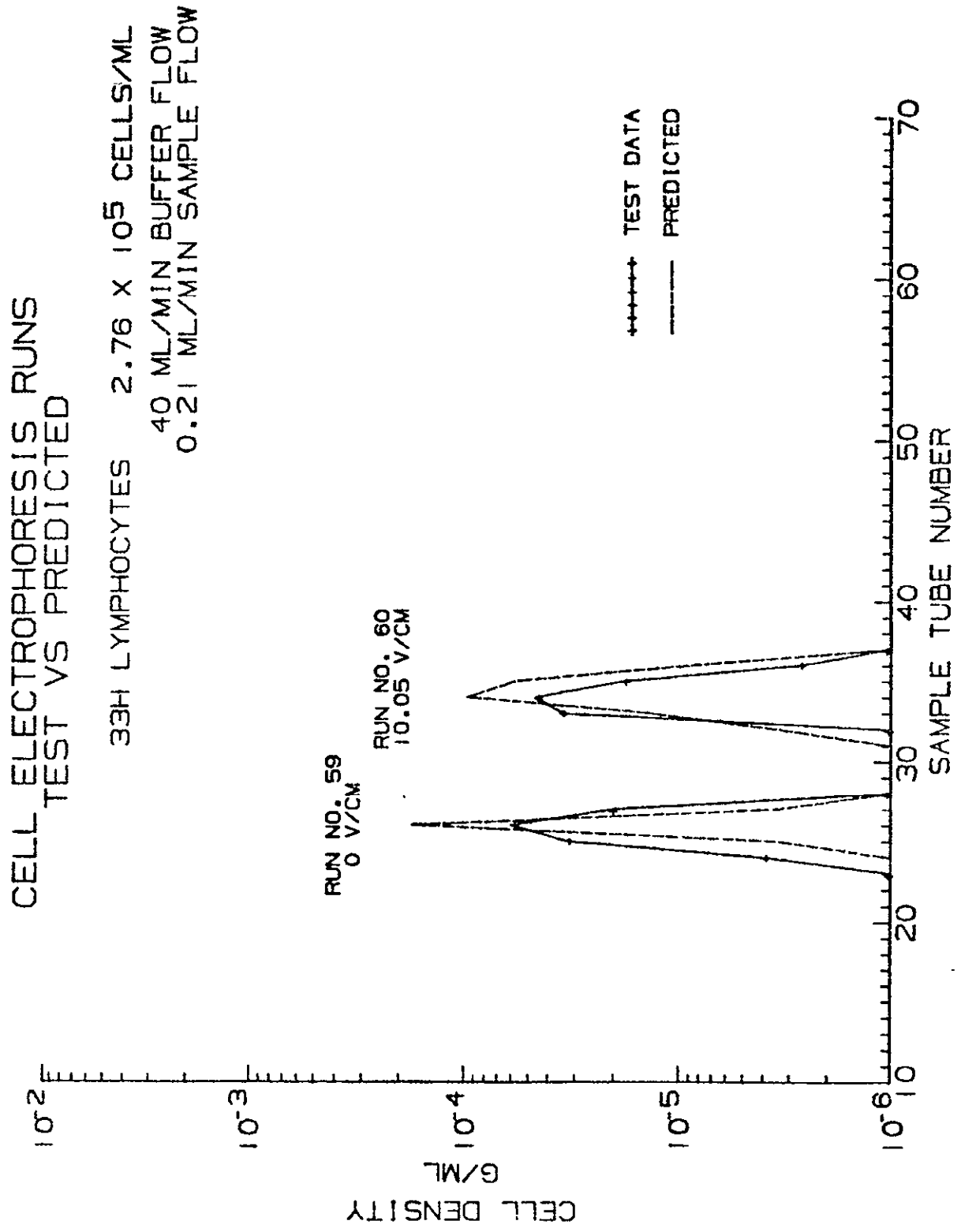
CELL ELECTROPHORESIS RUNS
TEST VS PREDICTED
33H LYMPHOCYTES 2.76 X 10⁵ CELLS/ML
40 ML/MIN BUFFER FLOW
0.21 ML/MIN SAMPLE FLOW
TEST DATA
PREDICTED
RUN NO. 59
0 V/CM
RUN NO. 60
10.05 V/CM
CELL DENSITY
G/ML
SAMPLE TUBE NUMBER

FIGURE 6-8

7.0 SAMPLE CONCENTRATION EFFECTS

Previous studies in the MDAC-St. Louis laboratories have shown that limited concentrations of proteins and cells can be processed by free flow electrophoresis in a one-gravity environment (8,9). Basically, the limitations are caused by the increasing specific gravity that occurs in a solution when increasing amounts of protein solute are added. This increased specific gravity results in an increased weight of the sample stream column flowing upward. When the sample stream column reaches a critical specific gravity, it fails to flow and falls back. This "fall-back" phenomenon can be avoided by increasing the carrier buffer flow rate, but this results in shorter residence times and poorer resolution capabilities. Human plasma must be diluted 1/50 to 1/70 times in distilled water in order to be processed in our unit at a carrier buffer flow rate of 20 ml/min (with sample flow at about 0.2 ml/min). If processed in zero gravity, it would flow without dilution and thus provide the potential of increasing sample throughput by 70 times.

Basic questions have arisen, however, concerning protein-protein interactions occurring in concentrated protein samples (but to a lesser degree in dilute samples) which may alter their fundamental characteristics and affect their electrophoretic mobility. If such were the case, utilizing the greater concentration possible in space would result in a decrease in resolution of the separated protein mixtures.

It is not practical at this time to conduct a space experiment solely to determine if concentration affects electrophoretic mobilities in the free flow process although such an experiment should certainly be included as part of a space demonstration program.

In order to detect the possible effects of concentration on electrophoretic mobility, we employed three common ground based electrophoretic procedures and studied the mobilities of various proteins in human plasma at several concentration. Tests with agar gel plates, and polyacrylamide disc gel electrophoresis showed that no significant differences in the fundamental electrophoretic mobility of the major protein components occurred over a concentration range of nearly two orders of magnitude. Tests with cellulose acetate strips provided only inclusive results because of erratic performance by the instrument employed.

7.1 TEST METHODS

AGAR GEL PLATE ELECTROPHORESIS - Agar coated plastic plates (Corning No. 470100) and a Corning Model No. 470130 electrophoresis chamber were used for this series of tests. Gelman 51104 buffer, pH 8.6 and 0.03 ionic strength, was used as the electrolyte and carrier fluid.

Samples were applied to the gel using the Corning Sample Dispenser Model No. 470152 in 1.0 µl aliquots and the plates placed in the electrophoresis chamber. After positioning the plates, voltage (85 volts) was applied to provide a field strength of about 15 volts/cm.

Samples were electrophoresed for 40 minutes after which time the plates were removed and rinsed in deionized water and dried at 67°C for 60 minutes. They were then stained in 0.5% Coomassie Brilliant Blue R250 (BIO-RAD No. 161-0400 dissolved in 45% methanol, 45% water, and 10% glacial acetic acid, V/V/V) for five minutes. The plates were then rinsed in the above solution (but without added Coomassie Blue) until the protein bands were visible. They were then dried in a 67° oven for one hour. The distance each protein band moved during electrophoresis was then determined by direct measurement of the distance from the original starting position to the center of each band.

POLYACRYLAMIDE DISC GEL ELECTROPHORESIS - For these tests, a BIO-RAD Model No. 150A electrophoresis apparatus was employed. In this method, glass tubes, dimensions 5 mm diameter x 125 mm long, were filled with polyacrylamide gel and run according to the standard procedure of the Miles Laboratories, Elkhart, Indiana. Test samples were mixed with loading gel which was placed at the top of the column in 100 µl aliquots and the column then placed in the electrophoresis chamber. Tris-glycine buffer, pH 8.1 and ionic strength 0.2, was used for the electrolyte and carrier fluid. Samples were electrophoresed for 75 minutes with 150 applied volts which resulted in a field strength of approximately 12 volts/cm and 40 milliamps (5 milliamps per column; 8 columns employed).

After electrophoresis, the polyacrylamide gel columns were removed from the glass column, fixed in 2.5% trichloroacetic acid overnight, rinsed with water, then stained in 1% Coomassie Blue G-250 in 7% acetic acid. They were then rinsed in 7% acetic acid 50% methanol and the gels preserved in 7% acetic acid in water.

The distance each protein band moved during electrophoresis was determined by direct measurement of the distance from the top of the separation gel to the center of each band.

SAMPLE PREPARATION - Standard Normal Plasma (SNP) samples obtained in dried form from Dade Diagnostics, Miami, Florida, were used as the protein samples for these tests. In all cases, the dried plasma was rehydrated prior to use with distilled water. Each SNP vial contains premeasured plasma such that rehydration with 1.0 ml of water will result in a solution representative of normal plasma, containing about 7% total protein. Various sample concentrations were obtained by adding 0.25 ml of water (to obtain a sample containing 28% protein), 0.5 ml for a 14% solution, and so on, to obtain samples containing from 0.109% (one vial in 64.0 ml of water) to 28% (one vial in 0.25 ml of water).

7.2 TEST RESULTS

AGAR GEL PLATES - The results of these tests are shown in Figures 7-1 and 7-2 and are summarized in Figures 7-3 and 7-4. In run 1, samples containing 7.0%, 3.5%, and 1.75% protein were used. A photograph of the stained electrophoresis gel plate is shown in Figure 7-1. The 7% sample clearly separated into six distinct bands representing (from top to bottom) albumin, alpha-1-globulins, alpha-2-globulins, beta-1-globulins, fibrinogen, and gamma globulins. The 2.5% sample also separated into six distinct bands. In the 1.75% sample, only albumin, beta-1-globulins, and fibrinogen were visible, and in the lowest concentration, 0.875%, only albumin, beta-1-globulins, and fibrinogen were visible. This loss of visualization was a result of dilution of the proteins bands beyond the point at which dye would bind sufficiently to be visible to the naked eye.

In run 2 test samples consisted of duplicate samples containing 7% and 28% protein, and a 7% sample which had been prepared originally at 28%, allowed to react at room temperature for two hours and then rediluted to its original 7% protein concentration. A photograph of the stained electrophoresis gel is shown in Figure 7-2. In all cases, the samples showed six distinct separated bands on the original gel plate. Unfortunately, the photographic reproduction does not show the resolution obtained with the 28% sample.

CORNING AGAR GEL PLATE ELECTROPHORESIS OF HUMAN PLASMA PROTEINS

0.875% TO 7.0%

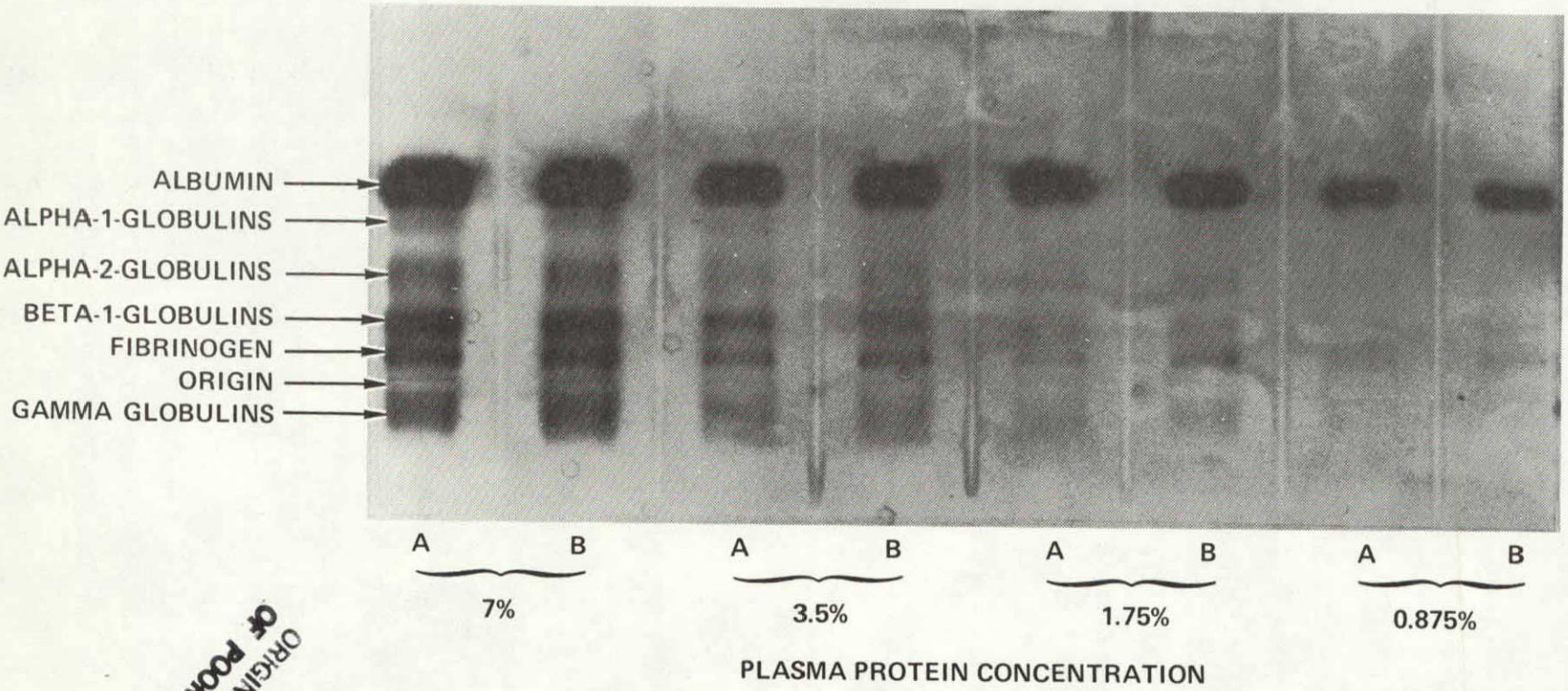

Figure 7—1

CORNING AGAR GEL PLATE ELECTROPHORESIS OF HUMAN PLASMA PROTEINS

7.0% TO 28%

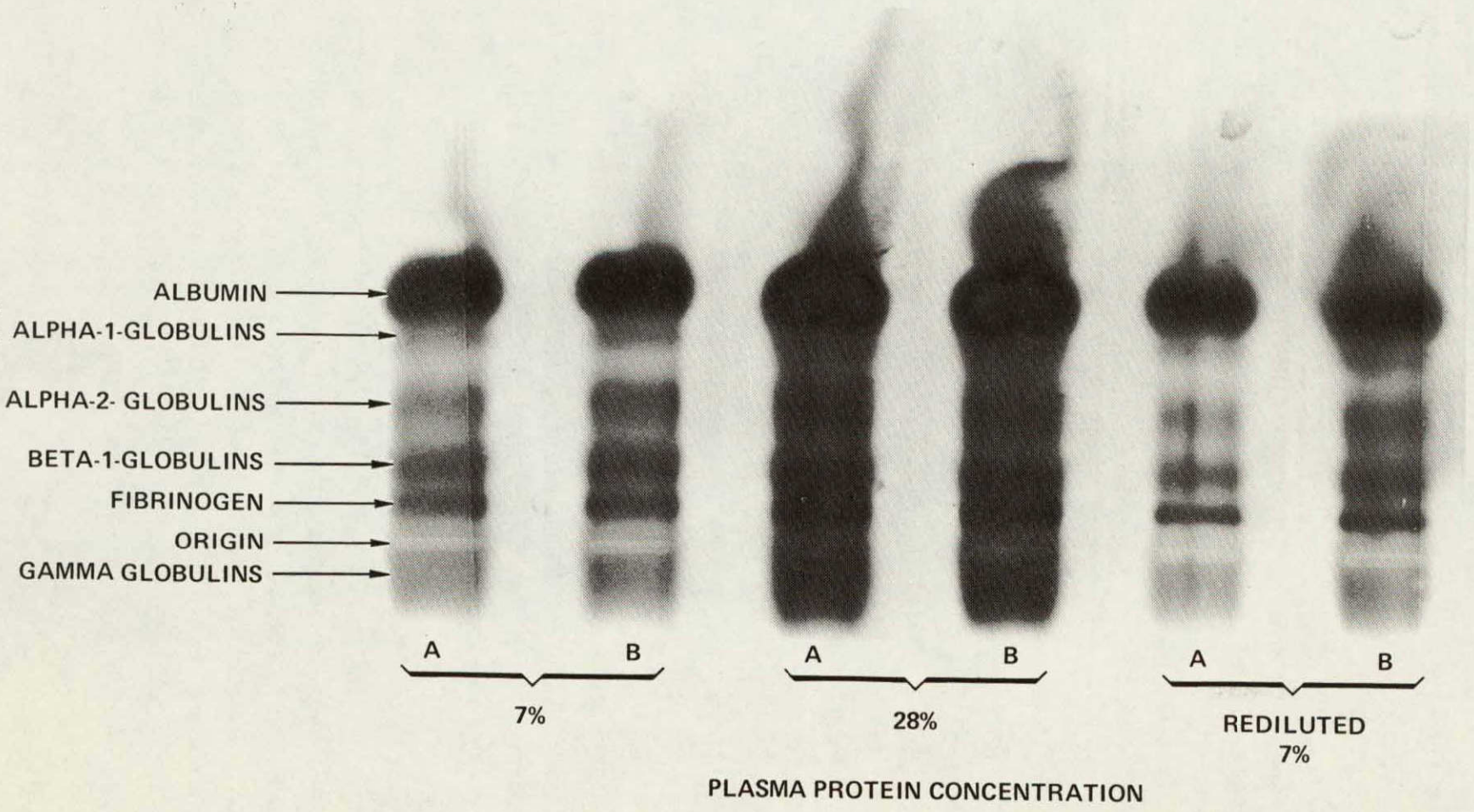

Figure 7–2

Visual inspection of Figures 7-1 and 7-2 reveals that no significant differences in mobility occurred as a result of the starting sample concentration. More precise measurements, made from the origin to the center of each band, are shown in Figures 7-3 and 7-4.

In the first experiment (Figure 7-3) albumin moved a distance of 18 mm, regardless of the concentration of the starting sample. Similarly, all of the other major proteins moved consistently regardless of concentration. In this procedure, the gamma-globulins migrated in the opposite direction to the other proteins and their migration distance is indicated as such by the minus (-) sign. Where N.V. appears in the table, no measurements were possible because the bands were not visible. Measurements of the mobilities in the second experiment are shown in Figure 7-4. As in the first set of data, all the protein bands showed consistent mobilities regardless of the concentration of the starting sample. In addition, the mobilities of most of the proteins were identical from one run to another. Albumin mobility varied only from 18 mm in Run 1 to 19 mm in Run 2, or only about 5.5%; the beta-1-globulins varied from 0.55 to 0.60 or only about 8.3%. The other protein bands moved identically in both runs.

These data indicate that the agar gel electrophoresis provides consistent results from day to day. Using this method, no differences in mobility of the major plasma proteins as a function of the concentration of the starting sample could be detected.

POLYACRYLAMIDE DISC GEL ELECTROPHORESIS - The results of these tests are shown in Figure 7-5 and the data summarized in Figure 7-6. Although many details of the separation were lost during photographic representation, sufficient details are present to visually analyze the results.

Figure 7-5 is a photograph of plasma separations from samples ranging in protein concentration from 0.109 to 7%. From this photograph we selected seven bands or band groups for mobility comparison purposes. These bands were identified as (from top to bottom) gamma-globulins, a group of alpha-2-globulins, a single alpha-2-globulin, beta-1-globulins (hemoglobin and transferrin), an alpha-1-globulin, albumin and prealbumin. These identifications were made by comparing our electrophoretic pattern to that of Clarke(10), who identified all the various bands obtainable by this procedure.

MIGRATION OF PLASMA PROTEINS ON CORNING AGAR GEL PLATES

RUN 1

% PLASMA CONCENTRATION	PROTEIN MEASURED					
	ALBUMIN	α-1 GLOBULIN	α-2 GLOBULIN	β-1 GLOBULIN	FIBRINOGEN	γ GLOBULIN
	DISTANCE MOVED (cm) AT 85 VOLTS; FIELD STRENGTH 15 VOLTS/cm					
7.0	1.8	1.5	1.0	0.60	0.25	—0.25
3.5	1.8	1.5	1.0	0.60	0.25	—0.25
1.75	1.8	N.V.	1.0	0.60	0.25	N.V.
0.875	1.8	N.V.	N.V.	0.55	0.25	N.V.

N.V. — BANDS WERE NOT VISIBLE DUE TO DILUTION

Figure 7–3

MIGRATION OF PLASMA PROTEINS ON CORNING AGAR GEL PLATES

RUN 2

% PLASMA CONCENTRATION	PROTEIN MEASURED					
	ALBUMIN	α-1 GLOBULIN	α-2 GLOBULIN	β-1 GLOBULIN	FIBRINOGEN	γ GLOBULIN
	DISTANCE MOVED (cm) AT 85 VOLTS; FIELD STRENGTH 15 VOLTS/cm					
7.0	1.9	1.55	1.0	0.65	0.25	−0.25
28.0	1.9	1.55	1.0	0.65	0.25	−0.25
7.0 (REDILUTED)	1.9	1.55	1.0	0.65	0.25	−0.25

Figure 7–4

POLYACRYLAMIDE DISC GEL ELECTROPHORESIS OF HUMAN PLASMA PROTEINS

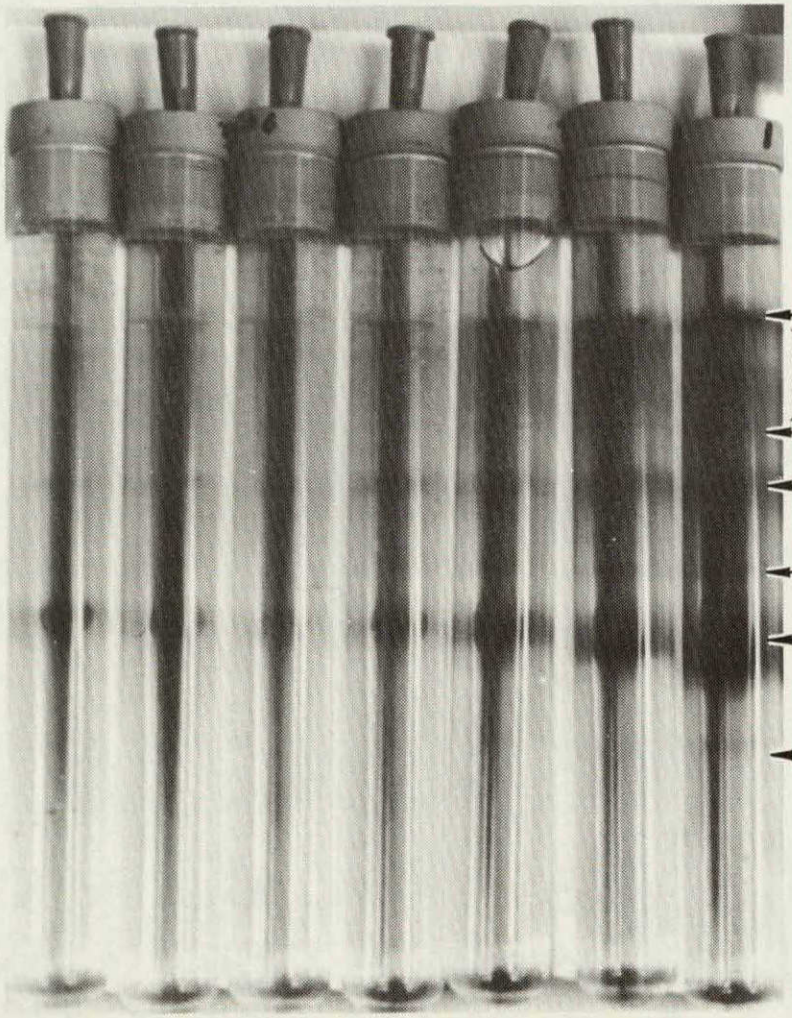

Figure 7–5

MIGRATION OF PLASMA PROTEINS IN POLYACRYLAMIDE DISC GEL ELECTROPHORESIS

% PLASMA CONCENTRATION	PROTEIN MEASURED					
	PRE-ALBUMIN	ALBUMIN	α-1 GLOBULIN	β-1-GLOBULINS (HEMOGLOBIN AND TRANSFERRIN)	α-2 GLOBULIN	γ GLOBULIN
	DISTANCE MOVED (cm) AT 150 VOLTS, FIELD STRENGTH, 12 VOLTS/cm					
7	5.8	4.4	3.3	2.1	1.4	0
3.5	5.8	4.4	3.3	2.2	1.4	0
1.75	N.V.	4.3	3.4	2.3	1.4	0
0.875	N.V.	4.2	3.3	2.3	1.4	0
0.437	N.V.	4.2	N.V.	2.2	N.V.	0
0.218	N.V.	4.2	N.V.	2.2	N.V.	0
0.109	N.V.	4.1	N.V.	2.1	N.V.	0

N.V. — NOT VISIBLE DUE TO DILUTION

Figure 7–6

The gamma-globulins were visible in all tubes and remained at the origin during electrophoresis. Although not visible in the photograph, seven distinct close-moving alpha-2-globulins were visible to the naked eye in the freshly stained gels down to a concentration of 0.875%, and showed no visible differences due to sample concentration. The alpha-2-globulin band was visible in the photograph in all tubes down to 0.875% and visual inspection indicated that this material moved about the same distance from the origin in each concentration. The beta-1-globulins, hemoglobin and transferrin moved as a single band, were visible in all tubes and also appeared to migrate the same distance regardless of concentration. Similar results are apparent with the alpha-1-globulin band, visible down to 0.875%, albumin, visible in all tubes, and prealbumin, visible only in the 7% and 3.5% samples. In two tubes, those containing 3.5% and 1.75% samples, slight smearing occurred in the area between the gamma-globulins and the group of alpha-2-globulins. The smearing is not visible in the photographic representation but was visible in the freshly stained gels. Those same bands, although very faint, were not smeared in the other tubes and all showed similar migration patterns. The reason for the smearing in those tubes was likely due to improper sample placement on the column.

Visual inspection of the general pattern of band migration in the gel column indicated that no significant differences in migration occurred from one test sample to another. More precise measurements, made from the origin to the center of each band are shown in Figure 7-6. Where N.V. appears in the table it indicates that the protein in that sample was too diluted to bind sufficient dye to be visible to the naked eye.

In the case of all the proteins except albumin, no significant differences were apparent as a function of protein concentration. The gamma-globulins all remained at the origin, the alpha-2-globulin moved 1.4 cm in every case, the beta-1-globulins showed migrations of 2.1 to 2.3 cm with an apparent slight increase with the intermediate concentrations, the alpha-1-globulin moved 3.3 to 3.4 cm with no apparent trend toward differences as a function of concentration, and prealbumin, in the two concentartions available for measurement, both migrated 5.8 cm.

Albumin, however, did appear to migrate slightly farther in the concentrated sample than in the most dilute sample. The differences of 2.1 and 2.3 noted for the beta-2-globulins and of 3.3 and 3.4 noted for the alpha-1-globulin are probably not

significant because of measuring error, slight deviations in gel thickness, or possible small differences in field strength across the gel discs. With albumin, however, a distinct trend is apparent indicating increased mobility of the albumin in concentrated samples. One possible explanation is that the albumin has oversaturated the gel disc molecular sieve pores and thus some of the albumin molecules are no longer retarded in mobility by the gel pores. These excluded molecules would be under the same electromotive force as all the other albumin molecules, but, not being retarded by molecular sieve action, as are all the others, would migrate farther giving the appearance of increased electrophoretic mobility.

Whatever the explanation of the increased albumin migration, the differences noted were not significant (about 7.3%) and did not interfere with the migration of the two species which move near albumin, i.e., prealbumin and the alpha-1-globulin. In addition, whereas it might have been expected that proteins in higher concentrated samples would possess retarded mobilities, these data indicate that if concentration does affect mobilities, even if only slightly, it does so with opposite results.

CELLULOSE ACETATE STRIP ELECTROPHORESIS - Tests conducted with the Gelman Model No. 51211 electrophoresis apparatus gave erratic and inconclusive results. It was found that differences in field strength occurred across separate cellulose acetate strips which caused erroneous interpretation of early test results. In effect, samples placed at the top of the apparatus always showed greater migration distances, regardless of concentration, when compared to migration distances obtained on strips placed at the bottom of the apparatus. Additionally, day to day variations in mobilities of up to 46% occurred, also regardless of sample concentration, which discounted meaningful interpretation of the data. No simple means of controlling these erratic results were available and so this method was not investigated further.

7.3 SUMMARY

Three conventional ground based electrophoretic procedures were employed to determine if sample concentration affected the electrophoretic mobility of the major plasma proteins. One of these methods, using cellulose acetate strips gave erratic and inconclusive results. These inconsistencies were shown to be a result of the apparatus itself and not a function of protein concentration. Using Corning gel

plates, consistent results were obtained from one experiment to another providing reliable data which showed that no differences in separation occurred as a result of protein concentration over the range of 0.875% to 28%. The third method employed, polyacrylamide gel electrophoresis, gave similar results over a concentration range of 0.109% to 7.0% protein. A slight increase in the migration of albumin noted during this procedure was probably not due to an increase of electrophoretic mobility but to overloading of the polyacrylamide gel by this major constituent of human plasma.

These results indicate that no significant differences in electrophoretic mobility are apparent, as a function of protein concentration, over the range of 0.109% to 28%.

8.0 CONCLUSIONS AND RECOMMENDATIONS

8.0 CONCLUSIONS AND RECOMMENDATIONS

The purpose of this study was to demonstrate the effects of gravity on the free flow electrophoretic process and to compare the demonstrated effects with predictions made using mathematical models. The effort included eighteen test runs to investigate the effects of gravity on the carrier buffer flow and forty-two test runs to investigate the effects of gravity on samples of biological materials, both proteins and cells. During the runs, electrical field, buffer flowrate and sample concentration were the independent variables. The dependent variables for the buffer gravity effects investigation were the vertical centerline velocity distributions and the horizontal centerline velocity distributions. For the sample gravity effects investigations, the dependent variable was outlet concentration distribution.

From the results of the buffer gravity effects, tests and data correlation the following conclusions can be drawn:

- Correlation between measured vertical centerline velocity distributions and analytical predictions with no field applied was generally good, except that test profiles are more rounded.
- With field applied to the chamber, the peaks in the velocity distribution near the membranes, with a larger peak on the cathode side, were predicted analytically and were evidenced by peaks in the horizontal dye fronts. These same peaks could not be numerically differentiated reliably from dye front coordinates, due to nearly vertical slopes in the dye fronts near the membranes.
- With field applied to the chamber, the measured vertical centerline velocities were generally less than those predicted by analysis. The analytical predictions are strongly dominated by the axial flow and the solution may not have converged sufficiently to accurately predict the additive velocities due to convection cells. Further correlation effort in this area is recommended.
- Correlation between measured horizontal centerline velocity distributions and analytical predictions was good considering that the error in measuring these velocities, which are about two orders of magnitude less than the vertical velocities, is almost as great as the velocities themselves.

From the results of the sample gravity effects tests and data correlation, the following conclusions can be drawn:

- Widening of the sample stream to about plus or minus one outlet tube width (±.08 cm) more than analytically predicted was obtained even with no field applied. Some of this widening is probably a characteristic of the test setup.

- Correlation between the outlet concentration distribution of single proteins during electrophoresis and the predicted distributions is generally good. except at low buffer flowrates. The larger measured movement at 20 ml/min buffer flowrate is a result of greater residence time for the sample than was analytically predicted. This is evidenced by the buffer gravity effects tests, where vertical velocity was less than predicted by analysis.

- Inconsistent results were obtained in estimating wall electroosmotic velocity for the buffers used from data obtained in the literature for other buffers. Further investigation of electroosmotic velocity for the buffers used is recommended. For a given estimate of wall electroosmotic velocity, the experimental results were consistent.

- The effects of gravity on the samples at the highest protein concentrations and lowest flowrate was about a 5% increase in movement under electrophoresis. Greater effect would have been noted at higher protein concentrations; however, consistent results would have been more difficult to obtain.

- The outlet concentration distributions obtained for 33H human lymphocytes show results similar to those obtained for proteins.

A general conclusion of this study is that three dimensional mathematical models, if they include gravity induced buoyant forces, can be used to effectively predict electrophoresis chamber separation performance.

The results of tests performed using various methods of electrophoresis using supportive media show that the mobility and the ability to separate are essentially independent of concentration, providing promise of being able to perform electrophoresis with higher inlet concentrations in space.

This investigation provides a starting point for meaningful comparison of free flow electrophoresis chamber performance, i.e. output and separation capability, on earth and under microgravity conditions and additional work in this area is recommended.

9.0 REFERENCES

9.0 REFERENCES

1. Barlow, G. H., et. al. Electrophoretic Separation of Human Embryonic Kidney Cells in Space. Colloquium on Bioprocessing in Space, LBJ Space Center, Houston, Texas (1976).
2. Hannig, K. H., et. al., Column Electrophoresis on the Apollo-Soyuz Test Project. Experiment MA-011, PP II-1 to II-38. In NASA Technical Memorandum NASA TMX-73360. Apollo-Soyuz Test Project Composite of MSFC Final Science Report. MSFC (1977).
3. Allen, R. W. et. al., Column Electrophoresis on the Apollo-Soyuz Test Project. Experiment MA-014. PP I-1 to I-68. In NASA Technical Memorandum NASA TMX 73360. Apollo-Soyuz Test Project - Composite of MSFC Final Science Report MSFC (1977).
4. Strickler, A., and T. Sacks, Continuous Free-Film Electrophoresis: The Crescent Phenomenon. Prep. Biochem., 3, 269 (1973).
5. Michl, H., Techniques of Electrophoresis. PP 252-286, In Chromatography 2nd Ed., Editor, Erich Heftmann, Pub. Van Nostrand Reinhold Company, 1971.
6. Vanderhoff, J. W., et. al. Electrophoresis Experiment for Space, NASA-CR-149925, MSFC (1976).
7. Lowry, O. H., et. al., Protein Measurement with the Folin Phenol Reagent. J. Biol. Chem., 193, 265-275, (1951).
8. Investigation of the Free Flow Electrophoresis Process. McDonnell Douglas Report E1721(1977).
9. Independent Research and Development - Calendar Years 1978-1979, McDonnell Douglas Report Q0853-2(1979).
10. Clarke, J. T., Simplified Disc Polyacrylamide Gel Electrophoresis, Ann., N. Y. Acad. Sci., 121, 428-436(1964).

MCDONNELL DOUGLAS ASTRONAUTICS COMPANY-ST. LOUIS DIVISION

Box 516, Saint Louis, Missouri 63166 (314) 232-0232

MCDONNELL DOUGLAS

CORPORATION